

2010

# A computational kinematics and evolutionary approach to model molecular flexibility for bionanotechnology

Athina N. Brintaki  
*University of South Florida*

Follow this and additional works at: <http://scholarcommons.usf.edu/etd>

 Part of the [American Studies Commons](#)

---

## Scholar Commons Citation

Brintaki, Athina N., "A computational kinematics and evolutionary approach to model molecular flexibility for bionanotechnology" (2010). *Graduate Theses and Dissertations*.  
<http://scholarcommons.usf.edu/etd/1579>

This Dissertation is brought to you for free and open access by the Graduate School at Scholar Commons. It has been accepted for inclusion in Graduate Theses and Dissertations by an authorized administrator of Scholar Commons. For more information, please contact [scholarcommons@usf.edu](mailto:scholarcommons@usf.edu).

A Computational Kinematics and Evolutionary Approach to Model Molecular Flexibility  
for Bionanotechnology

by

Athina N. Brintaki

A dissertation submitted in partial fulfillment  
of the requirements for the degree of  
Doctor of Philosophy  
Department of Industrial and Management Systems Engineering  
College of Engineering  
University of South Florida

Major Professor: Susana K. Lai-Yuen, Ph.D.  
Les Piegl, Ph.D.  
Alfredo Cardenas, Ph.D.  
Tapas Das, Ph.D.  
Kimon Valavanis, Ph.D.  
Ali Yalcin, Ph.D.

Date of Approval:  
November 3, 2009

Keywords: collision detection, molecular conformational search, flexible molecules,  
molecular stability, computational geometry, differential evolution

© Copyright 2010 , Athina N. Brintaki

## Dedication

*To the living memory of my father Nikolao E. Brintaki for his exceptional strength,  
boundless love and support as well as for his unforgettable spirit!  
And to my mom ... my love harbor!*

## Table of Contents

|  |    |
|--|----|
| List of Tables   | iv |
| List of Figures  | v  |
| Abstract   | ix |
| Preface  | xi |
| Chapter 1: Introduction  | 1  |
| 1.1 Motivation   | 1  |
| 1.2 Dissertation Objectives and Contributions                  | 2  |
| 1.3 Dissertation Outline                                       | 4  |
| Chapter 2: Literature Review                                   | 5  |
| 2.1 Molecular Mechanics Model                                  | 5  |
| 2.2 Evolutionary Algorithms (EAs)                              | 6  |
| 2.2.1 EAs in Molecular Docking                                 | 6  |
| 2.2.2 EAs in Molecular Conformational Search                   | 7  |
| 2.3 Haptic Rendering Approaches                                | 8  |
| 2.4 Computational Geometry                                     | 9  |
| 2.4.1 Collision Detection in Molecular Conformational Search   | 9  |
| 2.4.2 Geometric-Based Molecular Docking                        | 11 |
| 2.5 Current Literature Limitations                             | 12 |
| Chapter 3: A Geometric Interpretation of Molecular Mechanics   | 14 |
| 3.1 Background on Molecules                                    | 14 |
| 3.2 Molecular Energy   | 17 |
| 3.3 A Geometric Molecular Methodology from Molecular Mechanics | 18 |
| Chapter 4: BioGeoFilter (BGF) Methodology                      | 23 |
| 4.1 Overview of the Proposed BGF Model                         | 23 |
| 4.2 BGF: Lower Level Hierarchy                                 | 24 |

|   |    |
|---|----|
| 4.3 BGF: Upper Level Hierarchy  | 27 |
| 4.3.1 Constructing the Hierarchy  | 27 |
| 4.3.2 Molecular Geometric Constraints                                     | 28 |
| 4.3.3 Updating the Hierarchy and Self-Collision Detection                 | 29 |
| 4.4 Computer Implementation and Results                                   | 29 |
| 4.5 Conclusions   | 33 |
| <br>  |    |
| Chapter 5: Enhanced BioGeoFilter (eBGF) Molecular Model                   | 34 |
| 5.1 Differences Between eBGF and BGF Models                               | 34 |
| 5.2 Proposed eBGF Overview  | 35 |
| 5.3 eBGF: Lower Layer Hierarchy   | 36 |
| 5.4 eBGF: Upper Layer Hierarchy   | 38 |
| 5.4.1 Constructing the BVH  | 39 |
| 5.4.2 Randomization   | 40 |
| 5.4.3 Updating the Hierarchy  | 40 |
| 5.4.4 Self-Collision Detection  | 41 |
| 5.5 Computer Implementation and Results                                   | 44 |
| 5.6 Conclusions   | 49 |
| <br>  |    |
| Chapter 6: Generic Enhanced BioGeoFilter (g.eBGF) Model                   | 50 |
| 6.1 Differences Between eBGF and g.eBGF Models                            | 50 |
| 6.2 Ligand Modeling   | 51 |
| 6.3 Protein Modeling  | 51 |
| 6.4 Proposed g.eBGF Methodology   | 53 |
| 6.4.1 Overview of the Proposed g.eBGF Model                               | 53 |
| 6.4.2 Chemically-Artificial Bonds for the g.eBGF Method                   | 54 |
| 6.4.3 Description of the g.eBGF Algorithm                                 | 56 |
| 6.5 Computer Implementation and Results                                   | 58 |
| 6.6 Conclusions   | 65 |
| <br>  |    |
| Chapter 7: Identifying the Molecular Stability                            | 67 |
| 7.1 Fundamentals of Evolutionary Algorithms (EAs)                         | 67 |
| 7.2 EAs Advantages, Limitations and How to Compensate                     | 69 |
| 7.3 Differential Evolution  | 71 |
| 7.4 Proposed kDE Model  | 74 |
| 7.4.1 Overview of the Kinematics-Based Differential Evolution (kDE) Model | 74 |
| 7.4.2 Pre-Computation Module  | 75 |
| 7.4.3 DE-Loop Module  | 75 |
| 7.4.4 Computer Implementation and Results                                 | 77 |
| 7.4.5 Conclusions   | 82 |
| 7.5 Proposed BioDE Approach   | 83 |
| 7.5.1 BioDE Overview  | 83 |

|   |          |
|---|----------|
| 7.5.2 Input Files                                   | 85       |
| 7.5.3 Pre-Computation Module                        | 86       |
| 7.5.4 DE-Loop Module                                | 87       |
| 7.5.5 Computer Implementation and Results           | 88       |
| 7.5.6 Conclusions                                   | 93       |
| 7.6 Comparison Between the kDE and BioDE Approaches | 94       |
| <br>  |          |
| Chapter 8: Conclusions, Discussion and Future Work  | 97       |
| 8.1 Research Summary                                | 97       |
| 8.2 Future Research Work                            | 99       |
| <br>  |          |
| References  | 102      |
| <br>  |          |
| About the Author                                    | End Page |

## List of Tables

|           |  |    |
|-----------|--|----|
| Table 4.1 | Statistical data for four different ligand molecules                 | 32 |
| Table 5.1 | Performance analysis of the proposed eBGF algorithm for two proteins | 44 |
| Table 5.2 | Performance analysis of current approaches                           | 48 |
| Table 6.1 | Performance analysis of the proposed g.eBGF methodology              | 59 |
| Table 6.2 | Computational complexity comparison                                  | 65 |
| Table 7.1 | Performance analysis of the kDE algorithm on ligands                 | 78 |
| Table 7.2 | Performance analysis of the kDE algorithm on proteins                | 79 |
| Table 7.3 | RMSD performance of the kDE algorithm                                | 82 |
| Table 7.4 | Performance analysis of the BioDE algorithm on ligands               | 90 |
| Table 7.5 | Performance analysis of the BioDE algorithm on proteins              | 90 |
| Table 7.6 | RMSD performance of the BioDE algorithm                              | 93 |
| Table 7.7 | Comparison between kDE and BioDE approaches                          | 95 |

## List of Figures

|            |  |    |
|------------|--|----|
| Figure 1.1 | Receptor and ligand molecules used in drug design  | 2  |
| Figure 2.1 | Molecular manipulation and assembly with haptics   | 8  |
| Figure 3.1 | Graphical representation of three different molecular structures                             | 15 |
| Figure 3.2 | Graphical representation of amino acids' topology and link procedure through a covalent bond | 16 |
| Figure 3.3 | Pattern of a protein's backbone chain  | 16 |
| Figure 3.4 | Mechanical molecular model   | 19 |
| Figure 3.5 | Example of a drug-like molecule as an articulated body                                       | 19 |
| Figure 3.6 | Three geometric molecular models developed in this research work                             | 22 |
| Figure 4.1 | Overall structure of the proposed BioGeoFilter methodology                                   | 24 |
| Figure 4.2 | 1STP ligand molecule divided into AtomGroups based on the location of the torsion bonds      | 25 |
| Figure 4.3 | AtomGroups for a hypothetical small molecule   | 25 |
| Figure 4.4 | Local Cartesian coordinate frame assigned to $Group_i$ and $Group_{i-1}$                     | 26 |



|            |   |    |
|------------|---|----|
| Figure 4.5 | Schematic representation of the smallest enclosing sphere of spheres  | 27 |
| Figure 4.6 | Proposed hierarchical structure for 1STP ligand molecule  | 27 |
| Figure 4.7 | Computational time comparison for four different ligand molecules   | 30 |
| Figure 4.8 | Examples of random conformations for three ligand molecules   | 31 |
| Figure 5.1 | Overview of the proposed eBGF approach  | 36 |
| Figure 5.2 | Graphical representation of the degrees of freedom of a protein   | 37 |
| Figure 5.3 | Graphical representation of the AtomGroup concept along with the proposed splitting procedure for a hypothetical protein segment  | 37 |
| Figure 5.4 | Schematics representation of the rigid and flexible AtomGroups within a hypothetical protein segment and the accordance BVH   | 39 |
| Figure 5.5 | Graphical representation of the proposed collision detection algorithm  | 42 |
| Figure 5.6 | Two example macromolecules tested in this work  | 43 |
| Figure 5.7 | Comparison of the average collision time by the proposed eBGF vs. the average energy calculation time for different sets of pre-selected flexible-residues/dof                | 45 |
| Figure 5.8 | Average total time comparison between the proposed eBGF algorithm and the energy calculation approach to output feasibility for 1STP and 1DO3 proteins in a logarithmic scale | 46 |
| Figure 5.9 | Schematic demonstration of the accuracy of the proposed eBGF methodology  | 47 |
| Figure 6.1 | Examples of ligand molecules  | 51 |

|             |  |    |
|-------------|--|----|
| Figure 6.2  | VDW representation of two different protein molecule examples  | 52 |
| Figure 6.3  | Graphical representation of the degrees of freedom of a protein  | 52 |
| Figure 6.4  | Overview of the proposed g.eBGF methodology  | 54 |
| Figure 6.5  | Structure of the protein with PDB ID: 1NS1   | 55 |
| Figure 6.6  | Closest residue-pair between the first helices of the two 1NS1 protein's chains  | 55 |
| Figure 6.7  | Graphical representation of the AtomGroup concept along with the proposed splitting procedure for a hypothetical protein segment with two chains | 57 |
| Figure 6.8  | Time comparison between the traditional energy calculation approach and the proposed g.eBGF methodology for ligand molecules                     | 60 |
| Figure 6.9  | Time comparison between the traditional energy calculation approach and the proposed g.eBGF methodology for protein molecules                    | 61 |
| Figure 6.10 | Computational time performance of the proposed g.eBGF approach for molecules of different size and dof   | 62 |
| Figure 6.11 | Splitting threshold impact on the g.eBGF results for protein modeling  | 63 |
| Figure 6.12 | Accuracy comparison between the traditional energy calculation approach and the proposed g.eBGF method   | 63 |
| Figure 7.1  | One-point crossover (recombination) operator   | 68 |
| Figure 7.2  | Uniform mutation operator  | 68 |

|             |  |    |
|-------------|--|----|
| Figure 7.3  | Overview of the proposed kDE model                                     | 75 |
| Figure 7.4  | Schematic representation of the chromosome structure used in this work | 76 |
| Figure 7.5  | Ligand molecules tested with the kDE model                             | 77 |
| Figure 7.6  | Protein molecules tested with the kDE model                            | 78 |
| Figure 7.7  | kDE's convergence performance for ligands                              | 80 |
| Figure 7.8  | kDE's convergence performance for proteins                             | 81 |
| Figure 7.9  | Overview of the proposed BioDE approach                                | 84 |
| Figure 7.10 | Ligand molecules tested with the BioDE model                           | 89 |
| Figure 7.11 | Protein molecules tested with the BioDE model                          | 89 |
| Figure 7.12 | Convergence performance of the BioDE method for ligands                | 91 |
| Figure 7.13 | Convergence performance of the BioDE method for proteins               | 92 |

A Computational Kinematics and Evolutionary Approach to Model Molecular Flexibility  
for Bionanotechnology

Athina N. Brintaki

ABSTRACT

Modeling molecular structures is critical for understanding the principles that govern the behavior of molecules and for facilitating the exploration of potential pharmaceutical drugs and nanoscale designs. Biological molecules are flexible bodies that can adopt many different shapes (or conformations) until they reach a stable molecular state that is usually described by the minimum internal energy. A major challenge in modeling flexible molecules is the exponential explosion in computational complexity as the molecular size increases and many degrees of freedom are considered to represent the molecules' flexibility. This research work proposes a novel generic computational geometric approach called *enhanced BioGeoFilter* (*g.eBGF*) that geometrically interprets inter-atomic interactions to impose geometric constraints during molecular conformational search to reduce the time for identifying chemically-feasible conformations. Two new methods called *Kinematics-Based Differential Evolution* (*kDE*) and *Biological Differential Evolution* (*BioDE*) are also introduced to direct the molecular conformational search towards low energy (stable) conformations. The proposed *kDE* method kinematically describes a molecule's deformation mechanism while it uses differential evolution to minimize the intra-molecular energy. On the other hand, the proposed *BioDE* utilizes our developed *g.eBGF* data structure as a surrogate

approximation model to reduce the number of exact evaluations and to speed the molecular conformational search. This research work will be extremely useful in enabling the modeling of flexible molecules and in facilitating the exploration of nanoscale designs through the virtual assembly of molecules. Our research work can also be used in areas such as molecular docking, protein folding, and nanoscale computer-aided design where rapid collision detection scheme for highly deformable objects is essential.

## Preface

Four years of learning filled with contradictory experiences enforced facing myself, realizing my strengths and limitations while maturing me as a person and as a scientist. This has been a savory adventure within one's emotions: balancing between hope and despair, happiness and sadness, solitude and networking. For this reason, I have to express my sincere gratitude to those who made this journey possible and all people that helped and supported me during this adventure.

First and foremost, I would like to thank my advisor Dr. Lai-Yuen for providing the opportunity to work towards enhancing computer-aided molecular design and engineering which really captured my imagination and inspired me as both a student and a researcher. Her continuing support, guidance and encouragement throughout the challenging years we have worked together, has been invaluable. She allowed me to find my own research path, always listening to my ideas and offering sound advice. I have learned much from her on how to be a scientist, conduct research and, I hope, an inspiring teacher.

I would also like to thank Dr. Cardenas and his research group from the Department of Chemistry at USF, who taught me much of the biology I know, and for all their helpful discussions and suggestions. Their feedback and comments were very helpful in establishing the biological relevance of my work.

I owe special thanks to Dr. Piegl from the Department of Computer Science & Engineering at USF for letting me into his CAD & Graphics research group, supporting and guiding me throughout this research journey. Numerous times I have been challenged by Dr. Piegl on how to justify and support my research. I have learned much from him on how to present and project my work as a critical component of some of the emerging areas of engineering research in 21<sup>st</sup> century. I would also like to thank my CAD &

Graphics colleagues Olya and Khairan, for being always attentive and encouraging as well as for our exceptional collaboration.

My sincere thanks also to my colleagues Konstantino Dalamakidi and Soumayaroop Roy from the Department of Computer Science & Engineering at USF for helping me with C++ programming, being patient and accessible in answering my numerous questions.

Very genuine thanks to my former advisor Dr. Nikolos from the Production Engineering & Management Department at Technical University of Greece for initiating my research and teaching experiences. I am grateful for all his guidance, discussions and support that allowed my preparation for accomplishing this challenging adventure. I would also like to thank him for his collaboration in one of the projects that made up this dissertation as well as for allowing me to have at my disposal his lab equipment to conduct some of my final experiments.

I also owe very special thanks to my former advisor Dr. Valavanis from the Electrical & Computer Engineering Department at University of Denver for believing in me and inviting me to continue my Ph.D. studies at USF. I am truthfully grateful for the offered opportunity as well as for inspiring me to conduct robotics research and transfer this knowledge at the bionanoscale.

I am also extremely thankful towards my Committee Members Dr. Das and Dr. Yalcin and my committee Chair Dr. Tsokos for their insightful feedback, support and attention to my research work. I would like to give thanks to my colleagues Wilkistar, Chaitra, Vishnu, Patricio, Laila, Alfredo, Diana, Dayna, Andres, Alcides, Ozan, Sinan, Fethullah, all my IMSE Professors, Chair Dr. Zayas and of course Jackie and Gloria for our excellent collaboration, their support and attention to my research work and academic development.

I truthfully would like to thank my family and friends for their unconditional and continued support to this challenging and exciting adventure. I am extremely grateful for all the unreserved support and motivation received from my true friends Kaliopi, Katerina, Despoina, Nikoleta, Maria and of course my very good friend Ahna for always being there for me to strengthen my confidence during all the difficulties I faced. But

above all, my sincere thanks to my parents Nikolao and Euagelia, my sister Evi, my cousin Gianni, my aunt Vagia and my grandparents Athanasio and Pinelopi for strongly believing in me, supporting me throughout this long journey and all the years preceding it. I am deeply grateful to them for reinforcing me to pursue my dreams and accomplish this goal while teaching me to be a sincere person. They are the source of my strength, joy and love.

My only regret however, is for not finishing my dissertation earlier, before my father passed away. I miss watching my father's eyes filled with sincere love and pride. I am confident, though, that in his eternal peace he is proud of me as he was through all my life and as I have been proud of him. My sincere love, love without ego, for my father reinforced my efforts for accomplishing this work while he was fighting for his life. This is my gift to my father for all his courage, strength and for his unforgettable spirit!



## Chapter 1

### Introduction

The scope of this chapter is to introduce the motivation underneath this research work as well as the current molecular modeling challenges. The proposed research objectives and contributions are also discussed followed by the dissertation outline.

#### 1.1 Motivation

Bionanotechnology is the new frontier in research and technology and is vital for the realization of biomedical and nanoscale products. It consists of manipulating biological molecules to create structures or devices with new molecular arrangements. The control, manipulation, and assembly of molecules will enable the design of innovative materials, new pharmaceutical drugs, enhanced textiles, and precise nanoscale devices with new capabilities for diagnosis and treatment of diseases. It is estimated that within the next 10 years, “at least half of the newly designed advanced materials and manufacturing processes will be build at the nanoscale” [NIST].

To achieve bionanotechnology, it is crucial to enable real-time visualization of interactions between biological molecules during the design stage so that fully functional nanoscale products can be designed and evaluated prior to actual fabrication. A main key for enabling the visualization of biological components is the understanding and effective modeling of molecules' behavior. Molecules are very flexible in nature and can adopt many molecular conformations (or shapes) while searching for a stable or low-energy molecular state. The major challenge in modeling flexible molecules (or molecular conformations) lies on the exponential explosion in computational complexity as the molecular size increases and a large number of degrees of freedom (dof) are considered

to represent the molecules' flexibility. For example, Figure 1.1 shows a small drug molecule (called a ligand) that can dock or assemble into a larger molecule (called a receptor) leading to the identification of pharmaceutical drugs and new molecular arrangements with specific capabilities. Receptor molecules can consist of hundreds or thousands of atoms with hundreds or even thousands of degrees of freedom. Therefore, modeling molecular conformations is a highly intensive computational task and remains the main challenge in molecular design.

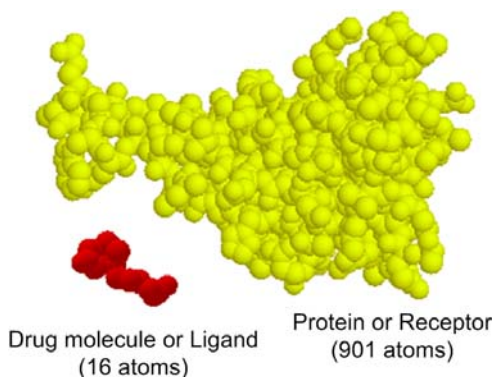


Figure 1.1: Receptor and ligand molecules used in drug design.

## 1.2 Dissertation Objectives and Contributions

The proposed research aims to address the main molecular modeling challenge and current literature limitations for modeling flexible molecules and identifying stable conformations. This research work presents a novel computational geometric and evolutionary inspired approach for the effective identification of chemically-feasible, low-energy molecular structures of any size, shape and topology.

The main expected research outcome is the design of novel algorithms to minimize molecular conformational search and to speed collision detection queries that will enable the visualization and virtual manipulation of flexible molecules for interactive molecular design. The major objectives of this dissertation are:

1. to develop a novel bounding volume data structure called *BioGeoFilter (BGF)* for the effective and real-time identification of feasible conformations for flexible drug-like or ligand molecules
2. to develop a generic biologically-inspired data structure called *generic enhanced BioGeoFilter (g.eBGF)* methodology for simplifying the molecular representation regardless of type, size and shape. This methodology considers certain chemical factors that influence the molecular flexibility to effectively provide more realistic and chemically-feasible molecular conformations.
3. to investigate and design a kinematics and evolutionary based direct search technique called *kinematics differential evolution* or *kDE* model that effectively searches for stable or low-energy molecular conformations with a good convergence performance.
4. to design a novel direct search method called *biological differential evolution (BioDE)* that will utilize our proposed *g.eBGF* approach as a surrogate approximation model to speed the search towards alternative low-energy molecular conformations and to achieve a good convergence performance.

The proposed computational geometric and evolutionary based research work contributes to the molecular modeling and differential evolution literature through the design of a new geometric-based model for simplifying the molecular representation and two innovative evolutionary-based algorithms for directing the search towards low-energy molecular conformations. This hybrid approach will impact nanoscale design by speeding the modeling of flexible molecules and enabling the development of an indispensable computer-aided design tool for bionanotechnology. The proposed research can be applied in areas such as molecular docking/ assembly and protein folding where a rapid collision detection scheme for highly deformable objects is essential.

This research has resulted in two journal papers [Brintaki and Lai-Yuen, 2008a, 2009a], two submitted journal papers [Brintaki et.al. 2010a,d], five conference proceedings [Brintaki and Lai-Yuen 2008a,b, 2009b, 2010b,c], three papers in progress and several poster presentations. The research work has been partially supported by NSF, SME and USF grants.

### 1.3 Dissertation Outline

Chapter 2 discusses current research work in molecular modeling, geometric techniques and evolutionary approaches in molecular applications. Chapter 3 describes our computational geometric interpretation of molecular inter-atomic interactions for addressing the molecular conformational search problem for highly deformable objects. Chapters 4, 5, and 6 present the development of three computational geometric models for the effective identification of feasible molecular conformations. The first model called *BioGeoFilter* or *BGF*, effectively identifies feasible conformations for small molecules in real-time as discussed in Chapter 4. The second model called *enhanced BioGeoFilter* or *eBGF* analyzes the structure of much larger molecules such as proteins to model them more effectively as discussed in Chapter 5. Chapter 6 introduces the *generic eBGF* or *g.eBGF* model that incorporates chemically-based constraints that result in more realistic molecular conformations for molecules of different type, size, shape and topology.

Chapter 7 proposes two new energy minimization algorithms: the *kinematics differential evolution* or *kDE* and the *biological differential evolution* or *BioDE* methods. Both kDE and BioDE models utilize our previously developed differential evolution (DE) algorithm to direct the search towards low-energy molecular conformations. The main algorithmic difference between the kDE and BioDE models is that the latest utilizes the g.eBGF data structure as a surrogate approximation model to speed convergence. Chapter 8 provides a summary of the research methodologies presented and future research work.

## Chapter 2

### Literature Review

This chapter provides the background on previous work in the areas of molecular modeling, evolutionary algorithms and computational geometry techniques in molecular applications. Previous work is analyzed and their limitations identified.

#### 2.1 Molecular Mechanics Models

The molecular mechanics or force-field method uses Newtonian procedure to describe a molecular structure and its properties energetically as a function of its conformation. Molecular mechanics approaches are widely used in molecular structure refinement, molecular dynamics (MD), Monte Carlo (MC), or molecular docking simulations. The molecular mechanics model considers atoms as spheres and bonds as springs that have the ability to move along different directions. The mathematics of spring deformation is used to measure the ability of the bond to stretch, bend and twist.

Dynamic-based simulation models such as molecular dynamics (MD) simulations [Leech 1996, Branner 2000, Renambot 2001, Tanfer 2004, Phillips 2005, Adcock 2006,] and Monte Carlo (MC) methods [Liu 1999, Kima 2002] are commonly used to obtain information related with the time evolution of molecular conformations. These methods aim to determine molecular feasibility by calculating atoms' position and hence their internal energy in small time steps. This results in a more accurate but slow progress towards the search of a feasible molecular conformation. As the number of atoms within a molecular structure increases, the time to calculate the intra-molecular energy for determining a molecule's feasibility (stability) increases significantly, making these methods unsuitable for interactive molecular design and assembly.

## 2.2 Evolutionary Algorithms (EAs)

The choice of an appropriate optimization method is essential for directing the conformational search to identify the desired solution or the best potential molecular conformation. The optimization of molecular geometry was one of the very first applications of evolutionary algorithms (EAs) in chemistry. EAs have shown good results in problems where other methods have struggled. In addition, their governing principles are clearly understood, intuitively appealing and relatively easy to implement. In this section, we focus on EAs applications in chemical problems that require optimization such as molecular docking and molecular conformational search. Detailed information on EAs is provided in Chapter 7.

### 2.2.1 EAs in Molecular Docking

Current literature in molecular docking demonstrates the effectiveness of Evolutionary Algorithms (EAs) for describing complex systems [Thomsen 2003, 2006] and for solving problems involving large search spaces, where traditional optimization techniques are less efficient [Yang 2001]. Genetic Algorithms (GAs) are presented as an effective local search method that behaves really well for median energy solutions [Westhead 1997, Jones 1997]. Additionally, Morris et al. compared the efficiency of Monte Carlo (MC) simulated annealing method against a classic GA and Lamarckian GA (LGA) for predicting the bound association of flexible ligands to macromolecule targets. Results showed that both LGA and GA are the most reliable, efficient and successful methods. However, many modifications have been proposed to improve the solution quality and to speed convergence.

One of the best EAs for solving real-valued energy functions is Differential Evolution (DE) initially proposed by [Storn & Price 1995, 2005]. DE is a population based stochastic function minimizer that adds the weighted difference between two individual vectors to a third vector (*donor*). Currently DE has been implemented by [Yang 2001, Thomsen 2003, 2006] for investigating the docking of a flexible ligand to a

rigid receptor where their numerical results indicate the algorithms' robustness and remarkable performance in terms of convergence speed.

### 2.2.2 EAs in Molecular Conformational Search

Wehrens presented a survey focused on the differences, strengths and weaknesses between EAs and other structure optimization methods such as distance geometry, eigen value decomposition, simulated annealing, Monte Carlo or molecular dynamics simulations [Wehrens 2000]. The main conclusion was that EAs are consistently among the best performing general search algorithms. On the other hand, GAs are particularly useful for rapidly producing a family of low energy conformations but are less successful in fine-tuning these conformations towards the exact global optimum.

Various evolutionary-based studies have been performed to study flexible ligand, flexible protein or polypeptide molecules conformational search. Wawer et al. [Wawer 2004] presented a real-coded (as opposed with the binary coding of the classic GAs) genetic algorithm to analyze the conformational behavior of Vitamin E (a small molecule). Wang and Ersoy [Wang and Ersoy 2005] presented a Mixture Gaussian Optimization (MGO) algorithm as a continuous stochastic approach for flexible ligand conformational search. The MGO method was compared against a systematic and a stochastic conformational search algorithm and it was concluded that the MGO algorithm can locate the global minimum faster as the molecular size increases. On the other hand, as the molecular size increases, the systematic search method became non-applicable whereas the stochastic was trapped in local minima. However, the MGO was tested for small molecular structures only and was not applied to large molecules such as proteins.

Chong and Tremayne [Chong and Tremayne 2006] presented a new DE algorithm based on Cultural Evolution concepts called CDE to study the structure search for ligand molecules. The CDE algorithm was compared against a classic DE method and it was concluded that both methods succeeded to find the global minimum and the convergence performance of the CDE algorithm was 54% faster.

Damsbo et al. [Damsbo 2004] presented the FOLDAWAY system, an evolutionary based approach for finding the low-energy conformations of polypeptides. The proposed model found large groups of low-energy structures within the expected low-energy globule that were not identified in previously developed MD simulations.

Bitello and Lopes [Bitello and Lopes 2004] used a DE algorithm to solve the protein folding problem. Their approach was consistent in finding the global minimum for structures consisted up to 64 amino acids (relatively small protein size) and performed better compared with a classic GA.

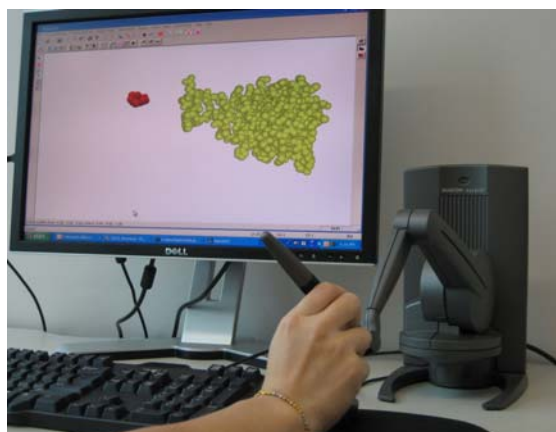


Figure 2.1: Molecular manipulation and assembly with haptics.

### 2.3 Haptic Rendering Approaches

In recent years, new methods have been investigated to facilitate molecular design and nanoscale engineering by providing real-time force feedback using haptic devices [Sherill, Baxter 1998, Nagata 2002, Grayson 2003, Lee 2004, Lai-Yuen 2006a,b, Morin 2007]. Haptic devices are electromechanical devices that exert forces on users giving them the illusion of touching something in the virtual world. These devices have been used to manipulate virtual molecules and to feel the forces as the molecules interact with each other providing an essential design and visualization tool as shown in Figure 2.1. However, current methods using haptics either model molecules as rigid bodies or are



limited to local molecular motions and short periods of simulation time. Modeling molecules as rigid bodies can simplify the calculation of forces but does not represent the molecular interactions realistically. To achieve a realistic molecular representation, it is necessary to model molecules as flexible bodies that attain different conformations while searching for a stable molecular state. Incorporating real-time haptic force feedback into molecular design requires rapid update and modeling of molecular conformations for providing realistic and continuous visualization and sense of touch to the users.

## 2.4 Computational Geometry

Recently, computational geometry has been successfully used in molecular design since important constraints influencing molecular behavior can have geometrical interpretation. The representation of intra-molecular interactions through a computational geometric approach can allow the approximation of molecules' behavior rapidly and efficiently for real-time molecular design. From a geometric point of view, a molecular conformation can be considered feasible when there are no overlapping atoms or all possible atomic interactions are collision-free. Collision detection (CD) is an essential problem in robotics, computational geometry, and computer graphics and is a major bottleneck in any interactive simulation. A wide range of techniques have been proposed to deal with collision detection such as hierarchical representations, spatial partitioning, analytical methods, and geometric reasoning. The algorithmic design depends on the representation of the model, the query types, and the simulated environment [Lin 1998].

### 2.4.1 Collision Detection in Molecular Conformational Search

Bounding volume hierarchies (BVH) are the most popular methods for capturing self-collision and collisions between objects [Teschner 2005]. The key idea is to use a hierarchical structure to describe the shape of an object at successive levels of detail. The

object of interest is enclosed by bounding volumes that can have various shapes such as spheres, axis-aligned bounding boxes (AABBs), and oriented bounding boxes (OBBs) [Lin 1998]. These bounding volumes become the tree leaves of the hierarchy that are enclosed by subsequent bounding volumes forming a hierarchical data structure.

For molecular structures, collision detection is a computationally expensive problem given the many degrees of freedom that a molecule can have. Lotan et al. [Lotan 2002] used a kinematics chain model to represent proteins flexibility. In respect to the chain topology the authors built a BVH using object-oriented bounding boxes to detect overlapping atoms. They tested various proteins of different size and concluded an updated and testing computational time ranging in hundreds milliseconds. Their proposed approach requires  $O(N)$  performance for building the BVH and  $O(N^{4/3})$  computational complexity for the collision detection queries.

Agarwal et al. [Agarwal 2004] used a BVH with the objects being modeled as spheres to detect collisions for deforming and moving necklaces (sequence of balls/beads). The authors built a balanced binary tree with spheres as bounding volumes to assist in the search for overlapping atoms within flexible protein molecules. They proposed two methods for computing the spheres: wrapped and layered hierarchy that provides an upper bound of  $O(N \log N)$  in 2D space or  $O(N^{2-3/d})$  in d-dimensional space for the collision detection plan.

Angulo et al. [Angulo 2005] proposed the BioCD algorithm for efficient self-collision search and distance computations. The algorithm maintains two levels of bounding volume hierarchies (BVH). In the low level, it identifies the rigid groups of the articulated model and builds a hierarchy for each of them. In the upper level, it arranges the roots of the low level hierarchies. The authors tested various proteins with different size and they reached a collision detection time measured in tens of milliseconds with  $O(N)$  performance and a  $O(N \log N)$  complexity for building the BVH.

Redon et al. [Redon 2005] proposed an adaptive dynamic algorithm (ADA) for articulated bodies built upon “the divide-and-conquer algorithm” (DCA). An articulated body is the recursive link pair of articulated parts. The series of the assembly actions is

represented by a binary tree. Each node in the tree represents a sub-assembly motion. Morin and Redon [Morin 2007] utilized the ADA algorithm and proposed a force-feedback algorithm for adaptive dynamic simulation of proteins. The authors used a multithreaded structure to couple the adaptive dynamic simulation loop from the computation of the force applied to the user (through the haptics) requiring a force feedback of  $O(\log N)$  complexity.

#### 2.4.2 Geometric-Based Molecular Docking

Current computational docking methods come from the areas of surface matching, object recognition and motion planning. Motion planning is a fundamental problem in robotics that consists of finding a valid sequence of configurations that moves an object from an initial position to a target point. Automatic motion planning is applicable not only to robotics, but also to virtual reality systems, computer-aided design and computational biology.

Recently, researchers realized that both automatic motion planning and molecular docking problem relies upon the same basic principles. A drug molecule can be considered like a robot with many degrees of freedom (dof) whose motion can be predicted by an automatic planner determining its ability to bind with a protein. The binding configuration should satisfy all the geometric, electrostatic and chemical constraints of the problem. A good binding site should also be reachable to the ligand from an outside location. Hence, the path to the binding site is highly important and motivates the use of motion planning in the molecular docking problem. These methods are known as probabilistic roadmap methods (PRMs) and are widely used in robotics, intelligent CAD systems and lately in computational biology. PRMs randomly construct a graph in  $C$ -space (configuration space), a roadmap, as it is called. The motion planning is then solved by connecting the start and goal configurations in the roadmap and searching for the feasible path on it [Bayazit 2003, Cortes 2003, 2005, 2007].

A modification of the PRM framework is the rapidly-exploring random trees (RRT) for solving single-query problems without preprocessing the complete roadmap.

These algorithms are well fitted for highly constrained problems [Cortes 2002, 2003, 2005, 2007, La Valle 1999, 2000a,b]. A recently developed PRM variation to study molecular motions is the Stochastic Roadmap Simulation (SRS) [Bayazit 2000, Apaydin 2002a, b, 2003, Chiang 2006]. A stochastic roadmap contains many Monte Carlo (MC) simulation paths at the same time. The SRS studied all the paths together in a closed form and resulted in significant computational time reduction.

Zhang and Kavraki [Zhang and Kavraki 2002] compared their proposed atom-group-local-frame method with the simple rotations and Denavit-Hartenburg model [Hartenburg and Denavit 1955]. It was concluded that the atom-group-local-frame method not only eliminates all the disadvantages of the other two but also resulted in a lazy evaluation of atom positions and in computational time reduction. This technique appears extremely useful in cases that deal with many conformations. Zhang et al. [Zhang 2005] extended the atom-group-local-frame work by adding a geometric screening phase for identifying feasible molecular conformations.

## 2.5 Current Literature Limitations

Although remarkable advances in computational biology have been performed over the years, modeling molecular flexibility remains the main challenge in molecular design. Most of the above discussed methods do not address the modeling of molecules for real-time rendering or only allow a limited number of degrees of freedom to change. In addition, a more generic methodology is required that:

1. is not limited to the topology of the molecules for self-collisions or collisions between them,
2. evaluates arbitrary conformations independently of the previous query,
3. is adaptive to the molecular structure by exploiting the fact that when limited degrees of freedom change some of the atomic distances remain constant,
4. identifies molecular feasibility rapidly, efficiently and is evaluated in terms of both computational time and accuracy,

5. incorporates the chemical information that controls molecules' flexibility into the molecular design to simplify and realistically represent the molecular interactions
6. effectively directs the search towards low energy and chemically-feasible molecular conformations.

To address current literature limitations, this research work presents a new biologically-inspired geometric method for simplifying the representation of molecules of different type, size, shape and topology while considering certain chemical factors that influence molecules' flexibility. To direct the search towards low-energy molecular conformations, we propose the use of a new evolutionary based algorithm that will utilize the developed geometric method as a surrogate approximation model for reducing the algorithm's convergence rate and finding the global minimum. The proposed work can facilitate interactive molecular modeling and nanoscale design.

## Chapter 3

### A Geometric Interpretation of Molecular Mechanics

This chapter introduces the basic molecular concepts and presents our proposed geometric interpretation of molecular mechanics. A brief background on the various types of molecules and their basic functions is provided where molecules are categorized into ligands and receptors. The central concepts on the internal molecular energy and our geometric interpretation of the molecular conformation mechanics are also explained in this chapter to provide the basis for our developed algorithms presented in Chapters 4, 5 and 6.

#### 3.1 Background on Molecules

A molecule is a sufficiently stable electrically neutral group of at least two atoms, in a definite arrangement, held together by very strong chemical bonds or covalent bonds. A covalent bond is a chemical bond where electrons are shared between atoms. As shown in Figure 3.1, the size, shape and topology of a molecular structure varies according to its chemical characteristics and function. These molecules are displayed using the VMD software [Humphrey 1999] as shown in Figure 3.1. Geometrically, a molecule can be considered as a collection of atoms and bonds between each atom pair. Each atom can be represented as a sphere with van der Waals radius while chemical bonds can be represented as springs.

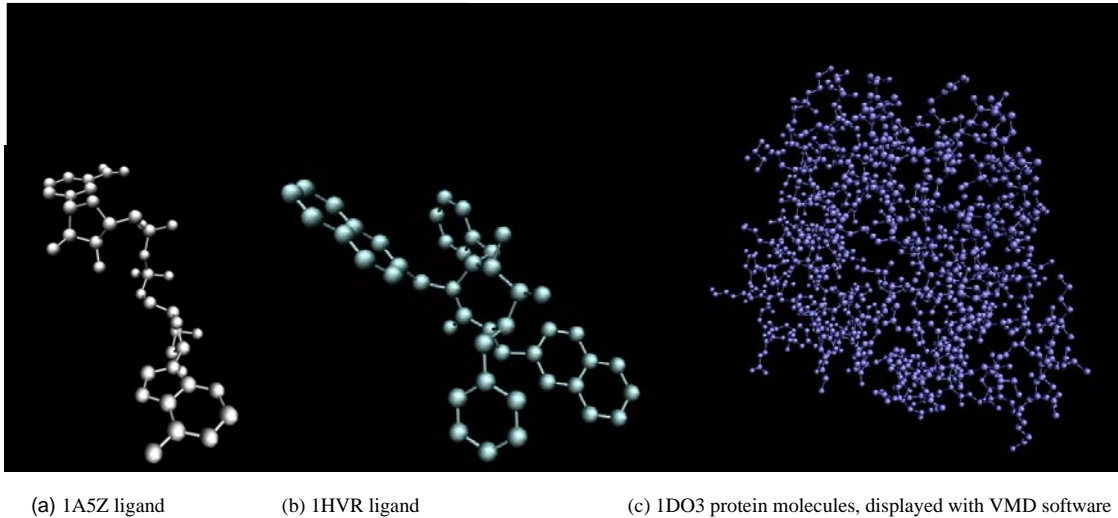


Figure 3.1: Graphical representation of three different molecular structures.

Molecules are essential to a variety of biological processes and activities of fundamental importance to life. There are four basic types of molecules that are the major players in biological systems: carbohydrates, lipids, nucleic acids and proteins. Both carbohydrates and lipids are small molecules that are less complex compared with the nucleic acids and proteins. Carbohydrates tend to be the least complicated molecular structures used as energy sources for cell processes. Lipids are also fairly simple organic molecules that have several uses in living organisms such as acting as water barriers in cell membranes. Lipids are also used for extra waterproofing or as insulation around nerves for long-term storage of energy in the form of fat, or used as heat insulation, as cushions, and as messenger molecules. Nucleic acids and proteins are typically much larger complex molecules. The primary role of the nucleic acids or DNA (one type of nucleic acid) is to store proteins' main information. Proteins are very important macromolecules in living organisms and perform many distinct functions. The functions of a protein depend on its 3-dimensional shape, which can be virtually infinite in variety. Most proteins are enzymes performing biochemical functions such as bond-making and bond-breaking reactions. Other proteins act as molecular motors or structural components by performing biophysical functions.

The understanding and modeling of the molecular functions and behaviors is very important in nanoscale design since many problems associated with the development of bionanotechnology require specifically-designed molecules. For example, drug design and discovery relies increasingly on structured-based methods for improving efficiency. The main objective in drug design is to find or build molecules (ligands) that target proteins (receptors) crucial to the proliferation of microbes, cancer cells or viruses. This is a very long and expensive process called molecular docking that typically requires years of research, experimentation, and resources.

A *ligand* or drug-like molecule is a small molecular structure that usually consists of at most 50 atoms as shown in Figure 3.1(a) and Figure 3.1(b). A ligand molecule has a tendency to bind to large molecules called *receptors* that can lead to the identification of new pharmaceutical drugs and the creation of new molecular structures with specific capabilities for diagnosis and treatment of diseases.

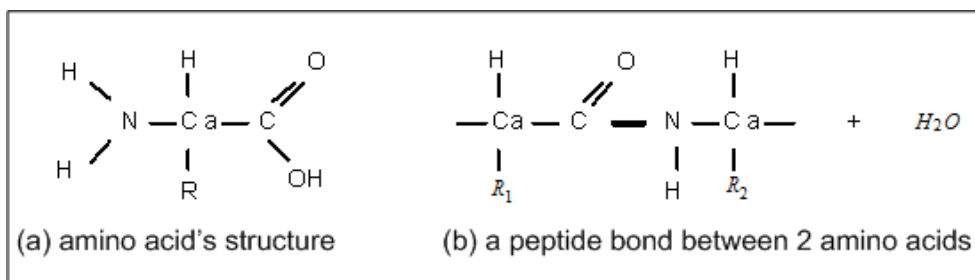


Figure 3.2: Graphical representation of amino acids' topology and link procedure through a covalent bond.



Figure 3.3: Pattern of a protein's backbone chain.

As shown in Figure 3.1(c), a protein or a receptor molecule is a much larger molecular structure that consists of hundreds or even thousands of atoms. Proteins are chains of smaller molecular entities called *amino acids*. The amino acids consist of a central carbon atom, denoted as  $C_a$ , connected to an amino group  $NH_2$ , a carboxyl



group  $COOH$ , a single hydrogen atom  $H$ , and a side chain  $R$ , specific for each amino acid, as shown in Figure 3.2(a). There are 20 basic amino acids that serve as building blocks of proteins. Amino acids differ from each other by their side chains, which also determine their chemical characteristics. The amino acids may be linked to each other by the peptide bond (a covalent bond) between an amino group of one amino acid and a carboxyl group of another amino acid releasing a water molecule, as shown in Figure 3.2(b). These peptide bonds lead to a linear sequence of amino acids forming a polypeptide chain. The backbone of the chain is formed by a peptide sequential pattern schematically shown in Figure 3.3. Therefore, any protein can be considered as a polypeptide chain characterized by the amino acid sequence along the chain in order.

### 3.2 Molecular Energy

Molecules are very flexible in nature and can attain different conformations. A feasible molecular conformation indicates a stable molecular state that is usually described by the minimum intra-molecular energy. This energy is a function composed of different energy factors that depict the interactions between bonded and non-bonded atoms. The major energy contributors are the non-bonded van der Waals (VDW) potential and electrostatic forces. A mathematical representation of the non-bonded molecular energy  $E_{nb}$  is given by Eqn. 3.1:

$$E_{nb} = \sum_{i=1}^n \sum_{j=1}^n \frac{B_{ij}}{r_{ij}^{12}} - \frac{A_{ij}}{r_{ij}^6} + \sum_{i=1}^n \sum_{j=1}^n k \frac{q_i q_j}{r_{ij}} \quad (3.1)$$

The first term in Eqn. 3.1 represents the VDW interaction that models the pair-wise potential over all pairs of non-bonded atoms  $i, j$ .  $B_{ij}$  and  $A_{ij}$  are the VDW repulsion and attraction parameters, respectively; and  $r_{ij}$  is the distance between every exclusive non-bonded atom pair  $i$  and  $j$ . The second term in Eqn. 3.1 represents the electrostatic forces between any non-bonded atom-pair. The electrostatic contribution is modeled

through a Coulomb potential where  $q_i, q_j$  represent the atomic charges,  $r_{ij}$  the inter-atomic distance, and  $k$  describes a molecular dielectric constant.

As the number of atoms within a molecular structure increases, the time to calculate the intra-molecular energy for determining a molecule's feasibility (stability) increases significantly. This makes the energy calculation method unsuitable for real-time molecular design and assembly. For this reason, alternative approaches for identifying feasible molecular conformations are needed. Recently, computational geometry has been successfully used in molecular design since important constraints influencing molecular behavior can have geometrical interpretation. The representation of intra-molecular interactions through a computational geometric approach can allow the approximation of molecules' behavior rapidly and efficiently. Hence, this research work focuses on developing a new computational geometry approach to effectively identify feasible molecular conformations for molecular design and assembly.

### 3.3 A Geometric Molecular Methodology from Molecular Mechanics

The molecular mechanics or force-field method uses Newtonian procedure to describe a molecular structure and its properties energetically as a function of its conformation. The internal forces experienced in the model structure are described using simple mathematics functions. For example, Hooke's law is commonly used to describe bonded interactions, whereas the unbounded atoms might be treated as inelastic hard spheres that interact according to the Lennard-Jones potential. Based on these mathematical models, molecular dynamics simulations numerically solve Newton's equation of motion to observe the structural motions with respect of time. These simulations consider atoms as spheres and bonds as springs that have the ability to move along different directions. The mathematics of spring deformation is used to measure the ability of the bond to stretch, bend and twist as shown in Figure 3.4.

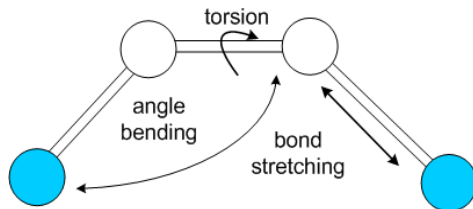


Figure 3.4: Mechanical molecular model.

As shown in Eqn. 3.1, the internal non-bonded energy is calculated based on the VDW potential and the electrostatic forces for every non-bonded atom pair within the molecular structure. Both VDW and electrostatic forces are usually computed for atoms connected by no less than two atoms (non-bonded atoms in a 1, 4 relationship or further apart). In the mechanical model, non-bonded atoms are those atoms linked by three or more chemical bonds as indicated by the blue-colored spheres in Figure 3.4.

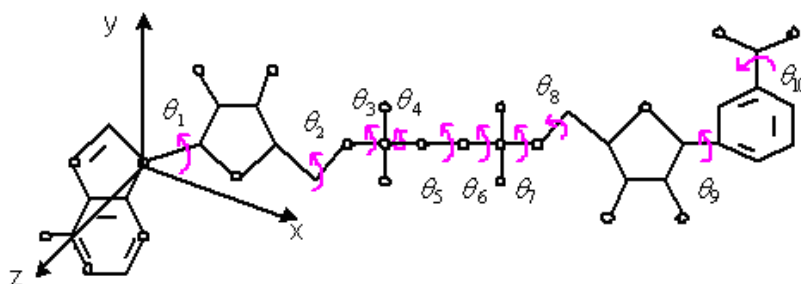


Figure 3.5: Example of a drug-like molecule as an articulated body.

From a geometric point of view, a molecule can be modeled as an articulated body with at least six degrees of freedom (dof): three translational and three rotational. In addition, each chemical bond  $b_i$  within a molecular structure carries information related to the van der Waals radius  $r_i$ . This information is linked to the bond length; the bond angle (the angle between bond  $b_i$  and  $b_{i-1}$ ) and the set of torsion angles  $\theta_i \in [0, 2\pi)$ . A torsion bond is the bond's capability to rotate along its own axis. In most molecular studies, the bond length and angles are kept fixed since they do not contribute

significantly to the molecular shape. Therefore, a molecular *conformation* is defined in this work as the changes in the angles of the torsion bonds  $\theta_i$  as shown in Figure 3.5.

From molecular mechanics, the VDW repulsion force between two non-bonded atoms increases exponentially as the distance between the atoms decreases. The VDW attraction occurs at short range until the non-bonded atoms' relative distance  $d$  is equal to their equilibrium distance  $d_0 = r_i + r_j$  and fades away as the interacting atoms move apart. A geometric interpretation of the VDW atomic interactions is given by Eqn. 3.2 under which an overlapping atom-pair exists:

$$\begin{aligned} d_{atoms_{i,j}} &< \rho (r_i + r_j) \\ 0 &< \rho \leq 1 \end{aligned} \quad (3.2)$$

Where  $d_{atoms_{i,j}}$  represents the distance between the non-bonded atoms  $i$  and  $j$ ;  $r_i, r_j$  are the VDW radii for the non-bonded atoms  $i$  and  $j$ , respectively; and  $\rho$  is a constant parameter that controls the impact of the VDW equilibrium distance on each non-bonded atomic interaction. The electrostatic potential provides a smooth transition between the attraction and repulsion regimes. The overall impact of the non-bonded atomic interactions can be geometrically interpreted by Eqn. 3.3:

$$\begin{aligned} d_{atoms_{i,j}} &< \rho (r_i + r_j) + r_{ij} \\ 0 &< \rho \leq 1 \end{aligned} \quad (3.3)$$

A stable molecular state can be represented by a feasible molecular conformation with low internal energy  $E$ . In a force field, the VDW forces are the dominant energy contributors while the electrostatic interactions dominate the computational time [Sherrill]. Thus, identifying a molecular conformation with  $E$  lower or equal than the VDW interactions guarantees that  $E$  will be less than or equal to the total non-bonded energy  $E_{nb}$  :

$$\begin{aligned}
E_{nb} &= \sum_{i=1}^n \sum_{j=1}^n \frac{B_{ij}}{r_{ij}^{12}} - \frac{A_{ij}}{r_{ij}^6} + \sum_{i=1}^n \sum_{j=1}^n k \frac{q_i q_j}{r_{ij}} \\
\text{given } \frac{B_{ij}}{r_{ij}^{12}} - \frac{A_{ij}}{r_{ij}^6} &\leq k \frac{q_i q_j}{r_{ij}} \text{ then} \\
\text{finding } E &\leq \sum_{i=1}^n \sum_{j=1}^n \frac{B_{ij}}{r_{ij}^{12}} - \frac{A_{ij}}{r_{ij}^6} \text{ guarantees that} \\
E &\leq E_{nb} \Leftrightarrow \text{stable molecular conformation}
\end{aligned} \tag{3.4}$$

Similarly, as shown in Eqn. 3.3, a molecular conformation is considered infeasible when overlapping atoms exist within the molecular structure. Finding a pairwise atomic distance  $d$  that satisfies Eqn. 3.2 ensures that a self-collision occurs as it is demonstrated below:

$$\begin{aligned}
d_{atoms_{i,j}} &< \rho (r_i + r_j) + r_{ij} \\
\text{where } 0 &< \rho \leq 1 \\
\text{given } \rho (r_i + r_j) &\leq r_{ij} \text{ then finding } d \leq \rho (r_i + r_j) \\
\text{guarantees that } d &\leq d_{atoms_{i,j}} \Leftrightarrow \text{self collision occurs}
\end{aligned} \tag{3.5}$$

Given that the VDW potential dominates the molecular interactions chemically and geometrically as demonstrated in Eqn. 3.6 and Eqn. 3.2, respectively, the intramolecular energy can be approximated by the VDW interactions only as follows:

$$E_{nb} \approx \sum_{i=1}^n \sum_{j=1}^n \frac{B_{ij}}{r_{ij}^{12}} - \frac{A_{ij}}{r_{ij}^6} \tag{3.6}$$

Given that the number of possible molecular conformations grows in proportion to the power of the number of torsion bonds, identifying feasible molecular conformations remains the main challenge in molecular design. This research work presents a biologically-inspired geometric method that incorporates the above assumptions on atoms' connectivity and chemical factors to rapidly identify chemically-feasible molecular conformations. Our approach aims to geometrically approximate the behavior of molecules of any size, shape, and topology efficiently while minimizing molecular conformational search and collision detection queries.

In the following three chapters, the development of three computational geometric molecular models for identifying molecules feasibility is discussed as shown in Figure 3.6. In Chapter 4, a biologically-inspired geometric method called BioGeoFilter (BGF) methodology is presented for modeling the behavior of drug-like molecules in real-time. The enhanced BioGeoFilter algorithm (eBGF) is presented in Chapter 5 to model the behavior of macromolecular structures such as protein molecules. Chapter 6 presents a generic computational geometric molecular approach (generic eBGF) for modeling the behavior of molecular structures of any size, shape and topology for real-time molecular design and assembly.

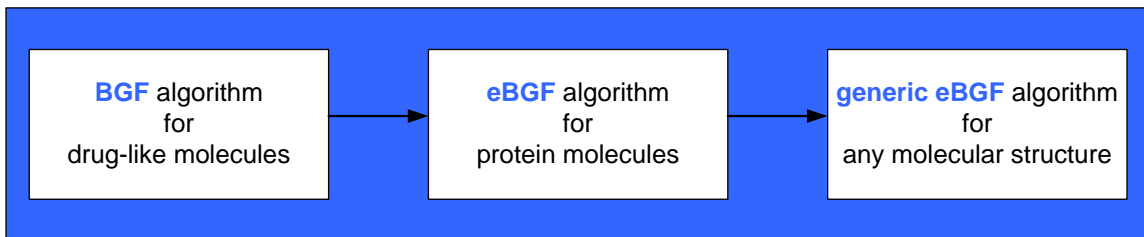


Figure 3.6: Three geometric molecular models developed in this research work.

## Chapter 4

### BioGeoFilter (BGF) Methodology

In this chapter, a new methodology called BioGeoFilter (BGF) is introduced to approximate drug-like molecules' behavior in real-time subject to both chemical and geometric constraints. The BGF approach consists of a two-layer hierarchical data structure that simplifies the molecular representation to effectively identify molecular self-collisions. Experimental results show that the BGF approach significantly decreases the computational time for identifying feasible conformations. This can facilitate the real-time modeling of molecular components to enable interactive molecular design and assembly.

#### 4.1 Overview of the Proposed BGF Model

The proposed BGF model consists of a hierarchical structure that comprises two layers: a lower level and an upper level as shown in Figure 4.1. At the lower level, the molecule is modeled as an articulated body with the internal degrees of freedom representing the number of torsion bond angles. At the upper level, a bounding volume hierarchy (BVH) is introduced to identify atoms within the molecule that are in collision. A new updating scheme for the BVH is presented to identify self-collisions during the update phase of the algorithm. This significantly speeds the computational time so the proposed BGF methodology can be used for both real-time molecular modeling and for reducing the energy minimization time. The following sections describe the two levels of the proposed BGF algorithm.

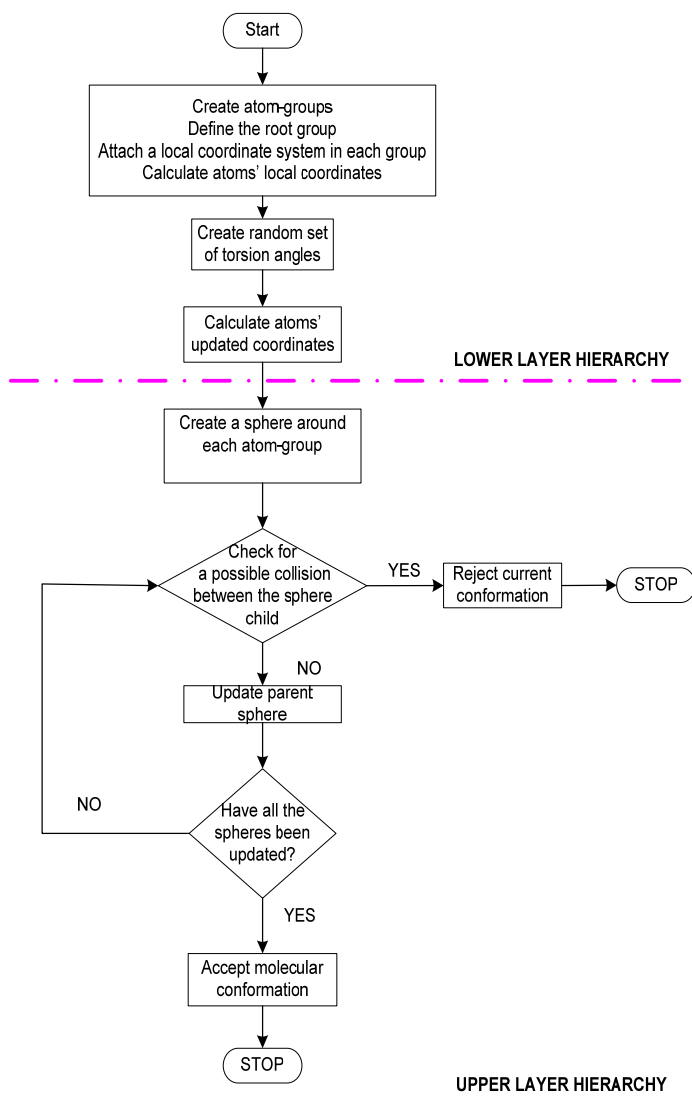


Figure 4.1: Overall structure of the proposed BioGeoFilter methodology.

## 4.2 BGF: Lower Level Hierarchy

As shown in Figure 4.2, a drug-like or ligand molecule is modeled as an articulated body, where an arbitrarily-selected atom acts as the base of the body. A flexible molecule has at least six degrees of freedom (dof): three translational and three rotational. In addition, each torsion bond angle  $\theta_i \in [0, 2\pi)$  accounts for an additional



dof. Hence, a molecular conformation is defined as the changes in the angles of the torsion bonds.

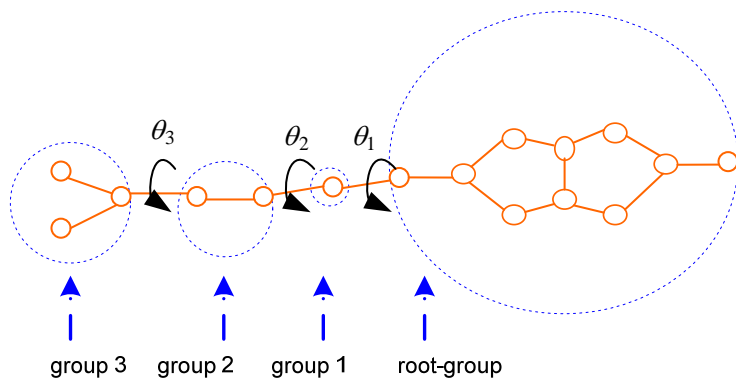


Figure 4.2: 1STP ligand molecule divided into AtomGroups based on the location of the torsion bonds.

To reduce the computational complexity of a molecular structure, atoms of a molecule are clustered into AtomGroups based on the approach by [Zhang and Kaviraki 2004]. Based on the location of the torsion bonds, atoms are clustered into AtomGroups. In other words, all the atoms within an AtomGroup are connected by rigid bonds while AtomGroups are connected by torsion bonds, as shown in Figure 4.2. Therefore, the number of the AtomGroups required to represent molecules' flexibility is equal to the number of the torsion angles plus one.

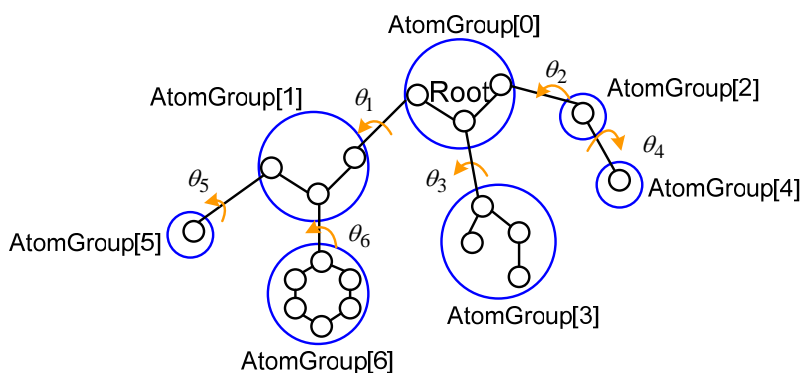


Figure 4.3: AtomGroups for a hypothetical small molecule.

Once the AtomGroups are defined, one group is chosen as the *root* Atomgroup. The *root* Atomgroup is important since it represents the base of the molecular structure where the molecular motions will be projected. The lower hierarchical layer of the proposed BGF is a tree where each vertex represents an AtomGroup and each edge denotes a torsion bond as shown in Figure 4.3.

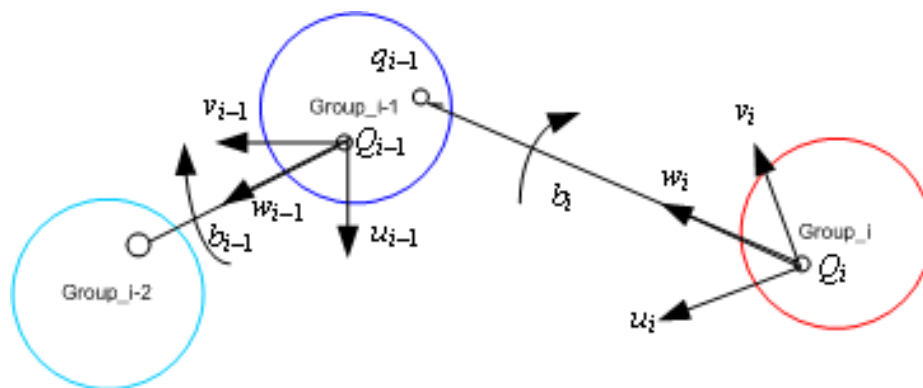


Figure 4.4: Local Cartesian coordinate frame assigned to  $Group_i$  and  $Group_{i-1}$ .

To speed the update of molecular conformations, each AtomGroup $_i$  is assigned a local Cartesian coordinate frame  $F_i$  and a relationship is generated between all the AtomGroups. Since each AtomGroup contains atoms whose distance will not change when torsion changes occur, the distance between atoms in the same AtomGroup do not need to be checked for collision. Only non-bonded atoms that correspond to different AtomGroups will be checked thus reducing the time to identify geometrically feasible conformations. This significantly reduces the computational time and decreases calculation inaccuracies when updating atom positions during conformational changes. The clustering of atoms in groups will be used to form the upper level hierarchy of the proposed BioGeoFilter approach as described in following section.

### 4.3 BGF: Upper Level Hierarchy

#### 4.3.1 Constructing the Hierarchy

Once the different AtomGroups of the molecule have been built at the lower level hierarchy, the smallest enclosing sphere that contains all the atoms within each AtomGroup is calculated as shown in Figure 4.5. The spheres (each containing an AtomGroup) are organized into a binary tree-like data structure that will serve to detect molecular self-collisions subject to both chemical and geometric constraints during conformational search.

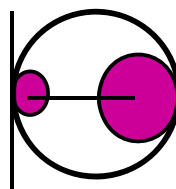


Figure 4.5: Schematic representation of the smallest enclosing sphere of spheres.

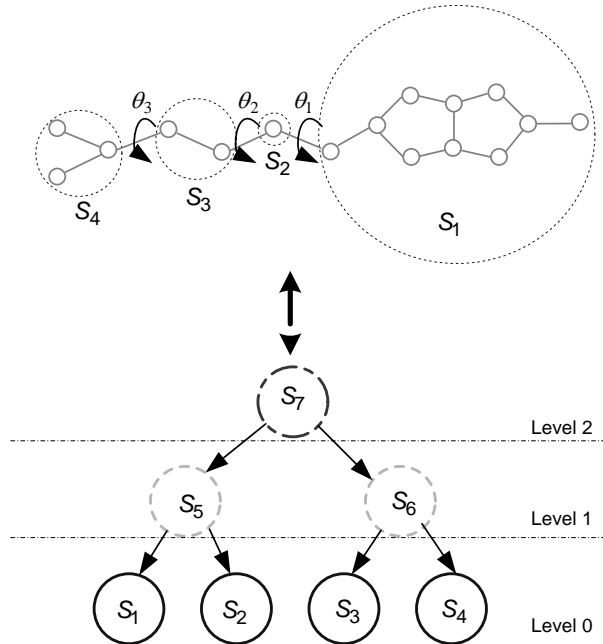


Figure 4.6: Proposed hierarchical structure for 1STP ligand molecule.

Figure 4.6 shows the proposed bounding volume hierarchy for the molecule previously shown in Figure 4.2. At the bottom of the tree there are four spheres (called leaf nodes) representing the four AtomGroups for the 1STP ligand molecule. For each pair of nodes, an intermediate node is created that encloses the two nodes. This process continues in a bottom-up manner until all the spheres result into one single root sphere as shown by the number *S7* in Figure 4.6.

#### 4.3.2 Molecular Geometric Constraints

The VDW interactions are converted into geometric constraints to decrease the time to identify infeasible molecular conformations. As discussed in Sections 3.2 and 3.3, the VDW repulsion between two non-bonded atoms increases exponentially as the distance between the atoms decreases. The VDW attraction occurs at short range until the non-bonded atoms' relative distance  $d$  is equal to their equilibrium distance  $d_0$ :

$d = d_0$ . Hence, based on these interactions, we introduce the first geometric constraint that no neighboring atoms or atoms within neighboring AtomGroups should be checked for self-collision.

The distance between non-bonded atoms within a molecule can often become very short leading to large values in the non-bonded energy and forces. For this reason, the VDW interaction for non-bonded atoms is modeled as a pair-wise potential over all pairs of atoms except 1-2 and 1-3 bonded atoms pairs based on the concept of [Dendzik 2005]. Thus, the second geometric constraint consists of considering as non-bonded atoms the atoms linked by four or more chemical bonds. Moreover, the detection of an actual self-collision between a non-bonded atom pair along with the algorithm's selectivity mechanism depends on the constant  $\rho$  of the equilibrium distance  $d_0$  where  $d_0 = (r_i + r_j)$ . Therefore, the third geometric constraint is the constraint given by Eqn. 3.2 that detects atoms self-collisions. If Eqn. 3.2 is satisfied, then an actual self collision occurs between the non-bonded atoms  $i$  and  $j$ .

By decreasing the  $\rho$  value, the output set of feasible solutions obtained by the BGF algorithm increases as it is further analyzed in Section 4.4. Therefore, based on the above geometric constraints, the BGF methodology rejects any molecular conformation that does not satisfy the geometric filtering as described in the following section.

#### 4.3.3 Updating the Hierarchy and Self-Collision Detection

As new conformations are being searched through changes in the torsion bonds, the new position of the atoms needs to be calculated. The new atom positions affect the location and radius of the spheres in the hierarchy so they need to be updated accordingly. In this work, the spheres in the hierarchy are updated in a bottom-up manner and one level at a time. Therefore, the tree nodes are updated from the leaf nodes to their parents and this process continues until the root node is reached and updated.

During the update phase, a new updating algorithm is introduced so that if a self-collision is detected, the algorithm will immediately stop and reject the conformation due to overlapping atoms (self-collision) as shown in Figure 4.1. The algorithm first updates the leaf nodes (e.g.,  $S1$ ,  $S2$ ,  $S3$ , and  $S4$  in Figure 4.6). One level at a time, the algorithm updates the spheres' radius and centers based on the new atom locations. Then, the parent nodes of the leaf nodes are tested for update. If there is a collision between the children nodes, the algorithm returns that the conformation is infeasible and stops. If no collision is detected, the process continues until the root node is reached and updated.

#### 4.4 Computer Implementation and Results

The presented method and algorithms have been implemented on Intel Pentium 4 with 2.7 GHz personal computers using Visual C++ programming language, the OpenGL and CGAL libraries [CGAL]. Four different molecules with different number of atoms and number of degrees of freedom were tested using the proposed BioGeoFilter methodology. The molecules were obtained from the Protein Data Bank (PDB) [Berman

2000] with PDB IDs as follows: 1HVR, 1HTB, 1A5Z, and 1JBO. Their corresponding number of atoms and degrees of freedom are indicated in Table 4.1 presented below.

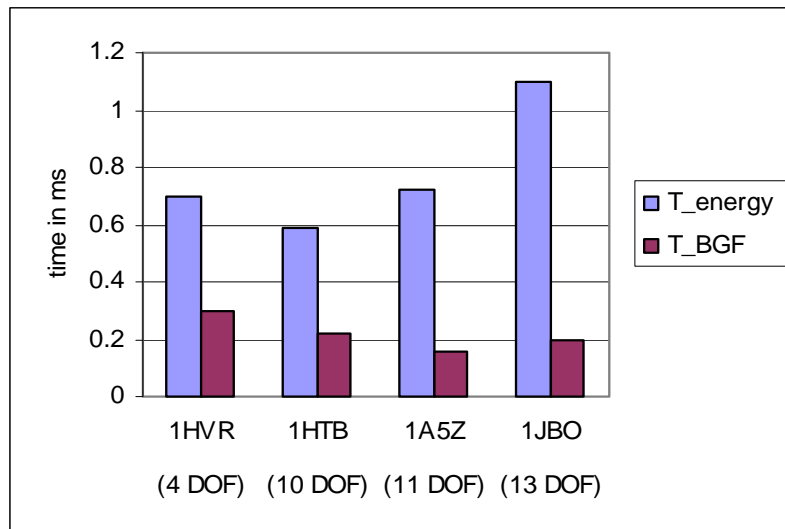


Figure 4.7: Computational time comparison for four different ligand molecules.

Figure 4.7 compares the performance of the proposed BGF algorithm and the energy calculation for the four different molecules with different pre-selected dof. For each example molecule, random conformations were generated and tested for feasibility using both methods. As shown in Figure 4.7, the proposed BGF methodology greatly reduces the computational time needed to identify feasible molecular conformations compared to the energy calculation approach. This reduction in time is significant as multiple flexible molecules will need to be modeled in real-time at the same time for nanoscale assembly. It can also be observed that as the dof increases, the time reduction percentage also increases. The computational times for all the tested molecules satisfy the real-time haptic constraint and scale well as the number of degrees of freedom increases.

Various feasible conformations obtained from the BGF approach are shown in Figure 4.8(c) for the example molecule 1A5Z. These conformations satisfy the geometric constraints of the BGF methodology and have been validated using the energy values obtained from the energy calculation method.

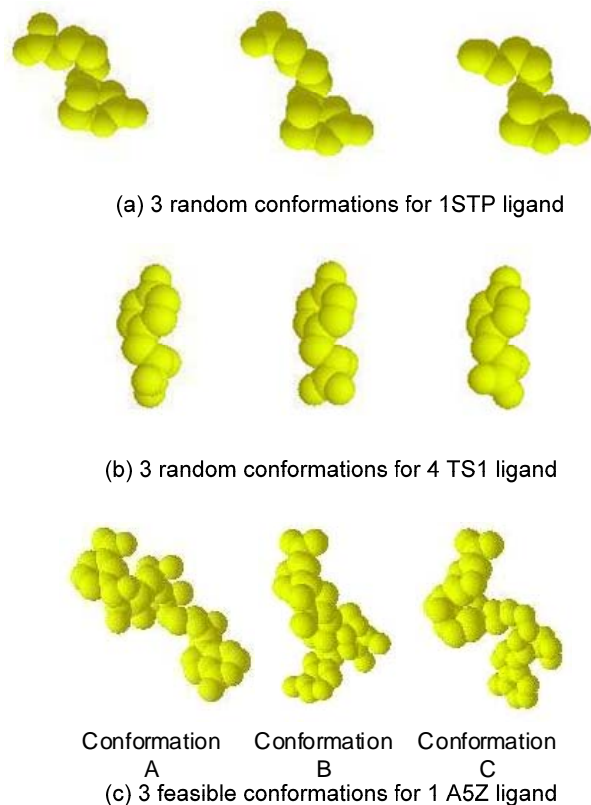


Figure 4.8: Examples of random conformations for three ligand molecules.

Table 4.1 shows the results in terms of computational time (milliseconds) and accuracy (number of feasible conformations identified) between the energy calculation approach ( $T_{en}$ , and  $F_{en}$ . columns) and BGF approach ( $T_{BGF}$ , and  $F_{BGF}$  columns). In the proposed methodology, the same molecular conformation is used for comparing the two methods. As shown in the percentage time reduction ( $T_{red}$ ) in Table 4.1, the proposed algorithm can identify feasible conformations at least twice faster than the energy calculation method and with similar accuracy. It can also be observed that as the dof increases, the time reduction percentage obtained from the BGF methodology also increases.

Table 4.1: Statistical data for four different ligand molecules.

| Ligand | # of atoms | DOF | $\rho$ | T_en. | T_BGF | F_en   | F_BGF  | T_red. |
|--------|------------|-----|--------|-------|-------|--------|--------|--------|
| 1A5Z   | 44         | 11  | 0.8    | 0.6   | 0.1   | 13/100 | 0/100  | 83%    |
|        |            |     | 0.7    | 0.5   | 0.2   | 14/100 | 6/100  | 60%    |
|        |            |     | 0.6    | 0.72  | 0.158 | 17/100 | 14/100 | 78%    |
| 1HTB   | 44         | 10  | 0.8    | 0.586 | 0.218 | 18/100 | 18/100 | 63%    |
|        |            |     | 0.7    | 0.6   | 0.3   | 43/100 | 39/100 | 50%    |
| 1HVR   | 46         | 4   | 1      | 0.7   | 0.3   | 0/100  | 2/100  | 57%    |
| 1JBO   | 43         | 13  | 0.8    | 0.7   | 0.4   | 69/100 | 43/100 | 43%    |
|        |            |     | 0.7    | 1.1   | 0.2   | 77/100 | 67/100 | 82%    |
|        |            |     | 0.6    | 0.6   | 0.1   | 85/100 | 78/100 | 83%    |

Table 4.1 also shows the sensitivity analysis performed to study the impact of the different values for  $\rho$  of the equilibrium distance on the results. The entire range of  $\rho$  values, where  $0 < \rho < 1$ , was tested for each molecule but only the most significant  $\rho$  values are shown in the table for explanation purposes. As shown in Table 4.1, it was found that by varying  $\rho$  and depending on the size of the molecule, the selectivity of the BGF methodology can be adjusted. As  $\rho$  decreases, BGF accepts more molecular conformations as feasible, which leads to a relaxed filtering. The main objective of the BGF methodology is to identify infeasible conformations while not rejecting any feasible conformations. Hence, the selection of an appropriate  $\rho$  value for each molecule depends on the molecule and the desired level of selectivity. In Table 4.1, the grey colored rows denote the best  $\rho$  values for each molecule in terms of selectivity and accuracy. An analysis on the relationship between the  $\rho$  value and the molecule's size is addressed in Chapter 5.

The sensitivity analysis was performed by relaxing the third geometric constraint ( $\rho$  value) only. The relaxation of the other geometric constraints was shown to increase the acceptance of unfeasible molecular conformations and computational time. For this reason, the sensitivity analysis only focused on relaxing the third constraint while keeping other constraints fixed.



## 4.5 Conclusions

This chapter presents a new method called BioGeoFilter (BGF) for modeling and approximating the molecular behavior subject to geometric constraints in real-time. BGF consists of a novel two-layer hierarchical structure that identifies self-collisions during the hierarchy's updating phase. The proposed methodology is presented as a filtering tool based on chemical and geometric concepts for effectively identifying feasible molecular conformations. Computer implementation and results demonstrate that the proposed BGF approach significantly decreases the computational time for identifying feasible ligand conformations to satisfy real-time update requirements. The proposed BGF methodology can facilitate the real-time modeling and visualization of molecular components and enable the development of an essential interactive nanoscale computer-aided design tool for bionanotechnology. The following chapter presents the extended BGF algorithm for macromolecular structures.

## Chapter 5

### Enhanced BioGeoFilter (eBGF) Molecular Model

This chapter analyzes the structure of much larger molecules such as proteins to model them more effectively using an enhanced BGF (eBGF) model. The proposed eBGF approach addresses current limitations in protein modeling through a biologically-inspired geometric filter for speeding self-collision detection queries. The presented eBGF methodology can facilitate the modeling of flexible macromolecules for applications such as molecular docking, nanoscale assembly, and protein folding.

#### 5.1 Differences Between eBGF and BGF Models

The proposed enhanced BioGeoFilter (eBGF) algorithm is similar to the BGF approach presented in Chapter 4 in that they both build a hierarchical data structure that consists of two layers: a lower level and an upper level. Both algorithms geometrically interpret the inter-atomic interactions to impose the geometric constraints that define a feasible molecular conformation. However, given that a protein molecule can consist of hundreds or thousands of atoms with hundreds or even thousands degrees of freedom, the modeling of proteins requires: 1. a further AtomGroup subdivision of the protein's backbone structure, 2. an independent updating of the BVH and collision detection functions, and 3. an additional geometric constraint for the collision detection queries. To effectively model protein molecules, the eBGF algorithm incorporates new algorithmic concepts. The core differences between the eBGF and BGF models are:

1. Given the particular structure of proteins, a new algorithm to divide the protein backbone into smaller groups is incorporated into the eBGF model to handle protein updating and collision detection more effectively.

2. The eBGF algorithm updates the BVH independently from the collision detection query compared to the combined updating and collision detection approach in the BGF model. This resulted in a significantly faster model that is more suitable for large molecules such as proteins.
3. To compensate with the not so tight fitting that results from the selection of spheres as bounding volumes, the eBGF algorithm incorporates an additional geometric constraint for the collision detection query.

## 5.2 Proposed eBGF Overview

Figure 5.1 shows the overview of the enhanced BioGeoFilter methodology that consists of two layers: the lower and upper hierarchical layers as indicated by the white colored boxes. At the lower layer of the hierarchy, the eBGF algorithm starts with any molecular conformation. The dof of the molecular structure are defined to form atom groups following the concept presented in Chapter 4. A further simplification in molecular representation is proposed by splitting the backbone atom cluster into smaller groups of atoms as it is discussed in Section 5.3. At the upper layer of the proposed approach, we build a BVH for the initial molecular conformation as it is described in Section 5.4. New random molecular conformations are obtained by arbitrary changing the values for each degree of freedom. For each candidate molecular conformation, the BVH is updated to incorporate the corresponding changes in the dof as it is presented in Section 5.4.3. A collision detection scheme is then performed to identify the feasibility of each random molecular conformation as it is described in Section 5.4.4. At the end of the eBGF algorithm, the intramolecular energy value for each random conformation is calculated for evaluating the proposed approach as it is discussed in Section 5.5. The following sections describe in details each hierarchical layer of the proposed eBGF methodology.

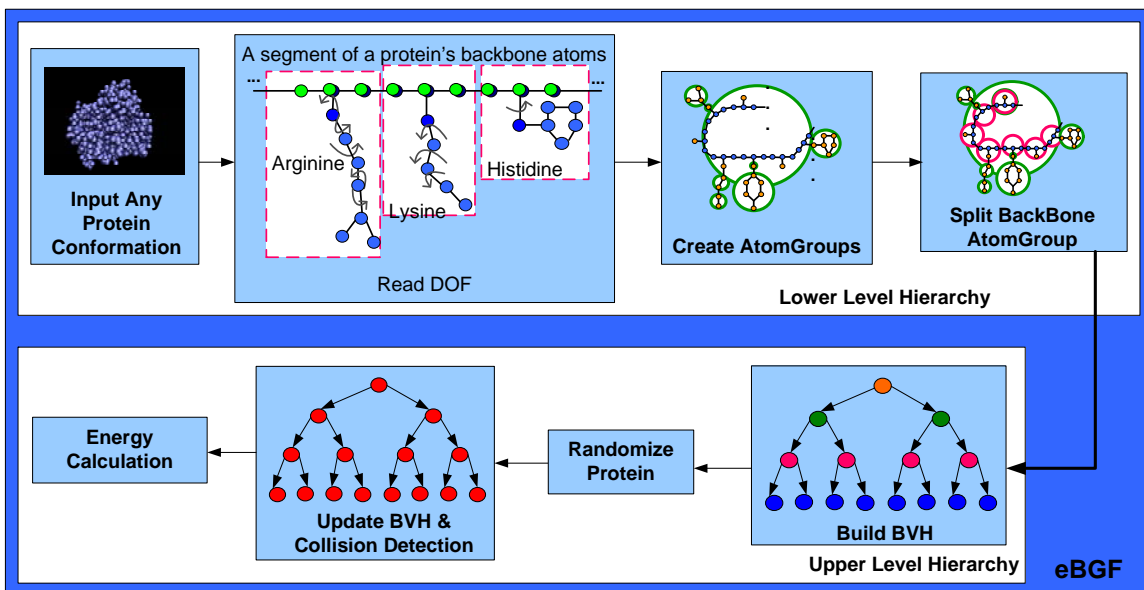


Figure 5.1: Overview of the proposed eBGF approach.

### 5.3 eBGF: Lower Layer Hierarchy

Torsion changes can occur anywhere within a protein's topology. However, considering random torsions within a protein's backbone can break its structure making it extremely difficult to evaluate whether the generated molecular conformation is chemically feasible. Therefore, in this paper, torsions are assumed only between the central carbon atom of a protein's backbone (CA) and a side chain atom (CB) or within the side chain atoms as shown in Figure 5.2. Furthermore, given the increasing complexity by a protein's size, torsions at the end of each side chain are neglected (i.e. the bond between CD and OE1 atoms in Figure 5.2(a) since they do not contribute significantly to the molecular conformation.

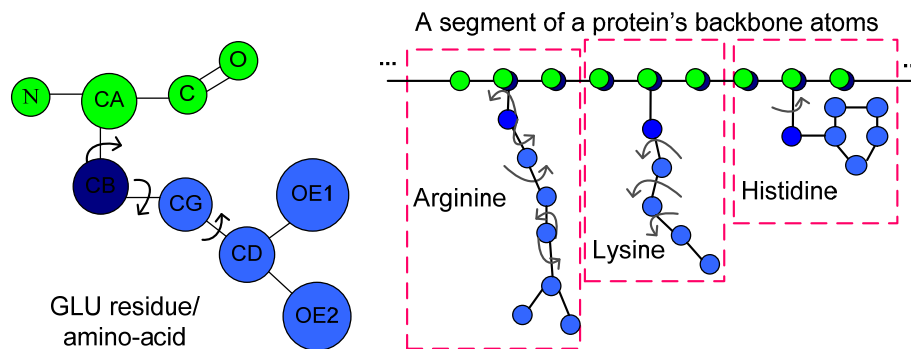


Figure 5.2: Graphical representation of the degrees of freedom of a protein.

Once the torsion bonds of a protein are identified, the atoms are clustered into AtomGroups based on the approach proposed by [Zhang and Kavraki 2004] and analytically shown in Chapter 4. However, the application of the AtomGroup concept in a protein molecule results in the generation of two different sized atom clusters: clusters of side chain atoms and a cluster of backbone atoms as shown in Figure 5.3(a). The cluster of backbone atoms contains hundreds of atoms whereas the clusters of side chain atoms contain tens of atoms. This large size difference in the atom clusters increases the time needed to determine if an actual molecular self-collision occurs.

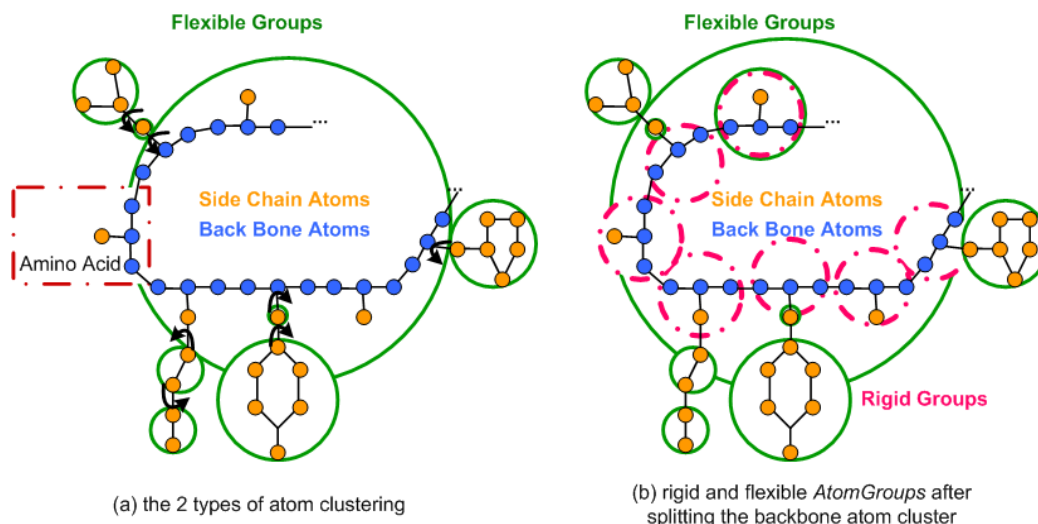


Figure 5.3: Graphical representation of the AtomGroup concept along with the proposed splitting procedure for a hypothetical protein segment.

To address this challenge, this research work proposes to split the backbone atom cluster into smaller AtomGroups based on a threshold defined by the maximum number of atoms allowed within each atom cluster. By splitting the backbone cluster, a flexible AtomGroup (i.e. the green and pink sphere in Figure 5.3(b) is obtained along with a number of rigid AtomGroups (i.e. the six pink/dashed-line spheres shown in Figure 5.3(b)). This splitting procedure further simplifies the molecular representation by reducing the collision queries while eliminating the collision searches between the rigid groups. Hence, the collision detection is now performed between similar sized flexible groups of atoms significantly reducing the computational time for identifying a molecule's feasibility.

The splitting of the backbone cluster into smaller groups of atoms significantly reduces the computational time for updating the atoms' positions by eliminating the calculation of the relation matrices for the rigid groups of atoms. As shown in Figure 5.3(b), the relation matrix for the big green sphere (initial flexible AtomGroup) is the same as the relation matrix of the green and pink sphere (modified flexible AtomGroup) and as the relation matrices of the pink/dashed-line spheres (rigid AtomGroups). Therefore, instead of calculating relation matrices for all the seven new groups of atoms, we just calculate a single relation matrix for the modified flexible group as depicted by the specific protein segment shown in Figure 5.3. The clustering of atoms into both rigid and flexible groups will be used to form the upper layer of the hierarchy of the proposed eBGF methodology as described in the following section.

#### 5.4 eBGF: Upper Layer Hierarchy

At the upper level of the eBGF method, a bounding volume hierarchy (BVH) depicted as a balanced binary tree similar to the BGF model is introduced to identify atoms' self-collisions. The main difference between the bounding volume hierarchies of the BGF and eBGF models is that the leaves in the BGF model only represent flexible group of atoms whereas the leaves of the eBGF model can represent both flexible and

rigid atom clusters. This impacts both the updating and collision detection time. Furthermore, an additional geometric constraint is proposed to compensate the not so tight fitting that results from the selection of spheres as bounding volumes.

#### 5.4.1 Constructing the BVH

Once the different AtomGroups (both flexible and rigid) have been defined at the lower layer of the hierarchy, the smallest enclosing sphere that contains all the atoms within each AtomGroup is calculated as in [Fischer and Gartner 2003]. The spheres (each containing an AtomGroup) are organized into a binary tree-like data structure that will serve to detect molecular self-collisions subject to both chemical and geometric constraints during conformational search as it will be discussed in Section 5.4.4.

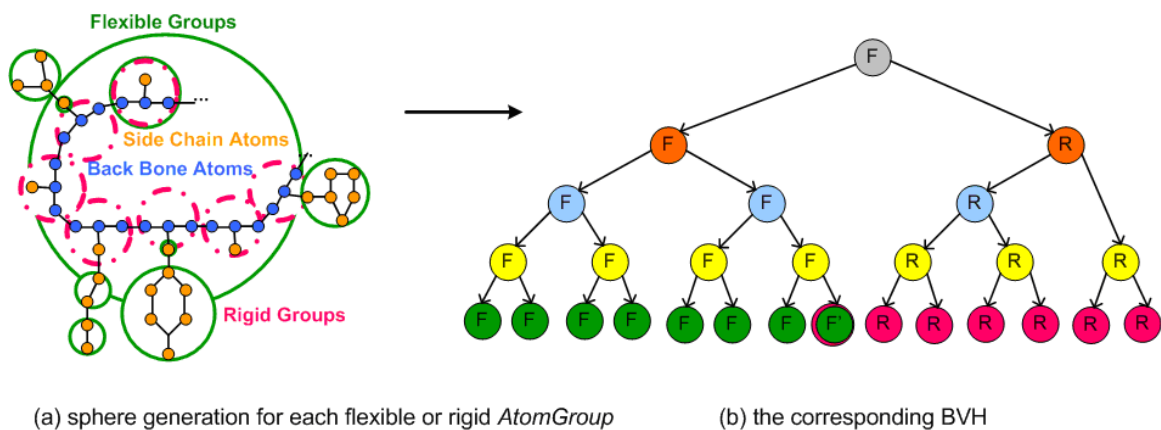


Figure 5.4: Schematic representation of the rigid and flexible AtomGroups within a hypothetical protein segment and the accordance BVH.

Figure 5.4(a) shows a hypothetical protein segment with its corresponding bounding volume hierarchy shown in Figure 5.4(b). At the bottom of the tree are the 14 spheres (called leaf nodes) representing the 14 AtomGroups of the molecule that includes flexible (green colored) and rigid (pink colored or dashed-lines). For each pair of nodes, an intermediate node is created that encloses the two nodes. This process continues in a bottom-up manner until all the spheres result into one single root sphere as shown by the

purple colored sphere in Figure 5.4, which is the sphere that encloses the whole protein segment.

The BVH is built only once at the beginning of the algorithm allowing a total construction time of  $O(N)$  where

$$\begin{aligned}
 N &= \text{DOF} + 1 + \text{rigidGroups} = \text{flexibleGroups} + \text{rigidGroups} \\
 \text{TotalNumberOfNodes} &= \begin{cases} 2N & \text{if } N \text{ odd} \\ 2N - 1 & \text{, o/w} \end{cases} \quad (5.1)
 \end{aligned}$$

#### 5.4.2 Randomization

As soon as the pre-selected dof have been defined for the specific protein molecule, a uniform generator is used to create random values for the torsion angles  $\theta_i$ , where  $\theta_i \in [0, 2\pi)$ . When random torsion changes occur, the new atom positions are updated based on the concept presented in Chapter 4 to obtain a new molecular conformation. For each new random molecular state, the BVH is updated and the new molecular conformation is tested for self-collision.

#### 5.4.3 Updating the Hierarchy

Every time the torsion bonds change, a new molecular conformation is generated. The new atom positions affect the location and radius of the spheres in the hierarchy so they need to be updated accordingly. In this work, the spheres in the BVH are updated in a bottom-up manner and one level at a time. Therefore, the tree nodes are updated from the leaf nodes to their parents until the root node of the tree is reached and updated.

As shown in Figure 5.4(b), the BVH is formed by both flexible (green colored) and rigid (pink colored) spheres. It can be observed that the updating of the spheres around the rigid groups (pink colored spheres and their parents) can be neglected since the atom distances within and between the rigid groups remain unchanged. This occurs when the atom cluster of the molecule's backbone has been defined as the root



AtomGroup or else the base of the molecule's body. Omitting the update of the rigid nodes ( $k$ ) results in a reduction of the computational time for updating the BVH and for identifying molecular feasibility. This contributes to a total updating time of  $O(\frac{N}{k})$  that never exceeds  $O(N)$ .

#### 5.4.4 Self-Collision Detection

The fundamental concept underneath the proposed collision detection algorithm is the geometric interpretation of the chemical information provided by the van der Waals (VDW) interaction as discussed in Chapter 3 and in Section 4.3.3. The main difference lies in that the collision search presented in the eBGF model is handled independently from the BVH update procedure. In other words, the BVH is updated first and then the tree is traversed down (in a top-bottom mode) to check for possible overlapping atoms.

The geometric constraints used in this work to handle the collision detection queries are depicted by Eqn. 5.2. As shown by the first relation in Eqn. 5.2, an additional constraint is considered to search for overlapping spheres.

$$\begin{aligned} d_{spheres_{ij}} &< \rho_1(sphereRadius_i + sphereRadius_j) \\ d_{atoms_{ij}} &< \rho_2(atomRadius_i + atomRadius_j) \\ 0 &< \rho_1, \rho_2 \leq 1 \end{aligned} \quad (5.2)$$

Where,  $d_{sphere_{i,j}}$  denotes the distance between the sphere objects  $i$  and  $j$ ;  $d_{atoms_{i,j}}$  represents the distance between the non-bonded atoms  $i$  and  $j$ ;  $\rho_1$  and  $\rho_2$  are constants that control the proposed algorithm's selectivity mechanism.

The first constraint in Eqn. 5.2 (the additional constraint for the eBGF model) embodies a primary filtering while checking for possible collisions between two spherical objects. If this constraint is satisfied, then a possible collision occurs between the sphere objects  $i$  and  $j$ . The second constraint in Eqn. 5.2 ensures that an actual self-collision occurs by comparing pair-wise atomic distances. The physical interpretation of the  $\rho_1$  parameter is that it controls the not so tight object fitting that result from the selection of

spheres as the type of bounding volumes. The  $\rho_2$  parameter controls the algorithm's selectivity or the number of feasible solutions generated. By decreasing the value of  $\rho_2$  selectivity parameter, the proposed eBGF algorithm accepts more solutions (molecular conformations) as feasible. From a biological point of view,  $\rho_2$  handles the impact that the VDW equilibrium distance has on the results.

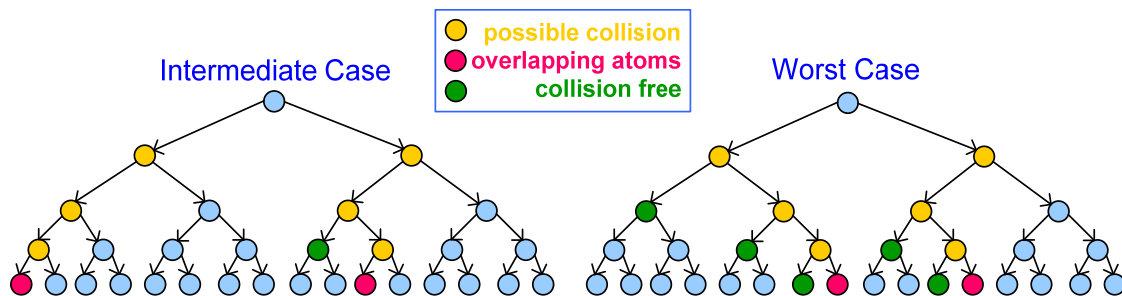


Figure 5.5: Graphical representation of the proposed collision detection algorithm.

Figure 5.5 shows an intermediate and the worst case scenario of the proposed collision detection scheme for a protein segment. During the tree traversal, each non-constraint pair of nodes is checked for a possible collision using the first constraint in Eqn. 5.2, where the actual self-collision detection is performed between non-bonded atom pairs by using the second constraint in Eqn. 5.2. A constrained node pair embodies any of the following properties:

1. For self-collision queries, collision detection between the root of the tree against itself should be omitted.
2. The collision search between rigid AtomGroups should be ignored since the atomic distances within and between these groups remain unchanged.
3. Collision queries between bonded neighboring AtomGroups should also be eliminated since the atomic distances between these two groups do not change significantly.

4. Given that the impact of the VDW interaction increases as the pair-wise atomic distances decreases, the collision detection between any atom pair linked by three or less chemical bonds should be avoided as discussed in Section 3.3. Therefore, non-bonded atoms are the atoms linked by four or more chemical bonds.

Under these assumptions, if the root's child nodes are collision free, then the specific molecular conformation is feasible and is accepted. Otherwise, the tree is traversed down to identify whether any atoms are actually in collision to reject the current molecular conformation. The computation collision detection time has  $O(\log \frac{N}{k})$  performance that never exceeds  $O(\log N)$ , where  $k$  is a constant that represents the number of constraint nodes (i.e. rigid AtomGroups) that are neglected in the proposed collision detection scheme. Finally, each random molecular conformation is tested with both the proposed eBGF approach and the traditional energy calculation method using Eqn. 3.4.

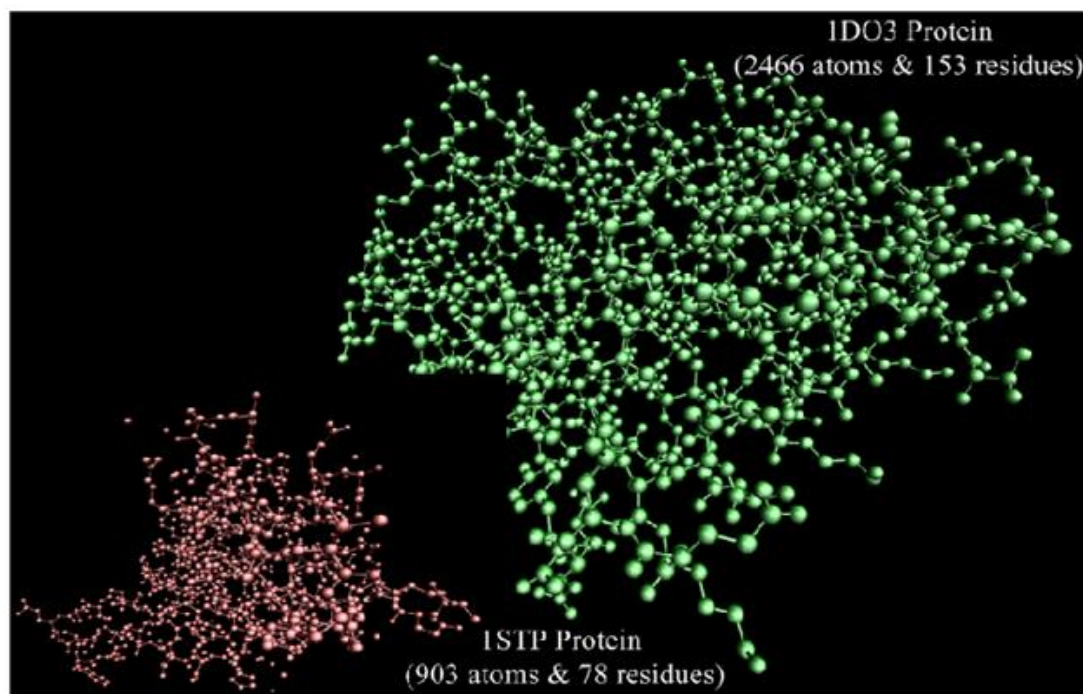


Figure 5.6: Two example macromolecules tested in this work.

## 5.5 Computer Implementation and Results

The presented method and algorithms have been implemented on a dual 3 GHz CPU workstation using Visual C++ programming language, OpenGL and CGAL libraries [CGAL]. Two different protein molecules with different number of atoms, residues, and number of degrees of freedom have been tested using the proposed *eBGF* methodology as shown in Figure 5.6. The molecules were obtained from the Protein Data Bank (PDB) [Berman 2000] with PDB IDs as follows: 1STP and 1DO3 protein molecules. They are displayed using the VMD [Humphrey 1999].

Table 5.1: Performance analysis of the proposed eBGF algorithm for two proteins.

| Molecule | # atoms | Time Energy | Time BVHUpdate | Time Collision | Time Rand | Feasible Energy | TH      | Feasible Collision | p1  | p2  | Free Residues | DOF |
|----------|---------|-------------|----------------|----------------|-----------|-----------------|---------|--------------------|-----|-----|---------------|-----|
| 1STP     | 903     | 212.42      | 2.42           | 0.13           | 0.3       | 100/100         | 10000   | 100/100            | 0.4 | 0.8 | 1             | 3   |
|          |         | 210.95      | 1.78           | 0.02           | 0.28      | 94/100          |         | 98/100             | 0.4 | 0.8 | 5             | 7   |
|          |         | 218.89      | 1.99           | 0.07           | 0.31      | 76/100          |         | 74/100             | 0.4 | 0.8 | 10            | 14  |
|          |         | 230.71      | 2.39           | 0.14           | 0.33      | 0/100           |         | 0/100              | 0.4 | 0.8 | 16            | 25  |
|          |         | 221.74      | 1.99           | 0.079          | 0.31      | 0/100           |         | 0/100              | 0.4 | 0.8 | 16            | 13  |
|          |         | 224.45      | 2.34           | 0.43           | 0.32      | 25/100          |         | 90/100             | 0.5 | 0.7 | 16            | 10  |
|          |         | 212.85      | 2.02           | 0.78           | 0.29      | 25/100          |         | 25/100             | 0.6 | 0.6 | 16            | 10  |
|          |         | 236.78      | 2.5            | 0.02           | 0.38      | 0/100'          |         | 0/100'             | 0.5 | 0.9 | 78            | 90  |
| 1DO3     | 2466    | 1771.99     | 6.12           | 0.044          | 0.89      | 10/100          | 100000' | 10/100             | 0.4 | 0.7 | 1             | 3   |
|          |         | 1649.68     | 5.27           | 0.38           | 0.78      | 40/100          |         | 75/100             | 0.5 | 0.7 | 5             | 9   |
|          |         | 1647.38     | 5.45           | 0.72           | 0.77      | 15/100          |         | 44/100             | 0.5 | 0.6 | 10            | 24  |
|          |         | 1707.17     | 5.1            | 0.24           | 0.83      | 0/100           |         | 0/100              | 0.5 | 0.9 | 35            | 36  |
|          |         | 1728.51     | 6              | 0.19           | 0.85      | 0/100           |         | 0/100              | 0.5 | 0.8 | 35            | 14  |
|          |         | 1695.27     | 5.59           | 0.56           | 0.81      | 28/100          |         | 29/100             | 0.5 | 0.6 | 35            | 22  |
|          |         | 1718.19     | 7.72           | 0.078          | 0.94      | 0/100           |         | 0/100              | 0.6 | 0.6 | 153           | 304 |

Table 5.1 shows a representative list of the performance analysis for the proposed eBGF method applied to the two example macromolecules. The molecules have been tested for feasibility after random torsion changes have occurred. The same conformations for both molecules have been examined with both the energy (*TimeEnergy*, *FeasibleEnergy*, and *TH* columns) and eBGF (*TimeBVHUpdate*, *TimeCollision*, *TimeRand*, *FeasibleCollision* columns) approaches and compared in terms of computational time (in milliseconds) and accuracy (percentage of feasible conformations identified). Furthermore, different case scenarios regarding the number, arrangement and the location of the pre-selected dof have been tested for assessing their

impact on the proposed eBGF methodology (*FreeResidues* and *DOF* columns). Column *FreeResidues* indicates the allowed number of completely flexible residues and column *DOF* represents the total number of dof assumed. For example, in 1DO3 protein section at the bottom of Table 5.1: column-pair 35-36 (*FreeResidues-DOF*) indicates that 35 completely flexible residues have been tested for the 1DO3 protein that results in a total of 36 dof; the pair 35-14 indicates that 14 dof were tested only between backbone and side chain atoms; and the pair 35-22 corresponds to torsions only within the side chains of the 35 flexible residues. Further discussion of the impact in molecular behavior by the pre-selected number of flexible residues and dof is performed below. In addition, different values for the algorithm's selectivity control parameters ( $\rho_1$ , and  $\rho_2$  columns) have been tested and discussed below.

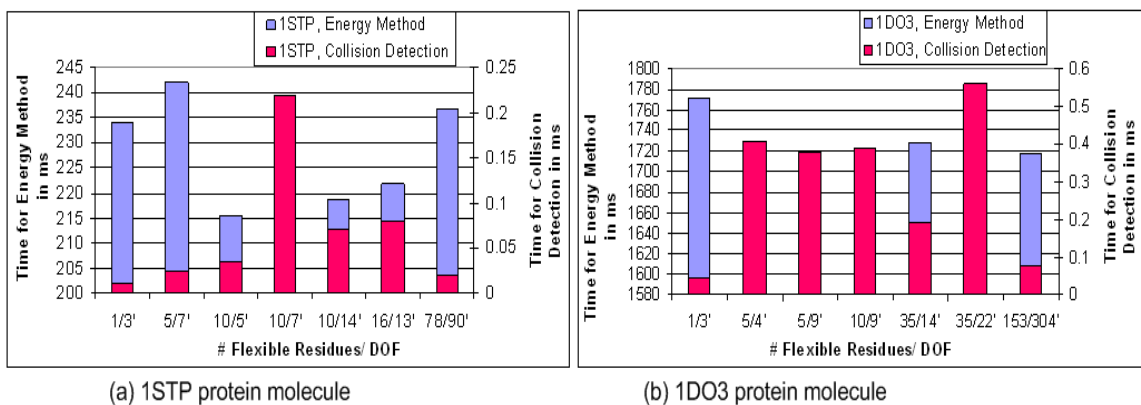


Figure 5.7: Comparison of the average collision time by the proposed eBGF vs. the average energy calculation time for different sets of pre-selected flexible-residues/dof.

Figure 5.7 compares the performance of the eBGF method against the energy calculation approach in terms of computational time needed to identify molecules' feasibility for the two protein (1STP and 1DO3) examples. As shown in Figure 5.7, the eBGF algorithm significantly reduces the computational time needed to identify feasible molecular conformations compared to the energy approach. In fact, the time reduction is so enormous that two different scales were needed to schematically display the two methods in the same graph. The left scale for both figures denotes the time in

milliseconds (ms) required by the energy approach to determine the feasibility of a molecular conformation whereas the right scale denotes the computational time (in ms) for the proposed collision detection algorithm to identify molecular feasibility. For both molecules and in all tested sets of pre-selected flexible-residues/dof, the eBGF requires less than 1ms to output if the tested molecular conformation is feasible. This time reduction is noteworthy as multiple flexible molecules will need to be modeled in real-time simultaneously for the molecular assembly or molecular docking problems.

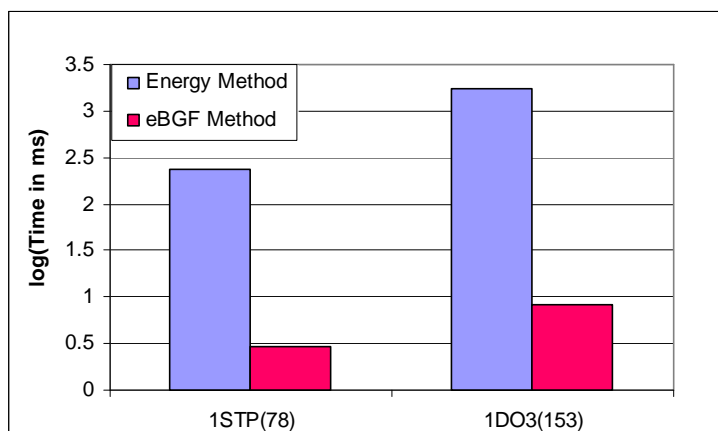


Figure 5.8: Average total time comparison between the proposed eBGF algorithm and the energy calculation approach to output feasibility for 1STP and 1DO3 proteins in a logarithmic scale.

Similarly, Figure 5.8 compares the computational time performance for the two methods (eBGF vs. energy calculation) while considering the scenario that both protein molecules are completely flexible (the total number of residues forming each protein structure assumed to be completely flexible). Analytically, Figure 5.8 displays the total computational time (in ms) for the eBGF method (the collision detection time + BVH update time + update atoms' position time) against the energy approach in a logarithmic scale. As it is shown in Figure 5.8, the proposed eBGF methodology is significantly faster than the energy calculation approach in identifying feasible molecular conformations. In addition, the eBGF algorithm scales very well as the protein size and problem's complexity increases.

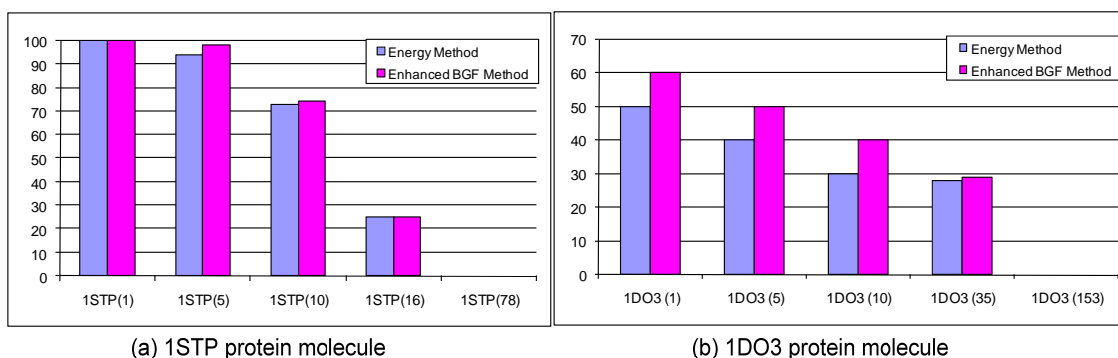


Figure 5.9: Schematic demonstration of the accuracy of the proposed eBGF methodology.

Figure 5.9 measures the accuracy (percentage of feasible conformations identified) of our proposed method under different considerations regarding the allowed number of flexible residues within each protein structure. For both protein examples, the two methods demonstrate similar accuracy. In fact, the selectivity of the eBGF algorithm can be adjusted by varying the control parameters ( $\rho_1$ , and  $\rho_2$ ). In other words, by decreasing the  $\rho$  values, the proposed algorithm can accept more molecular conformations as feasible leading to a relaxed filtering. The physical interpretation of  $\rho_1$  selectivity parameter is that it handles the not so tight object fitting resulted by the selection of spheres as the type of bounding volumes whereas the  $\rho_2$  selectivity parameter controls the impact that the VDW equilibrium distance has on the results as it has been analyzed in Section 5.3.4. The main objective of the eBGF approach is to identify infeasible molecular conformations rapidly while not rejecting any feasible ones. Hence, the selection of appropriate  $\rho$  values for each molecule depends on the molecule's size along with the desired level of selectivity by the user. It is also worth mentioning here that the molecules' feasibility is traditionally measured using the energy calculation shown in Eqn. 3.4. A conformation might be considered as feasible or not depending on the molecular internal energy value. If a candidate conformation has negative internal energy, then it corresponds to a stable molecular state. However, feasible molecular conformations exist while having positive intramolecular energy.

Therefore, a threshold (*TH* column in Table 5.1) has been selected based on the protein's size to define the maximum energy value for which a molecular conformation is considered to be feasible.

Moreover, as it is shown in Table 5.1 and Figure 5.9, there is a significant dependency among the pre-selected number of flexible residues and dof considered in each protein molecule and the output (percentage of feasible molecular conformations) derived by both (eBGF and energy) methods. Computer implementation and results demonstrate that as the number of dof considered increases, the output set of feasible solutions obtained by the energy approach decreases; whereas the output set by the eBGF algorithm can be adjusted as it has been discussed previously. In addition, when many dof are assumed between backbone atom and side chain atoms, the output set of feasible solutions by the energy calculation approach decreases. Therefore, an additional direct search method is essential to identify arbitrarily low energy molecular conformations after they have been filtered by the proposed eBGF methodology.

Table 5.2: Performance analysis of current approaches.

| <b>Methods</b>  | <b>Build BVH</b> | <b>Update BVH</b> | <b>Collision Detection</b> |
|---|------------------|-------------------|----------------------------|
| <i>ChainTree</i><br>[Lotan et.al. 2002]                 | $O(N)$           | $O(N)$            | $O(N^{4/3})$               |
| <i>SpatialAdaptiveHierarchy</i><br>[Angulo et.al. 2005] | ---              | $O(N \log N)$     | $O(N)$                     |
| <i>DeformingNecklaces</i><br>[Aqarwal et.al. 2004]      | $O(N \log N)$    | $O(N \log N)$     | $O(N^{4/3})$               |
| <i>BGF model</i><br>[Brintaki & Lai-Yuen 2008]          | ---              | $O(N)$            | $O(\log N)$                |
| <i>eBGF model</i><br>[Brintaki & Lai-Yuen 2009]         | $O(N)$           | $O(N)$            | $O(\log N)$                |



Table 5.2 demonstrates the worst case scenarios in terms of computational complexity for eBGF and current methods in the literature. The proposed eBGF methodology requires  $O(N)$  performance for building and updating the BVH and never exceeds  $O(\log N)$  when searching for overlapping atoms. Hence, the eBGF algorithm succeeds to keep the BVH complexity in the lower level ( $O(N)$ ) while significantly reducing collision detection complexity from  $O(N)$  to  $O(\log N)$ .

## 5.6 Conclusions

This chapter presents the enhanced BioGeoFilter (eBGF) methodology for modeling the behavior of macromolecules such as proteins. The proposed approach is presented as a rapid filtering tool for the identification of molecules' feasibility. The eBGF algorithm has been tested against the traditional energy calculation approach in terms of computational time and accuracy under different cases. Computer implementation and results demonstrate that the proposed eBGF algorithm significantly decreases the computational time for identifying feasible molecular conformations without sacrificing accuracy. Therefore, the eBGF method facilitates the modeling of flexible macromolecules that can be used in molecular modeling, protein folding, and nanoscale design.

## Chapter 6

### Generic Enhanced BioGeoFilter (g.eBGF) Model

This chapter presents the generic enhanced BioGeoFilter (g.eBGF) algorithm for simplifying the representation of molecules of different type, size, shape and topology by considering certain chemical factors that influence molecules' flexibility. The incorporation of chemically-based constraints can provide more realistic molecular conformations that will significantly improve molecular modeling. The proposed methodology can be used to enable the interactive modeling of molecules for molecular docking or assembly, and for protein folding applications.

#### 6.1 Differences Between eBGF and g.eBGF Models

Both geometric methods rely upon the same basic algorithmic concepts for modeling molecules conformation mechanism during conformational search. The main differences between the two methods are that the g.eBGF approach:

1. incorporates certain chemically-based factors that
  - a. control molecules flexibility for providing more realistic and chemically-feasible molecular conformations
  - b. further simplifies the molecular representation since they reduce the allowed number of degrees of freedom for the molecule.
2. is a generic model applicable to molecules of different type, size, shape and topology. The g.eBGF methodology can effectively model molecular structures such as ligands and proteins with one or multiple chains.

## 6.2 Ligand Modeling

A ligand or drug-like molecule is a small molecular structure that usually consists of at most 50 atoms. Ligand molecules may contain rings of atoms as graphically shown with [Humphrey 1999] molecular graphics software in Figure 6.1. These rings are considered rigid during modeling as the location of the ring atoms does not change with respect to each other. Therefore, torsion can be assumed everywhere within a ligand's topology except within the rings and within double- and triple-bonded atoms, which correspond to stronger (not easily breakable) chemical bonds. The proposed generic eBGF approach considers the above information for defining the chemically-feasible dof within a ligand molecule.

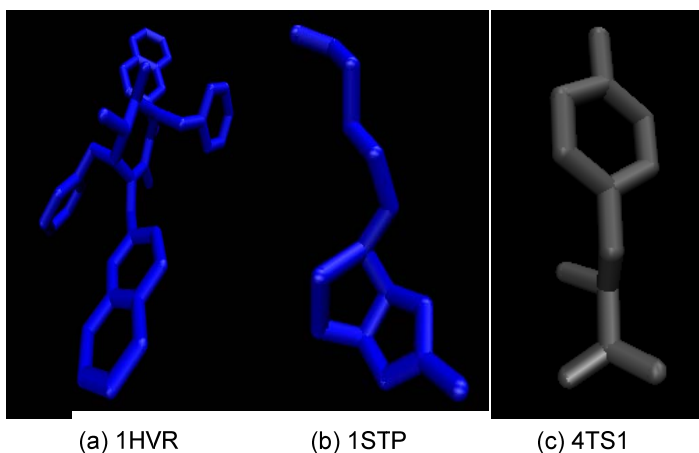
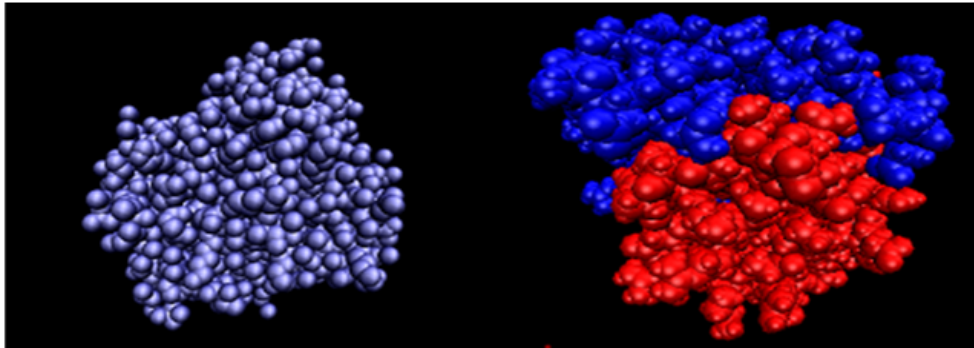


Figure 6.1: Examples of ligand molecules.

## 6.3 Protein Modeling

A protein molecule may contain one chain (backbone) as shown by using the molecular graphics software [Humphrey 1999] in Figure 6.2(a) or multiple chains as shown in Figure 6.2(b). Multiple chains are usually not connected by chemical bonds but by electrostatic forces that keep the chains close to each other. In contrast to ligand

modeling, macromolecules such as proteins consist of hundreds or thousands of atoms with hundreds or even thousands dof. A protein molecule can also be considered as a highly articulated body where an arbitrarily-selected atom or atom-group acts as the base of the body. A protein that contains more than one chain can be viewed as multiple kinematics chains with hundreds or thousands of links and joints.



(a) 1DO3 protein consisted by 1 chain (b) 1NS1 protein consisted by 2 chains  
Figure 6.2: VDW representation of two different protein molecule examples.

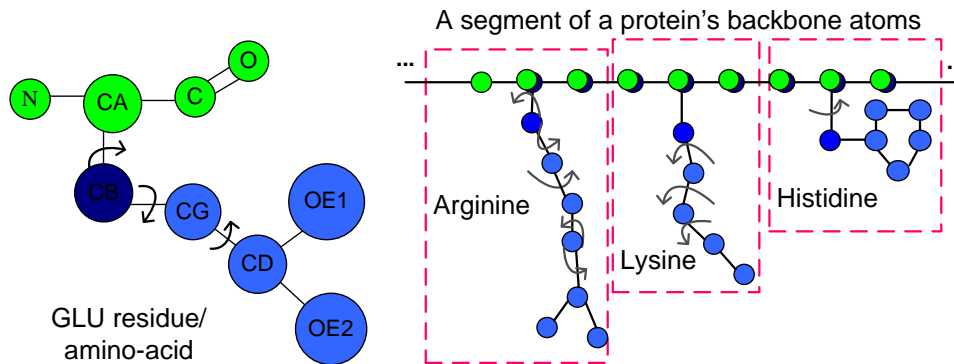


Figure 6.3: Graphical representation of the degrees of freedom of a protein.

Torsion changes can occur everywhere within a protein's topology, except within rings and double- and triple-bonded atoms. However, random torsions within a protein's backbone (chain) can break its structure making it extremely difficult to evaluate whether the generated molecular conformation is chemically feasible. For this reason, similar with Section 5.3 for the generic eBGF model, torsions are assumed only between the

central carbon atom of a protein's backbone (*CA*) and a side chain atom (*CB*) or within the side chain atoms as shown in Figure 6.3. Furthermore, torsions at the end of each side chain are neglected (i.e. the bond between *CD* and *OE1* atoms in Figure 6.3(a) since they do not contribute significantly to the molecular conformation.

Some regions within a protein structure attain higher flexibility. These higher flexible regions are the remote protein's portions or the amino acids (residues) located at the end of the chain. The residues within the *turns* of a protein's chain should also be considered as highly flexible molecular bodies since those have a tendency to move more. These highly flexible regions are considered in the proposed g.eBGF model for determining the chemically-feasible dof that controls the molecular flexibility.

## 6.4 Proposed g.eBGF Methodology

### 6.4.1 Overview of the Proposed g.eBGF Model

Figure 6.4 shows the overview of the proposed generic enhanced BioGeoFilter (g.eBGF) methodology that aims to effectively identify feasible conformations for molecular structures of different type, size, shape or topology while considering the underlying chemical information. The g.eBGF approach similarly with the BGF and eBGF models consists of two layers as indicated by the two larger boxes in Figure 6.4. At the lower layer of the hierarchy, any molecular conformation can be input into the g.eBGF algorithm. The pre-selected dof for a molecular structure are defined based on the concepts presented in Sections 6.2 and 6.3 to form the atom groups. A further simplification in macromolecular representation is proposed by splitting the backbone atom cluster (or clusters) into smaller groups of atoms. At the upper layer of the g.eBGF algorithm, the corresponding bounding volume hierarchy (BVH) of the initial molecular conformation is built. New random molecular conformations are obtained by arbitrarily changing the values for each degree of freedom. For each candidate molecular conformation, the BVH is updated and a collision detection scheme is performed to

identify the feasibility of the molecular conformation. At the end of the g.eBGF algorithm, the intramolecular energy value for each random conformation is calculated to evaluate the proposed approach.

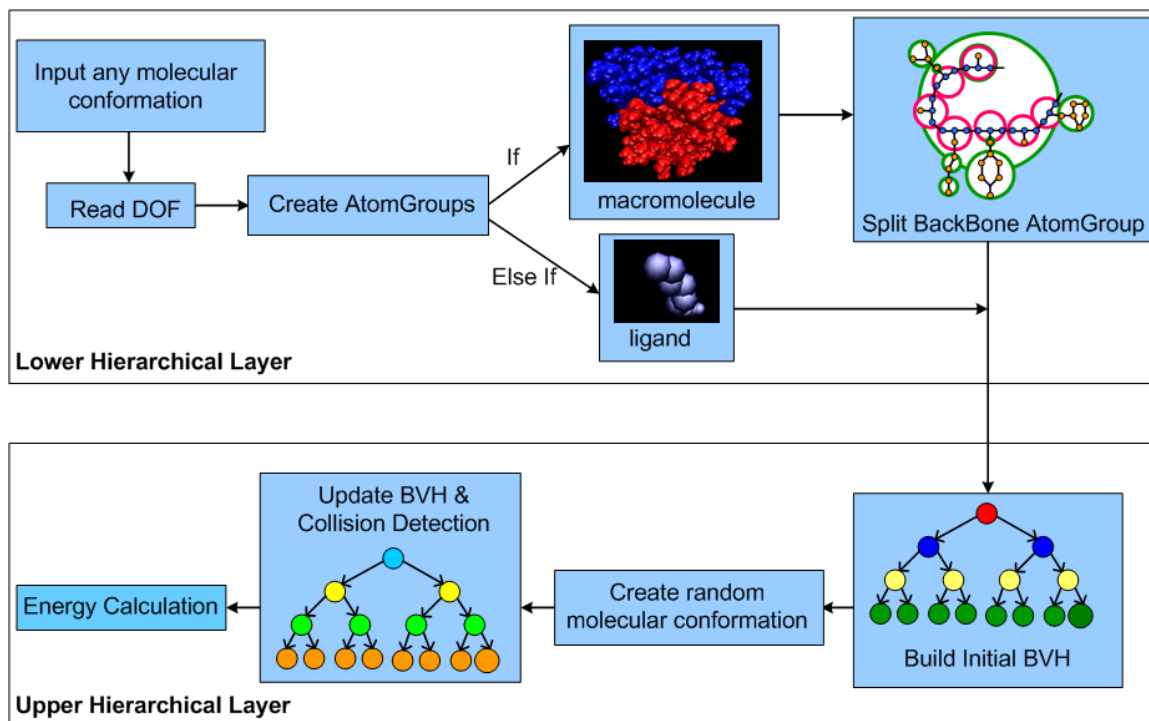
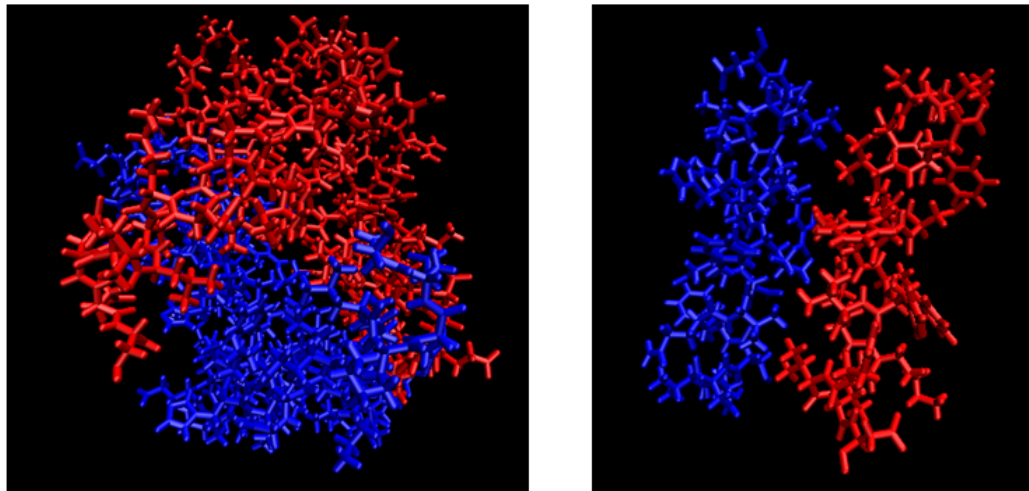


Figure 6.4: Overview of the proposed g.eBGF methodology.

#### 6.4.2 Chemically-Artificial Bonds for the g.eBGF Method

When a protein molecule contains more than one chain as shown with the VMD molecular graphics software [Humphrey 1999] in (Figure 6.5(a)), an artificial rigid bond is introduced between the closest residue-pair of the chains by the proposed generic eBGF approach. This artificial bond is used to simulate the electrostatic forces that keep the chains in contact and should be created in the least flexible region of the protein to avoid the risk of breaking its structure. For example, the least flexible region in the 1NS1 protein shown previously in Figure 6.5(a) is the area between the first helixes of the two chains as shown in Figure 6.5(b). However, an artificial bond should not be placed

arbitrarily between any residue-pair within the 1<sup>st</sup> helices but between the closest possible residue-pair as shown by the circle in Figure 6.6. Moreover, the selected residue pair should have the same polarity. In other words, the closest residues that are both either hydrophobic, polar or ionized would be good candidates for placing an artificial rigid bond.



(a) the 2 chains within 1NS1 protein      (b) blue: 1<sup>st</sup> helix of Chain A & red: 1<sup>st</sup> helix of chain B

Figure 6.5: Structure of the protein with PDB ID: 1NS1.

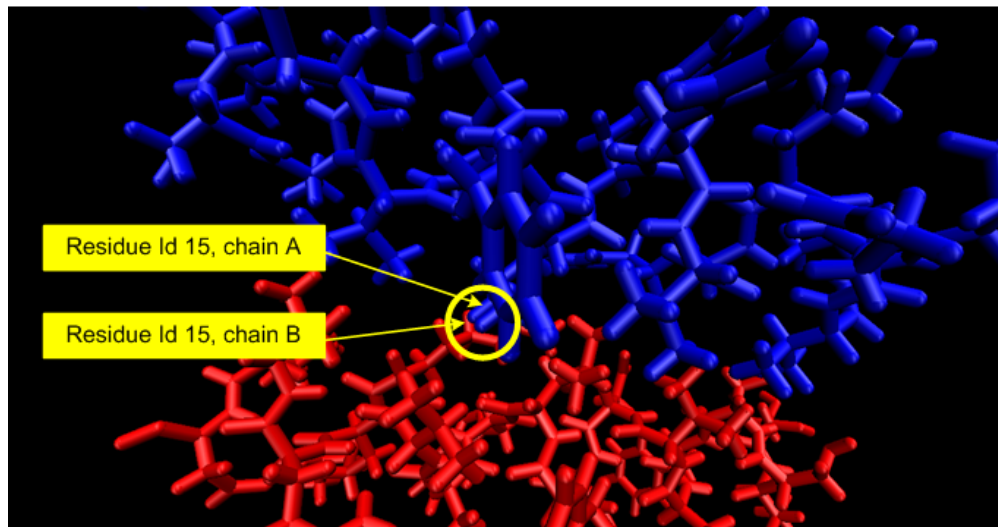


Figure 6.6: Closest residue-pair between the first helices of the two 1NS1 protein's chains.

### 6.4.3 Description of the g.eBGF Algorithm

The proposed g.eBGF methodology for identifying feasible molecular conformations requires two input files: the atomic coordinate information and the atoms within the molecular topology that share a torsion bond. The first input file is usually the PDB file obtained from the Protein Data Bank (PDB) [Berman 2000] and the second input file is the file that describes the pre-selected dof considered for each experiment. The VMD software [Humphrey 1999] is used to define atoms' connectivity information for proteins and to construct the first input file (coordinate file). If the protein contains multiple chains, an artificial bond is added as described in Section 6.4.2. Finally, to create the file that contains the pre-selected dof, the concepts about the allowed number and location of the pre-selected dof (torsion angles) presented in Sections 6.2 and 6.3 (i.e. torsions are not allowed within the rings or double-bonded atoms, etc.) are incorporated for studying chemically-feasible random molecular conformations.

Once the two required input files have been defined, groups of atoms are formed following the concept presented in Section 4.2 to create the lower layer of the proposed g.eBGF approach. Based on the location of the torsion bonds, atoms are clustered into AtomGroups where all the atoms within an AtomGroup are connected by rigid bonds while AtomGroups are connected by torsion bonds. Figure 6.7(a), schematically represents the Atomgroups for a hypothetical protein segment consisted by two symmetric chains. As it is shown in Figure 6.7(a), since the two chains are symmetric, the defined Atomgroups for both chains are the same in terms of both number and atom clustering.

If the tested molecular structure is a protein molecule, then an additional step within the g.eBGF algorithm is performed for splitting the backbone atom cluster (or clusters in the case of multiple chain proteins) into smaller AtomGroups. The purpose of this additional step is to reduce the time needed to identify an actual molecular self-collision while decreasing the computational time for updating the atoms' positions as discussed in Section 5.3. The size of these AtomGroups is based on a threshold defined by the maximum number of atoms allowed within each atom cluster. By splitting a



backbone cluster, a flexible AtomGroup (i.e. the green-pink sphere in Figure 6.7(b)) is obtained along with a number of rigid AtomGroups (i.e. the six pink spheres shown in Figure 6.7(b)) for each chain within a protein molecule. The splitting of the backbone group eliminates collision detection within and between the rigid groups since the atomic distances remain unchanged between and within these groups. Moreover, after splitting the backbone cluster, collision search is performed between similar sized flexible groups of atoms.

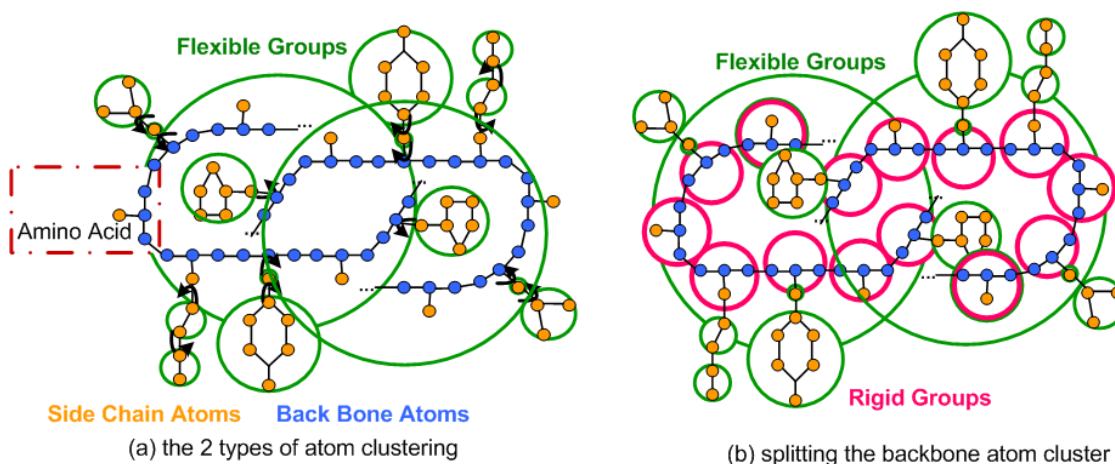


Figure 6.7: Graphical representation of the AtomGroup concept along with the proposed splitting procedure for a hypothetical protein segment with two chains.

At the upper hierarchical layer of the proposed g.eBGF method similarly with the eBGF model, a BVH depicted as a balanced binary tree is introduced to identify overlapping atoms. In respect the BVH the difference between the two models lays on the geometric representation of the preselected dof. Based on the location of the torsion bond angles (dof) within the molecule, groups of atoms are generated for both models. To construct the hierarchy a sphere is attached around each atom cluster. The spheres around each generated AtomGroup depict the leaves of the BVH for each method. As opposed to eBGF method the g.eBGF model defines the chemically-allowed torsion movements for each molecular structure. These chemically-oriented factors influence both the number and location of the generated AtomGroups and hence, the size and location of the

generated spheres for the BVH. Therefore, even if the same protein molecule is tested with both models (eBGF and g.eBGF) the resulted spheres for each method will have different size and location in respect to the world coordinate frame. In view that the chemically-allowed torsion movements (dof) provide a more realistic representation for molecules deformation mechanism, the g.eBGF compared with the eBGF model provides a more realistic geometric representation of molecules flexibility. The BVH is built only once at the beginning of the algorithm allowing a total construction time of  $O(N)$  where:

$$\begin{aligned}
 N &= \text{DOF} + 1 + \text{rigidGroups} = \text{flexibleGroups} + \text{rigidGroups} \\
 \text{TotalNumberOfNodes} &= \begin{cases} 2N & \text{if } N \text{ odd} \\ 2N - 1 & \text{o/w} \end{cases} \quad (6.1) \\
 \text{rigidGroups} &: \text{exist only when proteins are tested}
 \end{aligned}$$

Likewise with the eBGF model presented in Section 5.4.3, the BVH for the g.eBGF method is updated for each new molecular conformation as the torsion angles are randomly modified contributing to a total updating time of  $O(\frac{N}{k})$  that never exceeds  $O(N)$ . Where,  $k$  is the number of rigid nodes that remain unchanged.

As soon as the BVH is updated, a collision detection algorithm is performed to search for overlaps between non-bonded atoms within the new molecular conformation. The collision detection queries follow the same concepts of the eBGF model as analyzed in Section 5.4.4, attaining a total  $O(\log \frac{N}{k})$  performance that never exceeds  $O(\log N)$ .

Where,  $k$  is a constant that represents the number of constraint nodes (i.e. rigid *AtomGroups*).

## 6.5 Computer Implementation and Results

The presented method and algorithms have been implemented on a dual 3.0 GHz CPU workstation using Visual C++ programming language, OpenGL and CGAL libraries [CGAL]. Different molecules with different number of atoms, chains, residues and dof

have been tested with the proposed g.eBGF algorithm. The example molecules were obtained from the Protein Data Bank (PDB) [Berman 2000] with PDB IDs as follows: 1STP, 1A5Z, 1HVR, 1HTB, and 1JBO ligand molecules, along with 1STP, 1DO3, and 1NS1 protein molecules.

Table 6.1: Performance analysis of the proposed g.eBGF methodology.

| Molecule PDB Name | Number Chains | Number Atoms | Time Energy | Time BVHUpdate | Time Collision | Time Rand | % Feasible by Energy | TH Energy | % Feasible by Collision | Rho1 | Rho2 | Flex Helices | Flex Turns | Flex Residues | DOF | TH Split |
|-------------------|---------------|--------------|-------------|----------------|----------------|-----------|----------------------|-----------|-------------------------|------|------|--------------|------------|---------------|-----|----------|
| 1STP              | x             | 16           | 0.183       | 0.1            | 0.0016         | 0.0082    | 100                  | 100       | 100                     | 0.6  | 0.7  |              |            |               | 3   | x        |
| 1JBO              |               | 43           | 1.37        | 0.23           | 0.23           | 0.024     | 17                   |           | 20                      |      |      |              |            |               |     |          |
| 1HTB              |               | 44           | 1.38        | 0.21           | 0.014          | 0.025     | 52                   |           | 52                      |      |      |              |            |               |     |          |
| 1A5Z              |               | 44           | 1.72        | 0.23           | 0.016          | 0.024     | 56                   |           | 55                      |      |      |              |            |               |     |          |
| 1HVR              |               | 46           | 1.87        | 0.17           | 0.004          | 0.01      | 100                  |           | 100                     |      |      |              |            |               |     |          |
| 1STP              | x             | 16           | 0.18        | 0.1            | 0.0027         | 0.0088    | 100                  | 100       | 100                     | 0.7  | 0.8  |              |            | 3             | x   |          |
| 1JBO              |               | 43           | 1.58        | 0.24           | 0.018          | 0.024     | 9                    |           | 10                      |      |      |              |            |               |     |          |
| 1HTB              |               | 44           | 1.62        | 0.22           | 0.02           | 0.022     | 40                   |           | 43                      |      |      |              |            |               |     |          |
| 1A5Z              |               | 44           | 1.74        | 0.23           | 0.002          | 0.02      | 50                   |           | 41                      |      |      |              |            |               |     |          |
| 1HVR              |               | 46           | 1.42        | 0.17           | 0.004          | 0.018     | 100                  |           | 100                     |      |      |              |            |               |     |          |
| 1STP              | 1             | 903          | 233.16      | 1.5            | 0.21           | 0.32      | 85                   | 100000    | 90                      | 0.5  | 0.6  |              |            |               | 5   | 10       |
|                   |               |              | 220.96      | 0.74           | 0.73           | 0.3       | 80                   |           | 90                      |      |      |              |            |               | 15  |          |
|                   |               |              | 222.45      | 0.64           | 0.88           | 0.31      | 90                   |           | 90                      |      |      |              |            |               | 20  |          |
|                   |               |              | 224.15      | 1.38           | 0.12           | 0.33      | 80                   |           | 90                      |      |      |              |            |               | 10  |          |
|                   |               |              | 218.9       | 0.67           | 0.19           | 0.31      | 70                   |           | 70                      |      |      |              |            |               | 15  |          |
|                   |               |              | 219.56      | 0.57           | 0.2            | 0.28      | 70                   |           | 70                      |      |      |              |            |               | 20  |          |
|                   |               |              | 214.35      | 1.33           | 0.28           | 0.31      | 4                    |           | 5                       |      |      |              |            |               | 10  |          |
| 230               | 0.89          | 0.71         | 0.31        | 2              | 6              | 15        |                      |           |                         |      |      |              |            |               |     |          |
| 225.02            | 0.76          | 0.95         | 0.31        | 3              | 4              | 20        |                      |           |                         |      |      |              |            |               |     |          |
| 1NS1              | 2             | 2342         | 1456.04     | 4.47           | 0.3            | 0.8       | 30                   | 100000    | 25                      | 0.5  | 0.6  |              |            |               | 10  | 15       |
|                   |               |              | 1515.64     | 2.76           | 1.09           | 0.79      | 27                   |           | 30                      |      |      |              |            |               | 15  |          |
|                   |               |              | 1461.59     | 2.23           | 2.61           | 0.74      | 15                   |           | 15                      |      |      |              |            |               | 20  |          |
|                   |               |              | 1479.41     | 4.3            | 0.07           | 0.83      | 6                    |           | 3                       |      |      |              |            |               | 10  |          |
|                   |               |              | 1513        | 2.91           | 0.77           | 0.81      | 8                    |           | 10                      |      |      |              |            |               | 15  |          |
|                   |               |              | 1491.05     | 2.42           | 2.77           | 0.8       | 4                    |           | 2                       |      |      |              |            |               | 20  |          |
|                   |               |              | 1398.63     | 3.69           | 0.06           | 0.75      | 0                    |           | 0                       |      |      |              |            |               | 10  |          |
|                   |               |              | 1511.75     | 3.34           | 0.065          | 0.85      | 0                    |           | 0                       |      |      |              |            |               | 15  |          |
| 1469.47           | 2.76          | 0.13         | 0.78        | 0              | 0              | 20        |                      |           |                         |      |      |              |            |               |     |          |

Table 6.1 shows a representative list of the performance analysis for the proposed g.eBGF methodology on different example molecules. For each molecule, sets of random torsion angles were randomly generated. The same random molecular conformation was tested with both the g.eBGF (*TimeBVHUpdate*, *TimeCollision*, *TimeRand*, *%FeasibleByCollision* columns) and the energy (*TimeEnergy*, *%FeasibleByEnergy*, and *TH Energy* columns) approaches and evaluated in terms of computational time (in milliseconds) and accuracy (percentage of feasible conformations identified). A molecular conformation can be considered as feasible based on the internal molecular energy value. Therefore, a threshold (*TH* column in Table 6.1) has been

selected based on the molecules' size to define the maximum energy value for which a molecular conformation is considered to be feasible with the energy approach.

Different scenarios regarding the number, arrangement and the location of the pre-selected dof were studied for assessing their impact on the proposed g.eBGF algorithm. Columns *FlexHelixes*, *FlexTurns* and *FlexResidues* denote the number of flexible helixes, residues and turns respectively, where column *dof* states the total number of chemically and geometrically feasible dof considered for each experiment. In addition, different values for the algorithm's selectivity parameters ( $\rho_1$  and  $\rho_2$ ) have been tested for evaluating their impact on the g.eBGF results. Table 6.1 shows the results for the ligand molecules using two different pair-values for the selectivity parameters (*rho* values) and for the protein molecules using one selectivity parameter pair. A detailed analysis on the impact of the rho values on protein modeling can be found in our Chapter 5. Finally, three different values for the splitting threshold have been tested for each protein molecule as shown by the last column (*TH Split*) in Table 6.1.

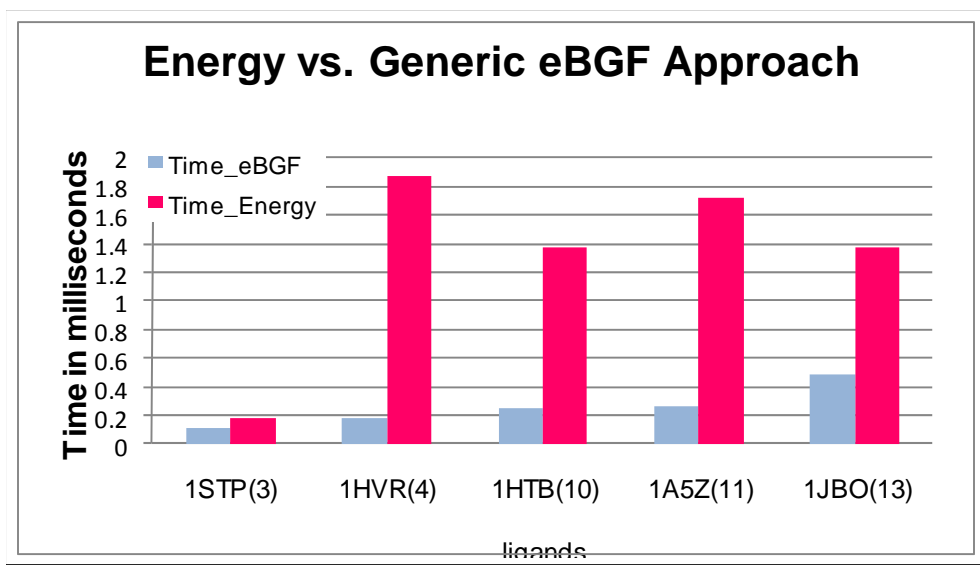


Figure 6.8: Time comparison between the traditional energy calculation approach and the proposed g.eBGF methodology for ligand molecules.

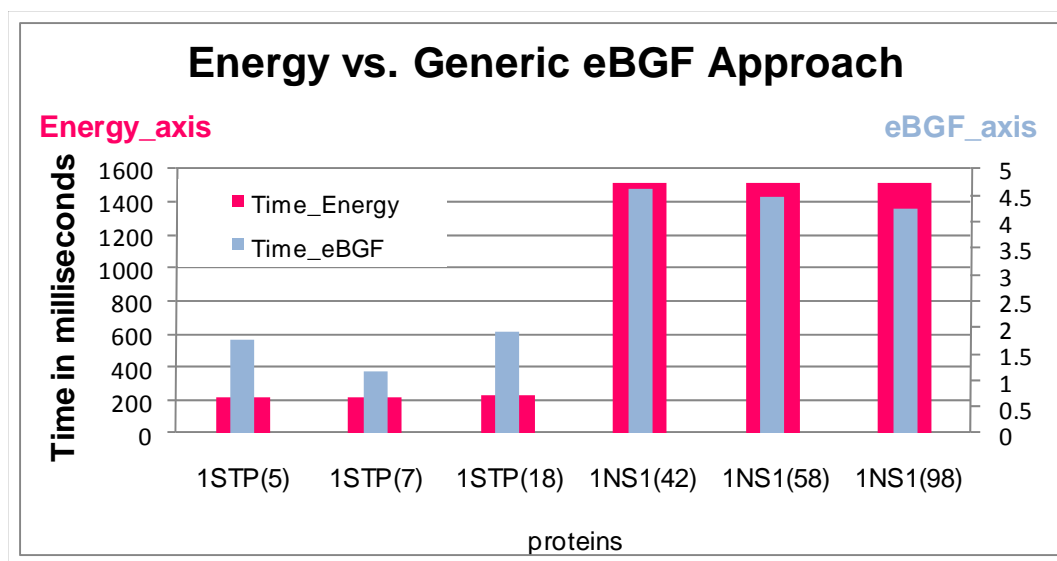


Figure 6.9: Time comparison between the traditional energy calculation approach and the proposed g.eBGF methodology for protein molecules.

Figure 6.8 and Figure 6.9 compares the performance of the proposed g.eBGF method (update atoms' position time + update BVH time + collision detection time) against the energy calculation approach in terms of computational time required to identify the molecule's feasibility. Figure 6.8 and Figure 6.9 show the computational time performance for both methods as the number of dof increases for ligand and protein molecules, respectively. Results show that the proposed approach significantly reduces the computational time compared to the energy approach for identifying the feasibility of a random molecular conformation. It was observed that as the molecular size and problem's complexity increases, the time benefit provided by the proposed g.eBGF method increases significantly. Moreover, as shown in Figure 6.9, the time difference between the two methods is so significant that two different scales were needed for displaying both methods in the same graph. The left scale in Figure 6.9 denotes the computational time (in ms) required by the energy calculation approach whereas the right scale denotes the computational time (in ms) for the proposed g.eBGF methodology.

Figure 6.10 displays the computational time performance of the proposed g.eBGF methodology while considering the scenario that all the example molecules are

completely flexible. The tested molecules are assumed to be fully flexible bodies by randomly varying the total allowed number of chemically-feasible dof as presented in Sections 6.2 and 6.3. Results show that the proposed g.eBGF approach scales very well as the molecular size and problem's complexity increase.

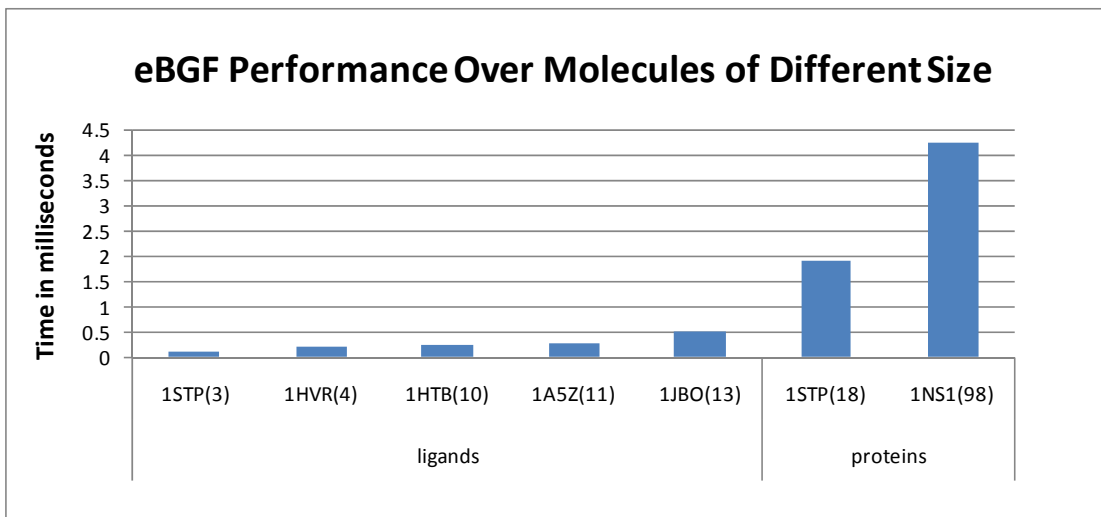


Figure 6.10: Computational time performance of the proposed g.eBGF approach for molecules of different size and dof.

The impact of the splitting threshold selection value on the g.eBGF algorithm is shown in Figure 6.11. As discussed in Section 6.4.3, the splitting threshold (*TH Split* column in Table 6.1) defines the maximum allowed number of atoms in each atom cluster. As the splitting threshold value decreases, it can be observed from Figure 6.11 that the following occur:

- the computational time required to update the BVH increases,
- the computational time for self-collision detection decreases, and
- the overall computational time for the g.eBGF algorithm remains approximately the same.

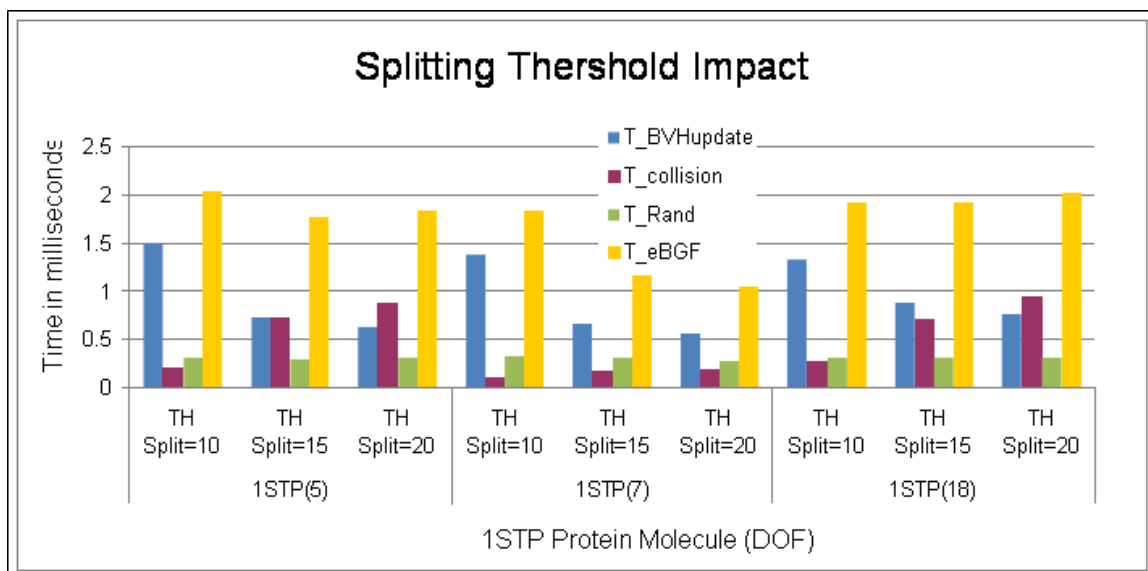


Figure 6.11: Splitting threshold impact on the g.eBGF results for protein modeling.

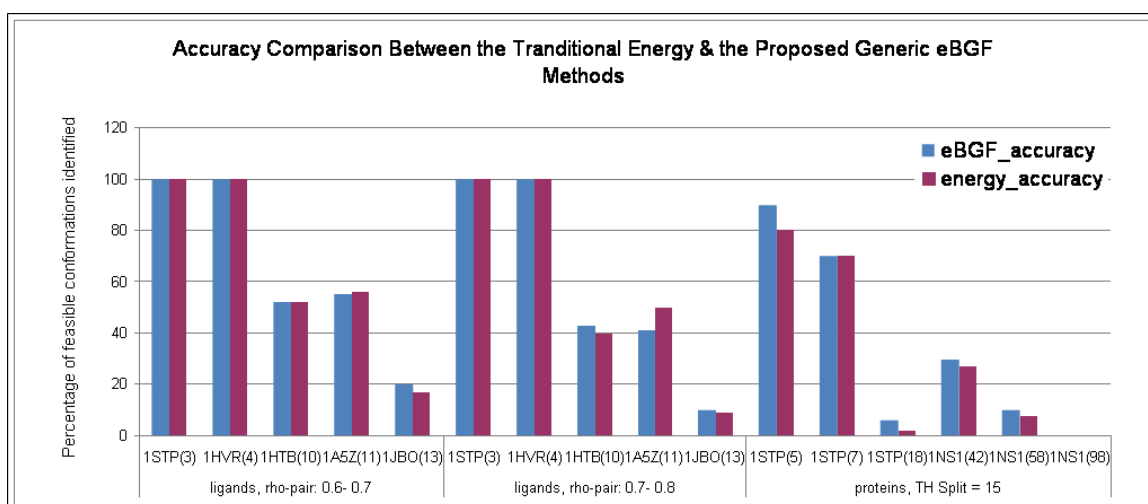


Figure 6.12: Accuracy comparison between the traditional energy calculation approach and the proposed g.eBGF method.

Therefore, incorporating the splitting concept for the backbone atom clusters into the proposed algorithm speeds the identification of molecular feasibility while it does not affect the overall performance of the algorithm. The best selection for a splitting threshold depends on the pre-selected set of dof. A good splitting threshold is a value that allows the construction of similar sized groups of atoms while reducing the

computational time for self-collision. In this work, it was found that a splitting threshold value of 15 atoms for each atom cluster provided similar-sized atom groups and the best results for self-collision detection time.

Figure 6.12 demonstrates the accuracy (percentage of feasible molecular conformations identified) between the traditional energy method and the proposed g.eBGF methodology. For the ligand molecules, two different pairs of the selectivity parameters are presented to show their impact on the results, whereas one selectivity pair is shown for the protein molecules. As shown in Figure 6.12, both methods (g.eBGF and Energy) demonstrate similar accuracy for all tested molecules. In fact, the selectivity of the g.eBGF algorithm can be adjusted by varying the control parameters ( $\rho_1$ , and  $\rho_2$ ). In other words, by decreasing the  $\rho$  values, the proposed algorithm can accept more molecular conformations as feasible leading to a relaxed filtering. It is important to select appropriate  $\rho$  values based on the molecule's size and the desired level of selectivity by the user to avoid rejecting molecular conformations that are feasible.

As shown in Table 6.1 and Figure 6.12, there is a significant dependency between the pre-selected number of chemically-feasible dof considered in each molecule and the percentage of feasible molecular conformations from both the g.eBGF and energy methods. Results demonstrate that as the number of dof increases, the output set of feasible solutions obtained by the energy approach decreases; whereas the output set by the g.eBGF algorithm can be adjusted as it has been discussed previously. In addition, when a macromolecule is assumed to be a fully flexible body, the output set of feasible solutions by the energy calculation approach decreases and tends to approach zero. Therefore, an additional direct search method is necessary to identify low-energy molecular conformations after they have been filtered by the proposed g.eBGF methodology.

Table 6.2 demonstrates the worst case scenarios in terms of computational complexity for g.eBGF and current methods in the literature. The proposed g.eBGF methodology requires  $O(N)$  performance for building and updating the BVH and never exceeds  $O(\log N)$  when searching for overlapping atoms. Hence, the g.eBGF algorithm



succeeds to keep the BVH complexity in the lower level ( $O(N)$ ) while significantly reducing collision detection complexity from  $O(N)$  to  $O(\log N)$ .

Table 6.2: Computational complexity comparison.

| <b>Methods</b>   | <b>Build BVH</b> | <b>Update BVH</b> | <b>Collision Detection</b> |
|--|------------------|-------------------|----------------------------|
| <i>ChainTree</i><br>[Lotan et.al. 2002]                      | $O(N)$           | $O(N)$            | $O(N^{4/3})$               |
| <i>SpatialAdaptiveHierarchy</i><br>[Angulo et.al. 2005]      | ---              | $O(N \log N)$     | $O(N)$                     |
| <i>DeformingNecklaces</i><br>[Aqarwal et.al. 2004]           | $O(N \log N)$    | $O(N \log N)$     | $O(N^{4/3})$               |
| <i>BGF model</i><br>[Brintaki & Lai-Yuen 2008]               | ---              | $O(N)$            | $O(\log N)$                |
| <i>eBGF model</i><br>[Brintaki & Lai-Yuen 2009]              | $O(N)$           | $O(N)$            | $O(\log N)$                |
| <i>Generic eBGF model</i><br>[submitted to CAD journal 2009] | $O(N)$           | $O(N)$            | $O(\log N)$                |

## 6.6 Conclusions

This chapter presented a new generic molecular modeling tool called enhanced BioGeoFilter (g.eBGF) for effectively identifying chemically-feasible conformations for molecules of different type, size and topology. The proposed g.eBGF methodology incorporates chemical factors that control molecules' conformation into a bounding volume hierarchy to rapidly identify chemically-feasible molecular conformations. The g.eBGF approach is presented as a filtering tool to rapidly identify molecular

conformations for speeding molecular conformational search and collision detection queries. Computer implementation and results demonstrate that the g.eBGF methodology significantly decreases the computational time for identifying feasible molecular conformations while maintaining accuracy. Therefore, the g.eBGF method can be used to facilitate the modeling of flexible molecular structures for applications such as molecular docking and assembly, and protein folding.

## Chapter 7

### Identifying the Molecular Stability

The scope of this chapter is to investigate the performance of evolutionary-based optimization methods on effectively searching for low-energy molecular conformations. Two novel differential evolution- based methods are presented. The first proposed method is a kinematics-based DE algorithm called kDE model that kinematically represents and simplifies the molecular representation to direct the conformational search towards stable solutions. The second approach, called Biological Differential Evolution (BioDE) is based on our previously developed differential evolution algorithm and our developed biologically-inspired geometric representation of molecules conformation mechanism. The BioDE algorithm utilizes the g.eBGF model as a surrogate approximation model to reduce the number of exact evaluations and to reduce the algorithm's convergence rate. Both proposed methodologies will be extremely useful in speeding the search for low-energy molecular conformations while enabling the modeling of flexible molecules for molecular design.

#### 7.1 Fundamentals of Evolutionary Algorithms (EAs)

Evolutionary Algorithms (EA) simulates the natural selection process using a number (population) of individuals (candidate solutions to the problem) to evolve through certain procedures. Similar to nature, each individual is represented as a chromosome – a string of numbers (bit strings, integers or floating point numbers) which contain the design variables for the optimization problem. Each individual's quality is represented by a fitness function tailored to the problem under consideration.

Classic Genetic Algorithms (GAs) use binary coding for the representation of the genotype. However, floating point coding moves EAs closer to the problem space. This allows the operators to be more problem specific while providing a better physical representation of the space constraints.

In general, EA starts by generating, randomly, the initial chromosome population with their genes (the design variables in the case of floating point coding) taking values inside the desired constrained space of each design variable. The lower and higher constraints of each gene may be chosen in a way that specific undesirable solutions may be avoided. Although the shortening of the search space reduces the computation time, it may also lead to sub-optimal solutions due to the lower variability between the potential solutions.

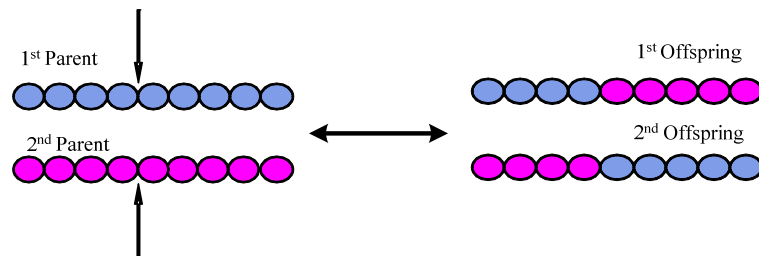


Figure 7.1: One-point crossover (recombination) operator.

After the evaluation of each individual’s fitness function, operators are applied to the population, simulating the natural processes. Applied operators include various forms of recombination, mutation and selection, which are used to provide the next generation of chromosomes. The first classic operator applied to the selected chromosomes is the one-point crossover scheme. In this operator, two randomly selected chromosomes are divided in the same (random) position while the first part of the first one is connected to the second part of the second one and vice-versa as shown in Figure 7.1. The crossover operator is used to provide information exchange between different potential solutions to the problem.

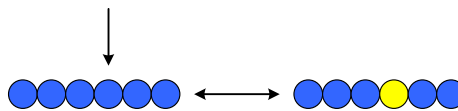


Figure 7.2: Uniform mutation operator.

The second classic operator applied to the selected chromosomes is the uniform mutation scheme. This asexual operator alters a randomly selected gene of a chromosome as shown in Figure 7.2. The new gene takes its random value from the constrained space that is determined at the beginning of the process. The mutation operator is used to introduce some extra variability into the population.

The resulting intermediate population is evaluated and a fitness function is assigned to each member of the population. Using a selection procedure (different for each type of EA), the best individuals of the intermediate population (or the best individuals of the intermediate and the previous population) will form the next generation. The process of a new generation evaluation and creation is successively repeated, resulting in individuals with higher values of fitness function.

## 7.2 EAs Advantages, Limitations and How to Compensate

Evolutionary algorithms are a class of search methods with remarkable balance between exploitation of the best solutions and exploration of the search space. They combine elements of directed and stochastic search and consequently, are more robust than directed search methods. The EAs are algorithms parallel by nature and may be easily tailored to the specific application of interest taking into account the special characteristics of the problem under consideration. In addition, the EAs are easy to implement in problems with a relatively high number of constraints and design variables, as well as with many and contradictory objectives [Michalewicz 1999, Goldberg 1989, Holland 1992].

However, EAs main limitations are the convergence uncertainty and trapping into local minima. To compensate for the algorithm's failure, the first step is to adjust the algorithm's selective pressure, which is defined as the predominance of exploitation versus exploration. By increasing the selective pressure, the algorithm's convergence rate and the probability of trapping into local minima are enhanced. Therefore, a balance between exploration and exploitation is essential. The crossover and mutation operators

are responsible for exploring the solution space (exploration) while leading to an increasing variation of the population. On the other hand, the selection process pushes the search into the region with the best fitness function values (exploitation) aiming to decrease the population variation. Thus, the balance between exploration and exploitation is given by the specific type of selection operator for the problem under consideration. Typically, high selective pressure requires high variation in the population to avoid any local minima traps.

Another way to compensate for algorithm's potential failure is to define "suitable" values for the control parameters of the EA. The control parameters for an evolutionary algorithm are the crossover and mutation probabilities. These probabilities remain constant during the search process while affecting the convergence behavior and algorithm's robustness. The values for the crossover and mutation probabilities are strongly dependent on the objective function, the characteristics of the problem, and the population size. Usually, when an algorithm is mostly based on a crossover operator, it requires low selective pressure to avoid trapping into local minima solutions. Additionally, when a high mutation probability is applied, the algorithm entails a high selective pressure to compensate for failure. Based on these concepts, a trial and error testing for the EA's control parameters will tune the algorithm's robustness and convergence rate.

An alternative approach is the use of a differential evolution (DE) algorithm since it has shown a better convergence performance compared with other EAs [Storn and Price 1995, 2005, Nikolos and Brintaki 2005a,b,c, 2007, Thomsen 2003, 2006]. Incorporating the scheme presented by [Hui-Yuan 2003] for determining the donor scheme for the mutation operator accelerates the algorithm's convergence rate, without sacrificing accuracy or the algorithm's robustness. In this scheme, the donor is randomly selected (with uniform distribution) from the region within the "hyper triangle" formed by the three members of the triplet. With this scheme, the donor comprises the local information of all members of the triplet. This provides a better starting-point for the mutation operation and results in a better distribution of the trial-vectors.

Besides using special operators, a substitute solution for compensating for the algorithm's convergence failure and for decreasing the computational time is the utilization of surrogating models and approximations. Surrogate models are auxiliary simulations that are less accurate, but also less computationally costly than the expensive (exact model) simulations. Surrogate approximations are algebraic summaries obtained from previous runs of the expensive simulation [Torczon 1998, Giannakoglou 2002]. Such approximations are the various types of Artificial Neural Networks (ANN) [Giannakoglou 2002, Nikolos and Brintaki 2005b, 2007]. The basic concept of using an approximation method is to replace the costly exact evaluations with fast inexact approximations while maintaining the algorithm's robustness. The surrogate model predictions replace exact and costly evaluations only for the less-promising individuals, while the more-promising ones are always exactly evaluated. Our developed biologically-inspired geometric filter (generic eBGF method) presented in Chapter 6 can also set the base for a surrogate approximation model as it is analyzed in Section 7.4.

### 7.3 Differential Evolution

In this work, a Differential Evolution (DE) algorithm based on the concepts by [Storn and Price 1995, 2005], improved by [Hui-Yuan 2003] and presented in [Nikolos and Brintaki 2005a,b,c, 2007] is used to direct the search towards low energy molecular conformations. The DE algorithm is a simple evolutionary algorithm to implement and demonstrates better convergence performance compared with other EAs. Differential Evolution embodies a type of evolutionary strategy (ES) especially formed to deal with continuous optimization problems often encountered in engineering design.

The classic DE algorithm evolves a fixed population size consisted by candidate problem solutions (population members or else chromosomes), randomly initialized. After initializing the population, an iterative process starts to direct the search towards better fitted population members. At each iteration (generation), a new population of candidate solutions is produced until a stopping condition is satisfied. At each generation,

each element (member) of the population can be replaced with a new generated one. The new element is a linear combination between a randomly selected population member and a difference between two other randomly selected members. Below is the analytical description of the algorithm's structure.

Given an objective function as shown by Eqn. 7.1:

$$F_{objective}(X) : R^{n_{param}} \rightarrow R \quad (7.1)$$

the optimization goal is to minimize the objective function value by optimizing the values of its parameters (design variables) as shown as follows:

$$X = (x_1, x_2, \dots, x_{n_{param}}), \quad x_j \in R \quad (7.2)$$

where  $X$  denotes the vector composed of  $n_{param}$  objective function parameters (design variables). The design variables take values between the specific upper and lower bounds:

$$x_j^L \leq x_j \leq x_j^U, j = 1, \dots, n_{param} \quad (7.3)$$

The DE algorithm implements real-number encoding for the design variables. Often, the only information available is the boundaries of the parameters. Hence, to obtain a starting point for the algorithm, we initialize the population by randomly assigning values to the design variables within their boundaries as given by Eqn. 7.4:

$$x_{i,j}^0 = r(x_j^U - x_j^L) + x_j^L, i = 1, \dots, n_{pop}, j = 1, \dots, n_{param} \quad (7.4)$$

where  $r$  is a uniformly distributed random value within the range [0, 1].

DE's mutation operator is based on a triplet of randomly selected individuals (different from each other). A new parameter vector is generated by adding the weighted difference vector between the two members of the triplet to the third one (the donor). In this way, a perturbed individual is generated. The perturbed individual and the initial population member are then subject to a crossover operation for generating the final candidate solution as shown as follow:

$$x_{i,j}^{(G+1)} = \begin{cases} x_{c_i,j}^{(G)} + F(x_{A_i,j}^{(G)} - x_{B_i,j}^{(G)}), & \text{if } (r \leq C_r \vee j = k) \vee j = 1, \dots, n_{param} \\ x_{i,j}^{(G)} & \text{o/w} \end{cases} \quad (7.5)$$



$$\left. \begin{array}{l} i = 1, \dots, n_{pop}, \quad j = 1, \dots, n_{param} \\ A_i \in [1, \dots, n_{pop}], \quad B_i \in [1, \dots, n_{pop}], \quad C_i \in [1, \dots, n_{pop}] \\ C_r \in [0, 1], \quad F \in [0, 1+], \quad r \in [0, 1] \end{array} \right\} \quad (7.6)$$

Where  $x_{c_i, j}^{(G)}$  is called the “donor”,  $G$  is the current generation, and  $k$  a random integer within  $[1, n_{param}]$ , chosen once for all members of the population. The random number  $r$  is seeded for every gene of each chromosome.  $F$  and  $Cr$  are DE control parameters, which remain constant during the search process and affect the convergence behavior and robustness of the algorithm. Their values also depend on the objective function, the characteristics of the problem, and the population size.

The population for the next generation is selected between the current population and the final candidates. If each candidate vector is better fitted than the corresponding current one, the new vector replaces the vector with which it was compared. The DE selection scheme for a minimization problem is described as follow:

$$X_i^{(G+1)} = \begin{cases} X_i^{(G+1)}, & \text{if } F_{obj}(X_i^{(G+1)}) \leq F_{obj}(X_i^{(G)}) \\ X_i^{(G)} & o/w \end{cases} \quad (7.7)$$

In this research work, the new improved scheme by [Hui-Yuan 2003] for determining the donor for the mutation operation is used to accelerate the convergence rate. In this scheme, the donor is randomly selected (with uniform distribution) from the region within the “hyper triangle”, formed by the three members of the triplet. With this scheme, the donor comprises the local information of all the members of the triplet, providing a better starting-point for the mutation operation that result in a better distribution of the trial-vectors. As it is reported in [Hui-Yuan 2003], the modified donor scheme accelerated the DE convergence rate, without sacrificing the solution precision or robustness of the DE algorithm. The random number generation (with uniform probability) is based on the algorithm presented in [Hui-Yuan 2003], which computes the remainder of divisions involving integers that are longer than 32 bits, using 32-bit (including the sign bit) words. The corresponding algorithm, using an initial seed, produces a new seed and a random number. In each different operation inside the DE algorithm that requires a random number generation, a different sequence of random

numbers is produced, by using a different initial seed for each operation and a separate storage of the corresponding produced seeds. By using specific initial seeds for each operation, it is ensured that the different sequences differ by 100,000 numbers.

## 7.4 Proposed kDE Model

In this section, a novel kinematics and evolutionary inspired approach called kinematics-based differential evolution (kDE) is proposed to model flexible biological molecules and to rapidly identify low-energy molecular conformations. The proposed kDE model consists of two modules: the pre-computation and the DE-loop. The kDE model provides the global minimum region for molecular structures of different type, size, shape and topology. This region consists of a number of alternative stable molecular conformations that attain the same low-energy value.

### 7.4.1 Overview of the Kinematics-Based Differential Evolution (kDE) Model

Figure 7.3 shows the overview of the proposed kinematics-based differential evolution (kDE) model that consists of two modules: the pre-computation and the DE-loops. During the pre-computation, a molecule is represented as a highly articulated body that can adopt different conformations. As shown in Figure 7.3, the kDE model starts with any random molecular conformation where the dof of the molecular structure are defined to form groups of atoms. During the DE-loop, our previously developed DE algorithm is incorporated to direct the search towards low-energy molecular conformations and to provide the global minimum region. This region includes a number of alternative stable molecular conformations that attain the same low-energy value.

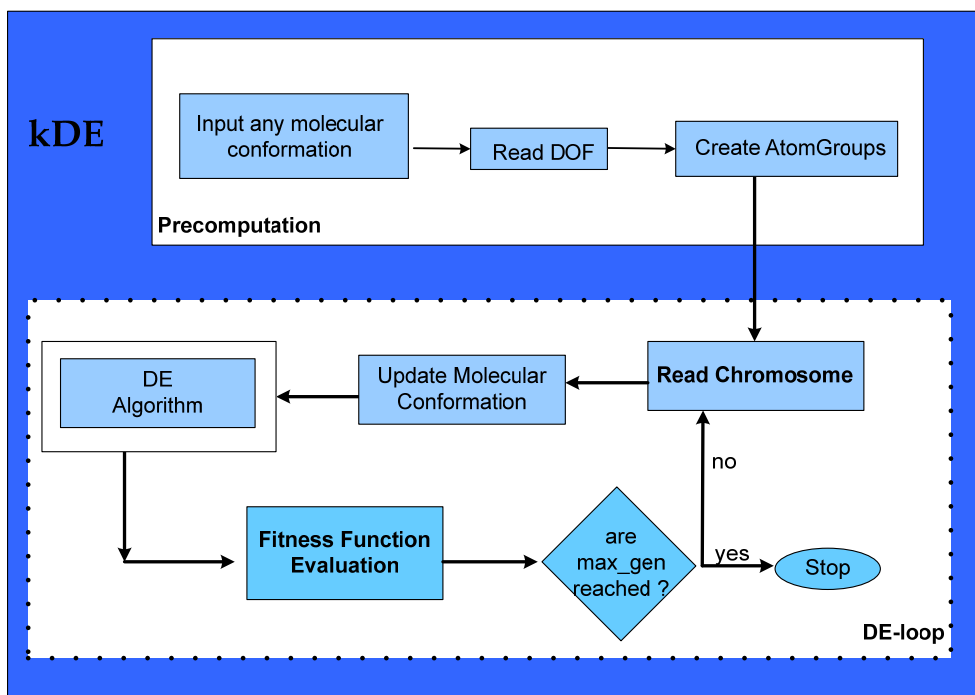


Figure 7.3: Overview of the proposed kDE model.

#### 7.4.2 Pre-Computation Module

During the pre-computation module, a geometric interpretation of the underlying chemical information is performed to represent the molecules' flexibility mechanism as discussed in Section 3.3. As a result, each molecular structure is represented as a highly articulated body able to deform and adopt different molecular conformations. A further simplification in the molecular representation is performed by applying the atom clustering approach presented in Section 4.2 to form groups of atoms based on the number and location of the torsion bonds.

#### 7.4.3 DE-Loop Module

Once the various atom clusters within each molecular structure are formed during the pre-calculation stage, the DE algorithm presented in Section 7.3 is incorporated into the kDE model. The DE algorithm is used to direct the search towards low-energy molecular conformations. As shown in Figure 7.3, two steps are required in the DE loop:

formulate the chromosome structure and define the fitness function. Each chromosome structure through the defined genotype represents a candidate solution to the problem under consideration, whereas the chromosome genes represent the design variables. Hence, to direct the search towards low-energy molecular conformations, the chromosome for the proposed kDE model should represent a candidate molecular conformation. The simplest possible chromosome structure for describing a molecular conformation is to consider each gene to be a degree of freedom or in our case, a torsion bond angle  $\theta_i$  as shown in Figure 7.4.



Figure 7.4: Schematic representation of the chromosome structure used in this work.

The fitness function ( $ff$ ) plays the role of the evaluation criterion for each candidate solution. Choosing a “good” mathematical representation for the  $ff$  is very important and challenging since it directs the search towards the optimal solution or in our case, towards stable (low-energy) molecular conformations. A good mathematical representation for the fitness function is the use of the total intra-molecular energy. As discussed in Section 3.2, the internal energy of a molecule is a function composed of different energy factors that depict the interactions between bonded and non-bonded atoms. However, the major energy contributors are the non-bonded van der Waals (VDW) potential and electrostatic forces. Given that the VDW potential dominates the molecular interactions chemically and geometrically at short-range and the electrostatic forces dominate the computational time, the internal molecular energy can be approximated by the VDW interactions measurement as demonstrated in Section 3.3. Therefore, to evaluate the fitness of each candidate chromosome (molecular conformation), we propose the use of the VDW non-bonded atoms potential as shown by Eqn. 7.8:

$$ff = \sum_{i=1}^n \sum_{j=1}^n \frac{B_{ij}}{r_{ij}^{12}} - \frac{A_{ij}}{r_{ij}^6} \quad (7.8)$$

Where  $B_{ij}$ , and  $A_{ij}$  are the VDW repulsion and attraction parameters, respectively; and  $r_{ij}$  is the distance between every exclusive non-bonded atom pair  $i$  and  $j$ .

#### 7.4.4 Computer Implementation and Results

The presented method and algorithms have been implemented on a dual 3.0 GHz CPU workstation using Visual C++, Visual Basic programming languages and OpenGL. Different molecules with different number of atoms, chains, residues and dof have been tested with the proposed kDE approach. The example molecules were obtained from the Protein Data Bank (PDB) [Berman 2000] with PDB IDs as follows: BTN, CYC, NAD, XK2 for ligand molecules and 1STP, 1DO3, 1NS1 for protein molecules. Figure 7.5 and Figure 7.6 show some of the tested molecules that are graphically displayed using the VMD package [Humphrey 1999].

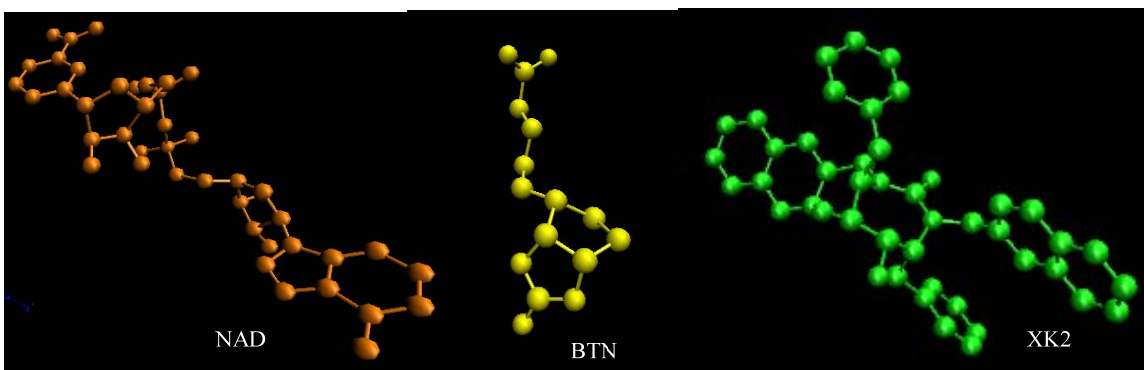


Figure 7.5: Ligand molecules tested with the kDE model.

The kDE algorithm's termination criterion for each experiment but the 1NS1 protein was set to  $maxgen = 500$  generations performed and  $popsiz e = 100$  candidate molecular conformations (population members) considered in each generation. For the 1NS1 protein, given the large number of dof considered in each experimental scenario, the  $maxgen$  was set to 600 generations and 300 population members used as  $popsiz e$ . Finally, the DE's control parameters used in all experiments were  $F = 0.6$  for the mutation parameter, and  $Cr = 0.45$  for the crossover probability.

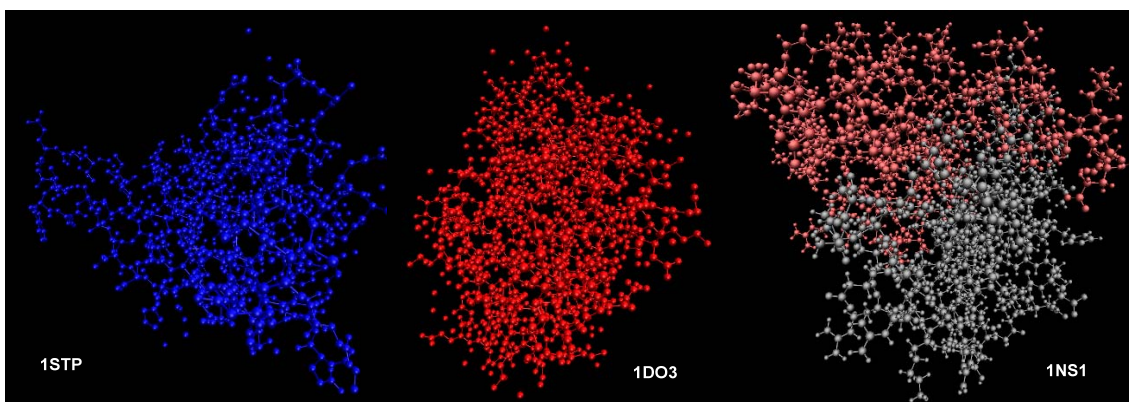


Figure 7.6: Protein molecules tested with the kDE model.

Tables 7.1 and 7.2, show a representative list of the performance analysis for the proposed kDE approach on different ligand and protein molecules, respectively. As shown in Tables 7.1 and 7.2, the first columns indicate the PDB IDs for the tested molecules. The second column in both tables specifies the number of atoms within each molecular structure and the third column shows the dof considered in each scenario. The preselected dof for each experiment are the chemically-allowed dof to study chemically-feasible molecular conformations.

Table 7.1: Performance analysis of the kDE algorithm on ligands.

| Ligands | Number Atoms | DOF | E_crystal<br>(kcal/mol) | E_kDE<br>(kcal/mol) | Conv.Gener. | T_kDE<br>(ms) |
|---------|--------------|-----|-------------------------|---------------------|-------------|---------------|
| BTN     | 16           | 3   | -3.25                   | -3.59               | 85/500      | 2.57          |
| CYC     | 43           | 13  | -16.75                  | -17.93              | 209/500     | 2.1           |
| NAD     | 44           | 11  | -12.42                  | -13.68              | 125/500     | 2.18          |
| XK2     | 46           | 4   | -10.91                  | -11.35              | 117/500     | 2.34          |

Table 7.2: Performance analysis of the kDE algorithm on proteins.

| Proteins | Number Atoms | DOF | $E_{crystal}$<br>(kcal/mol) | $E_{kDE}$<br>(kcal/mol) | Conv.Gener. | $T_{kDE}$<br>(s) |
|----------|--------------|-----|-----------------------------|-------------------------|-------------|------------------|
| 1STP     | 903          | 7   | -554.78                     | -576.16                 | 118/500     | 0.35             |
| 1DO3     | 2466         | 9   | -876.33                     | -876.37                 | 189/500     | 2.55             |
|          |              | 22  |                             | -881.53                 | 191/500     | 2.62             |
|          |              | 36  |                             | -879.38                 | 211/500     | 2.58             |
| 1NS1     | 2342         | 42  | -1126.35                    | -1127.49                | 170/600     | 2.3              |
|          |              | 58  |                             | -1128.061               | 172/600     | 2.27             |
|          |              | 98  |                             | -1126.076               | 138/600     | 2.25             |

To evaluate our proposed kDE molecular model, we compared our obtained results with the crystal structures published in the Protein Data Bank [Berman 2000]. Analytically, we calculated the van der Waals (VDW) energy for each crystal structure ( $E_{crystal}$ ) and compared it against the obtained VDW energy value by the kDE algorithm ( $E_{kDE}$ ) accordingly. As shown in Tables 7.1 and 7.2, the kDE algorithm succeeded to converge in a smaller VDW energy value compared with the corresponding VDW energy of the crystal structure for all the performed experiments. This phenomenon occurs since all the incorporated energy terms (i.e., VDW potential or electrostatic forces) in a molecule's internal energy are in fact an approximation of the potential energy and not the molecule's free energy, which requires entropy calculations, among others. Therefore, the proposed kDE model managed to output a stable molecular conformation for all the tested molecules. This is very important given that most evolutionary algorithms suffer from local minima traps.

The sixth column (*Conv.Gener.*) in Tables 7.1 and 7.2 indicates the generation when the BioDE algorithm converged. This convergence generation is the generation where the fitness function of the worst population member equals with the fitness function of the best one, which is also the same as the obtained  $E_{kDE}$  value. Moreover, Figure 7.7 shows the convergence performance of the kDE algorithm over different tested ligand molecules. Similarly, Figure 7.8 demonstrates the convergence performance of the kDE model for 1STP, 1NS1 and 1DO3 protein molecules over a selection of

experimental scenarios based on the dof considered. As shown in these figures, the kDE algorithm converges really fast. This is very important given that one of the main drawbacks in an evolutionary-based algorithm is the convergence uncertainty.

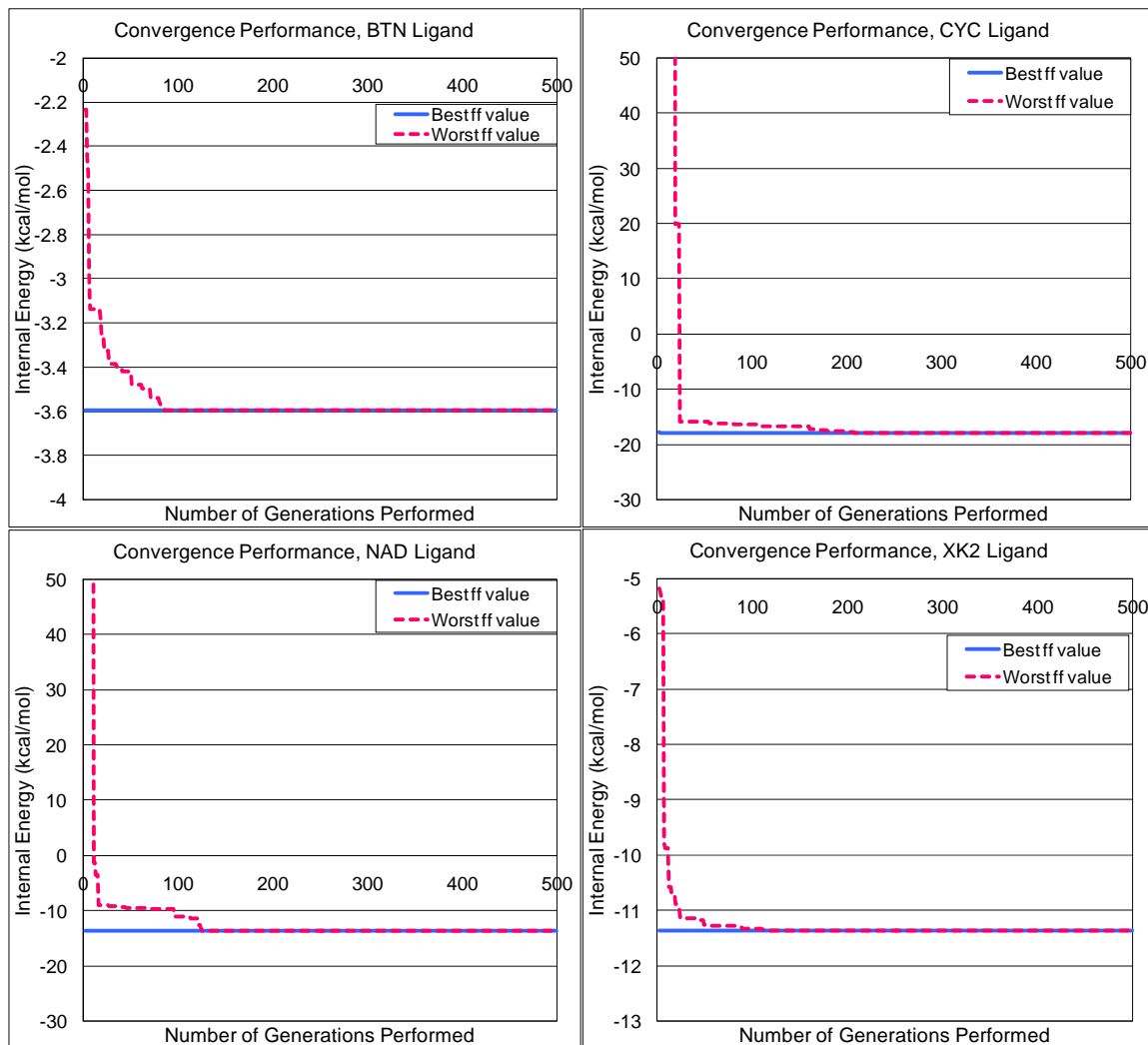


Figure 7.7: kDE's convergence performance for ligands.



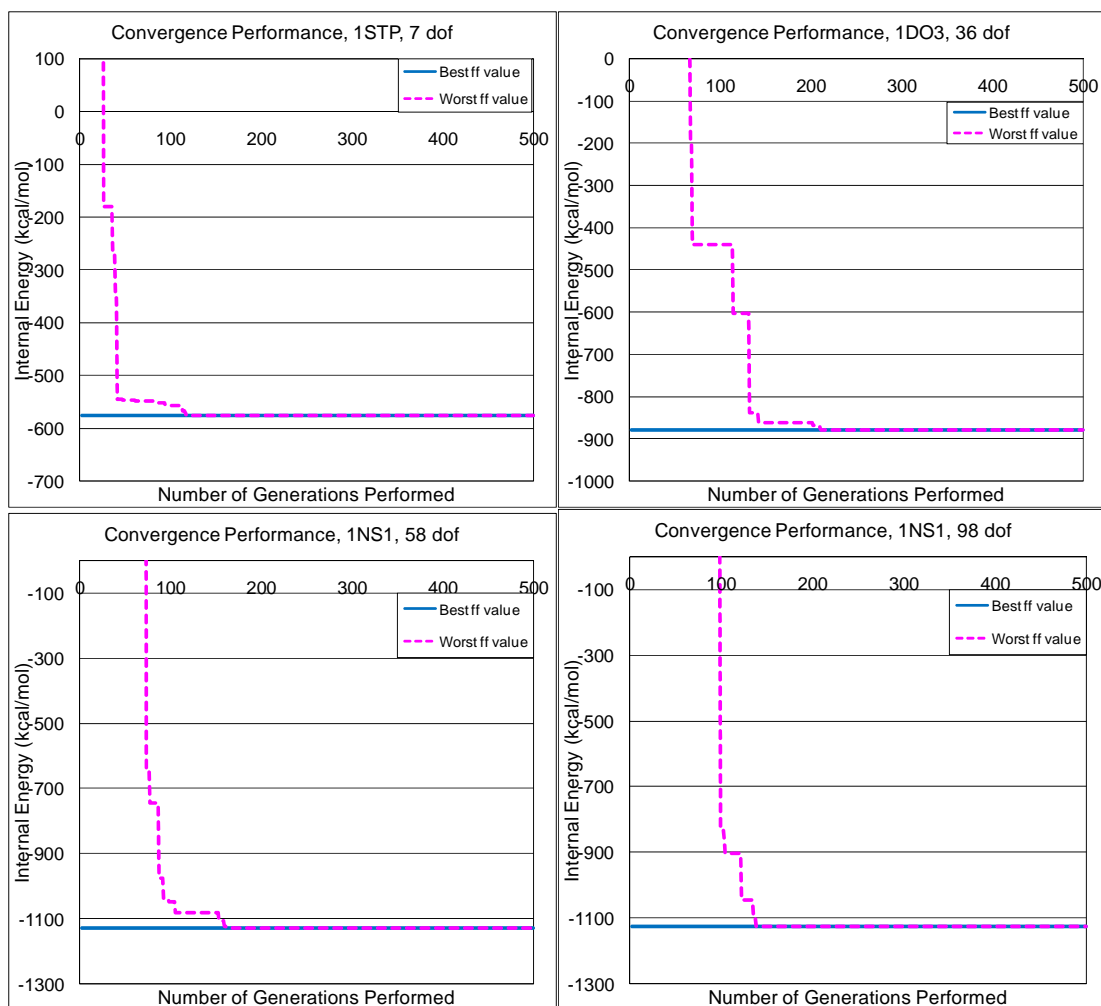


Figure 7.8: kDE’s convergence performance for proteins.

The last column in Tables 7.1 and 7.2 indicate the average computational time ( $T_{kDE}$ ) required by the kDE algorithm to evaluate each generation.  $T_{kDE}$  is given in milliseconds for the ligands and in seconds for the proteins. Considering the slowest experimental scenario depicted by the largest tested 1DO3 protein molecule, the required total computational time to output a stable conformation is  $T_{kDE} \times Converge\ Generation \times popsize = 2.68\text{ s/generation} \times 200\text{ generations} \times 100\text{ members} = 53600\text{ s} = 893.333\text{ min} = 13.89\text{ hours}$ . Therefore, in less than a day, a stable molecular conformation for a large enough protein molecule can be obtained using our proposed methodology.

Table 7.3: RMSD performance for the kDE algorithm.

|     |              | Ligands |         |         | Proteins |         |         |         |         |         |
|-----|--------------|---------|---------|---------|----------|---------|---------|---------|---------|---------|
| kDE | min_RMSD     | 2.09287 | 1.17923 | 1.4377  | 0.10494  | 0.15097 | 0.06455 | 0.28908 | 0.49195 | 0.94288 |
|     | max_RMSD     | 2.40881 | 9.94754 | 2.17494 | 0.35987  | 0.23343 | 0.24466 | 0.31183 | 0.69252 | 1.25286 |
|     | average_RMSD | 2.26475 | 6.11804 | 1.82515 | 0.23722  | 0.1942  | 0.1698  | 0.30067 | 0.61111 | 1.09315 |
|     | molecules    | CYC     | NAD     | XK2     | 1STP     | 1DO3    |         |         | 1NS1    |         |
| dof | 13           | 11      | 4       | 7       | 9        | 22      | 36      | 58      | 98      |         |

At the end, the kDE algorithm outputs the final population of stable solutions or the obtained global minimum region for any tested ligands and protein molecules. This final population contains a large number of different molecular conformations for each tested molecule that attains the same low-energy value. However, to evaluate the structural feasibility of each obtained molecular solution, we have calculated their Root Mean Square Deviation (RMSD) in Angstroms from their corresponding crystal structure. Generally, lower RMSD values indicate closer resemblance between observed and predicted structures with RMSD values below or near  $2.0 \text{ \AA}$  usually considered being sufficiently close.

As shown in Table 7.3, the kDE algorithm succeeded to identify stable structures with RMSD values in the range of 0.10 to 0.94 for any tested protein and in the range of 1.18 to 2.09 for the tested ligands. This means that the results of the kDE method lie within the acceptable structural range of  $[0, 3)$  for all tested molecules. Therefore, the kDE approach outputs a large number of alternative stable molecular conformations that can be clustered based on their structures to identify those closest to their crystal structure.

#### 7.4.5 Conclusions

This section presented a new kinematics-based differential evolution (kDE) model for effectively searching for low-energy molecular conformations. The proposed model consists of two modules: the pre-computation and the DE-loop. At the pre-computation module, a molecule is represented as a highly articulated body able to adopt different

molecular conformations. At the DE-loop, a differential evolution algorithm is used as a direct search technique towards low-energy molecular conformations. Computer implementation and results demonstrate that the proposed kDE approach rapidly and accurately finds low-energy (stable) molecular conformations for molecular structures of different size, shape and topology. Results also show that the kDE algorithm attains a very good convergence performance while it outputs the global minimum region for any tested molecule. This region provides a number of alternative stable molecular solutions that have the same low internal energy value. As demonstrated the proposed kDE model outputs sufficient molecular conformations with RMSD values below or near  $2.0 \text{ \AA}$ . The predicted molecular conformations can then be clustered based on their structure similarity to identify those closest to their crystal structure.

## 7.5 Proposed BioDE Approach

This section presents a new algorithmic scheme called Biological Differential Evolution (BioDE) to minimize the molecular energy based on the differential evolution algorithm presented in Section 7.3 and the hierarchical data structure presented in Chapter 6. The proposed BioDE utilizes our previously developed data structure called g.eBGF, as a surrogate approximation model to reduce the number of exact evaluations, speed molecular conformational search, and reduce the algorithm's convergence rate as discussed in this section.

### 7.5.1 BioDE Overview

The proposed BioDE methodology is a novel, generic evolutionary and geometric-based direct search technique to identify molecules' minimum internal energy. The BioDE algorithm aims to effectively identify stable conformations for any molecular structure regardless of type, size and shape while considering the underlying chemical information. The main algorithmic difference between the kDE and BioDE approaches is

that the latest utilizes our previously developed g.eBGF data structure as a primary filter of molecules' feasibility to speed convergence.

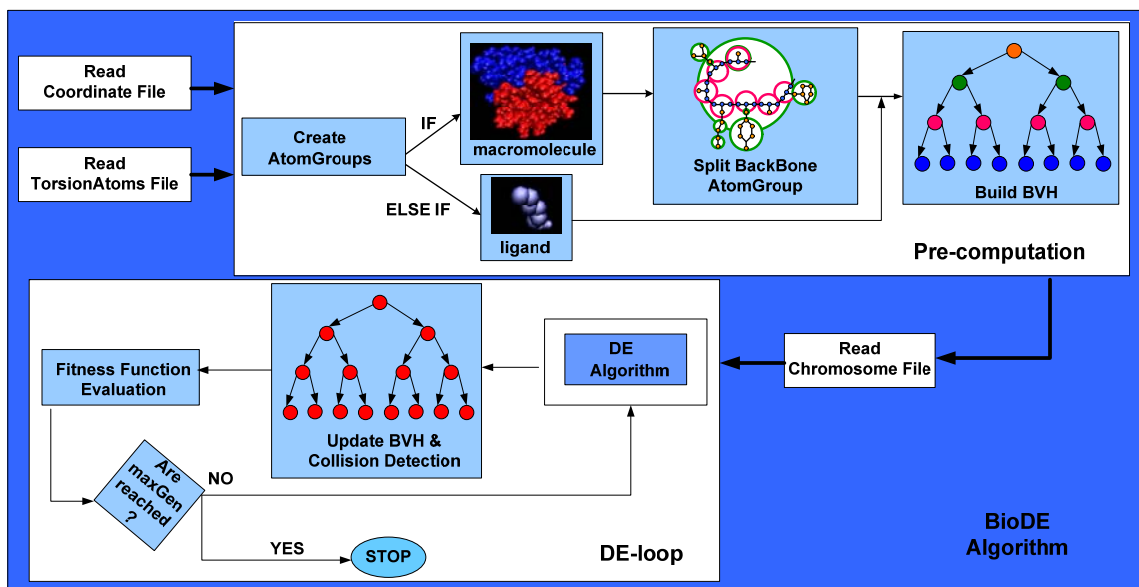


Figure 7.9: Overview of the proposed BioDE approach.

Figure 7.9 illustrates the overview of the proposed BioDE approach. As shown in Figure 7.9, the BioDE approach employs two modules: the pre-computation and the DE-loop modules. At the pre-computation stage, a geometric interpretation of the inter-atomic interactions is performed to set the constraints under which a molecular conformation is considered as feasible as discussed in Section 3.3. During this stage, our previously developed g.eBGF data structure is utilized as a primary filter for feasible molecular conformations. As shown in Figure 7.9, a molecular conformation (*coordinate* file) is input into the BioDE algorithm. The pre-selected dof (*TorsionAtoms* file) for a molecular structure are defined to form the atom groups. To further simplify the macromolecular representation, the backbone atom cluster(s) is split into smaller groups of atoms based on the concepts discussed in Section 5.3. A bounding volume hierarchy (BVH) denoted as a balanced binary tree is constructed for the initial molecular conformation to capture the molecular shape at successive level of details and to assist in

the collision detection queries. The type of bounding volumes used in this work is spheres since spheres are invariant to rotations and simpler to implement.

At the DE-loop module, the DE algorithm presented in Section 7.3 is used to direct the search towards low-energy minima or stable molecular conformations. For each candidate molecular conformation (population member) in each generation, the BVH is updated and a collision detection scheme is performed to determine the feasibility of the molecular conformation. The fundamental concept underneath the proposed collision detection algorithm is the geometric interpretation of the chemical information provided by the intra-molecular energy. If the collision detection queries output a feasible molecular conformation, then the fitness function for that conformation measures the van der Waals energy value; otherwise, a penalty function is computed to reject the specific unfit solution. This is an iterative process to provide better fitted individuals. As soon as the termination criterion denoted by the maximum allowed number of generations performed is satisfied, the BioDE algorithm outputs the final population of stable molecular conformations. This final population describes the global minimum region that provides a number of different molecular conformations that attain the same low-energy value and hence, provides alternative stable molecular solutions.

### 7.5.2 Input Files

The proposed BioDE methodology consists of two modules: the pre-computation and the DE-loop modules. Our proposed algorithm requires two input files for the pre-computation module: the atomic coordinate information (*coordinate* file) and the atoms within the molecular topology that share a torsion bond (*torsionAtoms* file). In addition, the BioDE algorithm requires one input file for the DE-loop module, the *chromosome* file.

The *coordinate* input file is usually the PDB file obtained from the Protein Data Bank (PDB) [Berman 2000]. The VMD software [Humphrey 1999] is used to define the atoms' connectivity information for proteins and to construct the *coordinate* input file.

The *torsionAtoms* input file is the file that describes the atoms that share a torsion bond and hence, depicts the number and the location of the pre-selected dof considered for each experiment. To create this file, the concepts about the allowed number and location of the pre-selected dof (torsion bond angles) presented in Section 6.2 and Section 6.3 are incorporated for studying chemically-feasible molecular conformations.

Finally, the *chromosome* file denotes the required dof or design variables for representing a candidate molecular conformation. Similar to nature, each chromosome structure through the defined genotype embodies a candidate solution to the problem under consideration whereas the chromosome genes represent the design variables that take values within their constrained space. Hence, to direct the search towards low-energy molecular conformations, the chromosome for the BioDE algorithm should represent a candidate molecular conformation with the genes accounting for the dof or the torsion bond angles  $\theta_i$  in the  $[0, 360)$  range.

### 7.5.3 Pre-Computation Module

During the pre-computation module, once the two input files (*coordinate* and *torsionAtoms* files) have been defined, groups of atoms are formed following the concept presented in Section 4.2 to simplify the molecular representation. If the tested molecular structure is a protein molecule, then an additional step within the BioDE algorithm is performed for splitting the backbone atom cluster (or clusters in the case of multiple chain proteins) into smaller AtomGroups as discussed in Section 5.3. As soon as the atom clusters both rigid and flexible have been defined, a bounding volume hierarchy (BVH) depicted as a balanced binary tree is introduced to capture the shape of the molecule at successive levels of detail and to facilitate the collision detection search for overlapping atoms. The BVH is built only once at the beginning of the algorithm during the pre-computation stage.

#### 7.5.4 DE-Loop Module

At the beginning of the DE-loop module, similarly to the kDE model, the *chromosome* file is input to the BioDE algorithm to define a candidate molecular conformation as a function of the torsion bond angles  $\theta_i$  as shown in Figure 7.4. The DE algorithm evolves a fixed population size (*popsize*) composed of candidate problem solutions (population members or chromosomes), randomly initialized. Consequently, each population member corresponds to a candidate molecular conformation. After initializing the population, an iterative process starts to direct the search towards better fitted population members or stable molecular solutions. At each generation (iteration), a new population of candidate solutions (conformations) is produced until a stopping criterion is satisfied. In this work, the termination criterion is the maximum allowed number of generations performed (*maxgen*). At each generation, each population member (candidate molecular conformation) can be replaced with a new generated one. The new member is a linear combination between a randomly selected member (the donor) and a difference between two other randomly selected members. Genetic operators (mutation, crossover, and selection) are applied to provide the next generation of better fitted candidate problem solutions (molecular conformations).

For each candidate molecular conformation (population member) in each generation, the BVH is updated and a collision detection scheme is performed to determine the feasibility of the molecular conformation. The BVH is updated for each new molecular conformation as the torsion angles are randomly modified. As soon as the BVH is updated, the collision detection algorithm presented in Chapter 5 and Chapter 6, is performed to search for potential overlaps between non-bonded atoms within the tested molecular conformation.

One of the major components in an evolutionary-based algorithm is to define an appropriate fitness function *ff*. The *ff* plays the role of the evaluation criterion for each candidate problem solution. Choosing a “good” mathematical representation for the *ff* is very important and challenging since it directs the search towards the optimal solution or in our case, towards stable molecular conformations. A good mathematical representation

for the  $ff$  is the use of the total intra-molecular energy. However, as discussed in Section 3.2, this would result in a very slow progress towards the search for low-energy solutions. Therefore, we propose an alternative fitness function definition utilizing our developed g.eBGF data structure as an approximation model of molecules feasibility. In other words, if the collision detection algorithm outputs a feasible molecular conformation, then the fitness function for that conformation measures the van der Waals (VDW) energy value, else a *penalty* function is computed to reject the specific bad solution as shown by Eqn. 7.9:

$$ff = \begin{cases} VDW_{potential} = \sum_{i=1}^n \sum_{j=1}^n \frac{B_{ij}}{r_{ij}^{12}} - \frac{A_{ij}}{r_{ij}^6} & \text{if conformation feasible} \\ penalty = m \cdot \sum_{k=1}^m (d_{0,k} - d_{i,j,k})^2 = m \cdot (1 - \rho_2) \sum_{k=1}^m (r_{i,k} + r_{j,k})^2 & o/w \end{cases} \quad (7.9)$$

Where,  $d_{0,k}$  and  $d_{i,j,k}$  are the equilibrium distance and the relative inter-atomic distance for the  $k^{th}$  colliding non-bonded pair of atoms  $i$  and  $j$ , and  $m$  is the total number of colliding atom pairs within the tested molecular conformation. As shown in Eqn. 7.9, the proposed *penalty* function is a distance function between the equilibrium and the relative inter-atomic distances for each overlapping atom pair within the molecular topology. The purpose of using this penalty function is to train the algorithm to avoid searching space regions mostly occupied by infeasible solutions. This training is defined as a function of “how” much infeasible these solutions are or alternatively how many overlapping atom pairs exist within the examined molecular conformation.

### 7.5.5 Computer Implementation and Results

The presented method and algorithms have been implemented on a dual 3.0 GHz CPU workstation using Visual C++, Visual Basic programming languages, OpenGL and CGAL libraries [CGAL]. As shown in Figure 7.10 and Figure 7.11, different molecular structures with different number of atoms, chains, residues and dof are tested with the proposed BioDE approach. The example molecules were obtained from the Protein Data



Bank (PDB) [Berman 2000] with PDB IDs as follows: BTN, CYC, NAD, XK2 ligand molecules and 1STP, 1DO3, 1NS1 protein molecules. These molecules are the same ones used to evaluate the kDE method presented in Section 7.4. Using these molecules as the test-bed for the BioDE algorithm, a performance comparison between BioDE and kDE models is provided in the following Section 7.6.

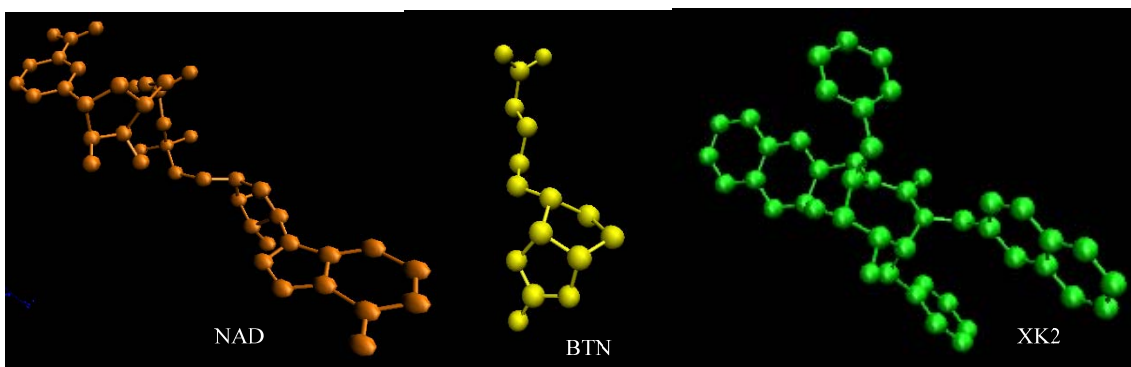


Figure 7.10: Ligand molecules tested with the BioDE model.

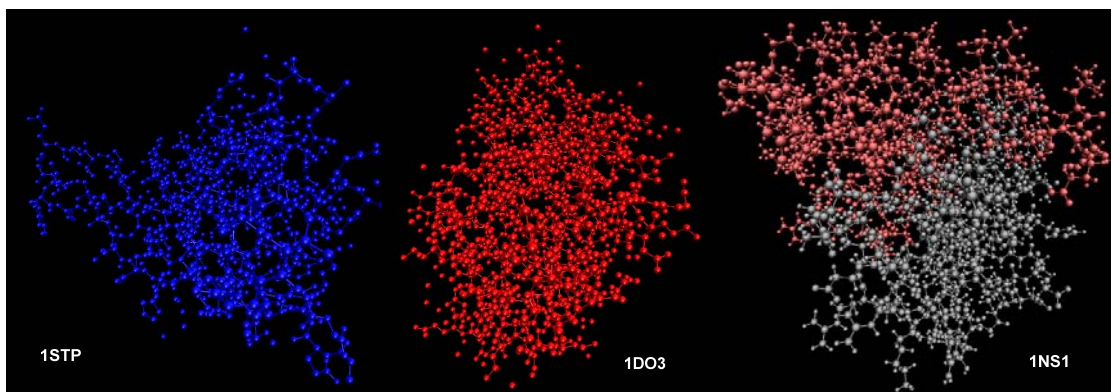


Figure 7.11: Protein molecules tested with the BioDE model.

The termination criterion for the BioDE algorithm was set to  $maxgen = 500$  generations performed and  $popsiz = 100$  candidate molecular conformations (population members) considered in each generation for each experiment except for the 1NS1 protein. For the 1NS1 protein, given the large number of dof considered in each experimental scenario, the  $maxgen$  was set to 600 generations and 300 population

members used as *popsize*. Finally, the DE's control parameters used in all experiments were  $F = 0.6$  for the mutation parameter, and  $Cr = 0.45$  for the crossover probability.

Tables 7.4 and 7.5, show a representative list of the performance analysis for the proposed BioDE approach on different ligand and protein molecules, respectively. As shown in Tables 7.4 and 7.5, the first columns indicate the PDB IDs for the tested molecules. The second column on each table specifies the number of atoms within each molecular structure, whereas the third column denotes the dof considered in each scenario. The preselected dof for each experiment are the chemically-allowed dof for the molecules.

Table 7.4: Performance analysis of the proposed BioDE algorithm on ligands.

| Ligands | Number Atoms | DOF | $E_{crystal}$<br>(kcal/mol) | $E_{BioDE}$<br>(kcal/mol) | Conv.Gener. | $T_{BioDE}$<br>(ms) |
|---------|--------------|-----|-----------------------------|---------------------------|-------------|---------------------|
| BTN     | 16           | 3   | -3.25                       | -3.59                     | 87/500      | 1.86                |
| CYC     | 43           | 13  | -16.75                      | -17.93                    | 132/500     | 2.07                |
| NAD     | 44           | 11  | -12.42                      | -13.68                    | 162/500     | 2.31                |
| XK2     | 46           | 4   | -10.91                      | -11.35                    | 117/500     | 2.36                |

Table 7.5: Performance analysis of the BioDE algorithm on proteins.

| Proteins | Number Atoms | DOF | $E_{crystal}$<br>(kcal/mol) | $E_{BioDE}$<br>(kcal/mol) | Conv.Gener. | $T_{BioDE}$<br>(s) |
|----------|--------------|-----|-----------------------------|---------------------------|-------------|--------------------|
| 1STP     | 903          | 7   | -554.78                     | -576.16                   | 187/500     | 0.34               |
| 1DO3     | 2466         | 9   | -876.33                     | -876.37                   | 180/500     | 2.49               |
|          |              | 22  |                             | -881.53                   | 188/500     | 2.49               |
|          |              | 36  |                             | -879.38                   | 175/500     | 2.46               |
| 1NS1     | 2342         | 42  | -1126.35                    | -1127.49                  | 150/600     | 2.28               |
|          |              | 58  |                             | -1128.061                 | 127/600     | 2.2                |
|          |              | 98  |                             | -1126.076                 | 150/600     | 2.21               |

To evaluate our proposed BioDE molecular model, we compared our results with the results for crystal structures published in the Protein Data Bank [Berman 2000]. Analytically, we calculated the van der Waals (VDW) energy for each crystal structure ( $E_{crystal}$ ) and compared it against the VDW energy value obtained from the BioDE

algorithm ( $E_{BioDE}$ ). As shown in Tables 7.4 and 7.5, the BioDE algorithm succeeded to converge in a smaller VDW energy value compared with the corresponding VDW energy for the crystal structure on all the performed experiments. This phenomenon occurs since when measuring a molecule's internal energy all the incorporated energy terms (i.e. VDW or electrostatic forces) are in fact an approximation of the potential energy and not the molecule's free energy, which among other requires entropy calculations. Therefore, the proposed BioDE algorithm succeeded to output a stable molecular conformation for all the tested molecules. This is very important given that most evolutionary algorithms suffer from local minima traps.

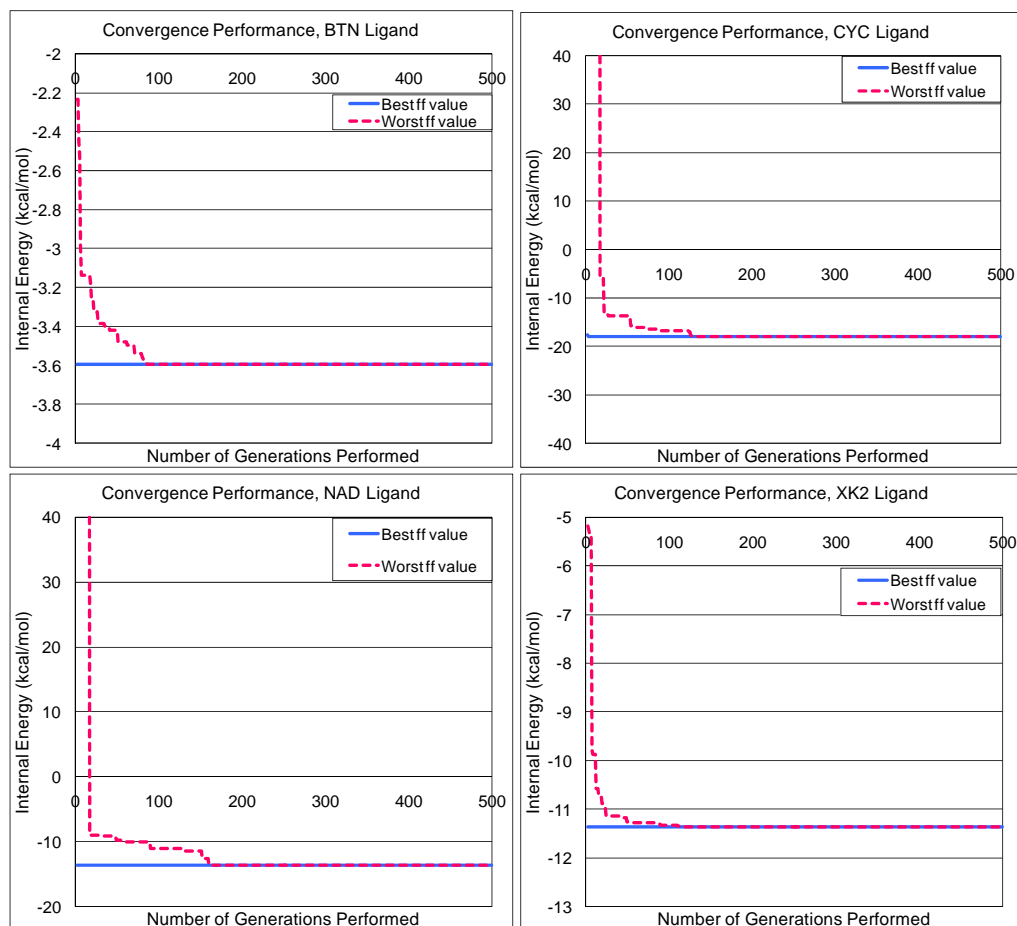


Figure 7.12: Convergence performance of the BioDE method for ligands.

The sixth column (*Conv. Gener.*) in Tables 7.4 and 7.5 indicates the BioDE algorithm's convergence generation. This convergence generation is the generation where the fitness function of the worst population member equals with the fitness function of the best individual, which is also the same as the  $E\_BioDE$  value. Figure 7.12 shows the convergence performance of the BioDE algorithm over the different tested ligand molecules. Figure 7.13 demonstrates BioDE's convergence performance for 1NS1, 1DO3 and 1STP proteins, over different number of dof. As shown in these figures, the BioDE algorithm attains a very good convergence performance. This is very important given that one of the main drawbacks in an evolutionary-based algorithm is the convergence uncertainty.

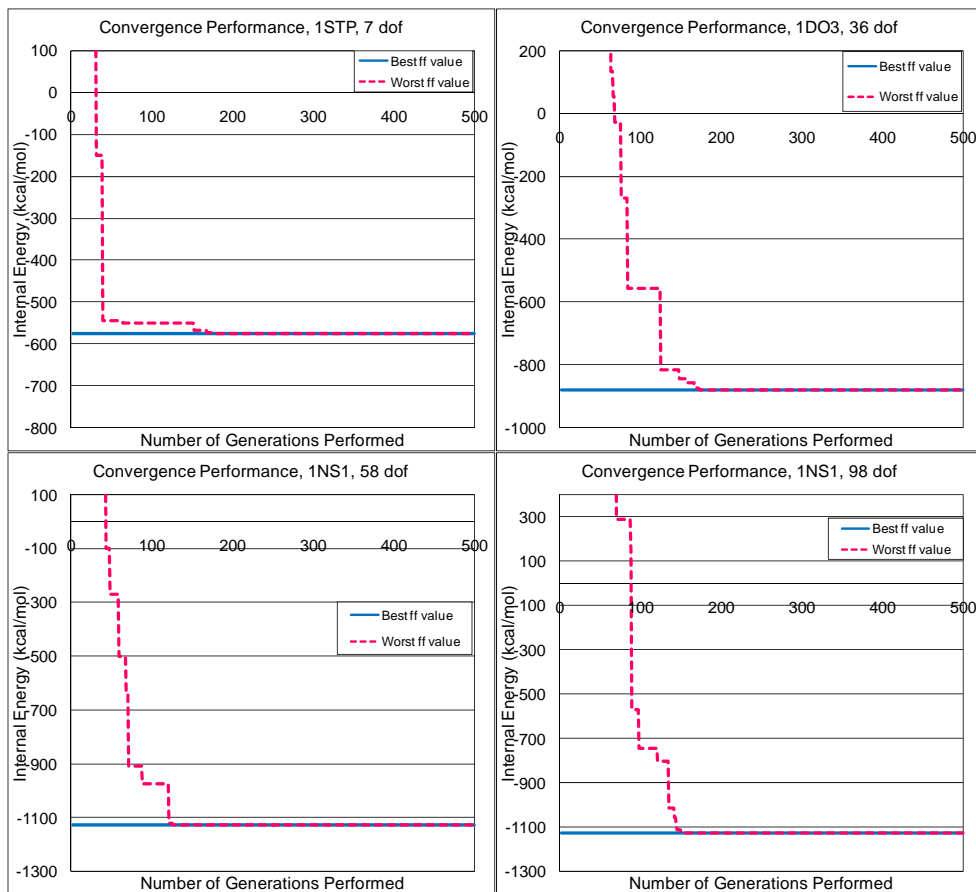


Figure 7.13: Convergence performance of the BioDE method for proteins.

The last column in Tables 7.4 and 7.5 indicates the average computational time ( $T_{BioDE}$ ) required by the BioDE algorithm to evaluate each generation. The  $T_{BioDE}$  is given in milliseconds for the ligands and in seconds for the proteins.

Similarly to the kDE model, at the end of the BioDE algorithm the final population of stable solutions is obtained. This final population contains a large number of different molecular conformations for each tested molecule that attains the same low-energy value. To evaluate the structural feasibility of each obtained molecular solution, we have calculated their Root Mean Square Deviation (RMSD) in Angstroms from their corresponding crystal structure. Generally, lower RMSD values indicate closer resemblance between observed and predicted structures with RMSD values below or near  $2.0 \text{ \AA}$  usually considered being sufficiently close.

Table 7.6: RMSD performance of the BioDE algorithm.

|       |              | Ligands |         |         | Proteins |         |         |         |         |         |
|-------|--------------|---------|---------|---------|----------|---------|---------|---------|---------|---------|
| BioDE | min_RMSD     | 3.13168 | 1.17923 | 1.4377  | 0.08278  | 0.00335 | 0.29471 | 0.44538 | 0.48878 | 0.88915 |
|       | max_RMSD     | 12.6164 | 10.0217 | 2.17394 | 0.50226  | 0.35859 | 0.51279 | 0.77254 | 0.6937  | 1.2621  |
|       | average_RMSD | 8.70862 | 6.21425 | 1.82367 | 0.33243  | 0.27351 | 0.40033 | 0.64655 | 0.60418 | 1.08408 |
|       | molecules    | CYC     | NAD     | XK2     | 1STP     | 1DO3    |         |         | 1NS1    |         |
|       | dof          | 13      | 11      | 4       | 7        | 9       | 22      | 36      | 58      | 98      |

As shown in Table 7.6, the BioDE algorithm succeeded to identify stable structures with RMSD values in the range of 0.003 to 0.889 for any tested protein and with RMSD values of 1.17 and 1.43 for NAD and XK2 ligands, respectively. However, the result for CYC ligand is relatively higher. This means that the BioDE method lies within the acceptable structural range of  $[0, 3)$  for all tested molecules except for the CYC ligand.

### 7.5.6 Conclusions

Section 7.5 presented a novel generic computational geometric and evolutionary-based molecular methodology called biologically-inspired differential evolution (BioDE)

approach for effectively identifying chemically-feasible and low-energy conformations for molecules of different type, size, shape and topology. The proposed BioDE approach employs a differential evolution algorithm to direct the search towards stable molecular conformations. It incorporates the underlying geometric interpretation of the inter-atomic interactions as a primary filter for feasible molecular conformations to reduce the number of exact evaluations performed and to speed the molecular conformational search. Computer implementation and results demonstrate that the proposed BioDE algorithm accurately and rapidly identifies low-energy molecular conformations for different molecular structures. The proposed BioDE approach attains a very good convergence performance while it outputs the global minimum region for the tested molecule. It also provides a set of alternative low-energy molecular conformations for researchers to test during molecular design. As demonstrated the BioDE algorithm outputs sufficient molecular conformations for all the tested proteins and most of the tested ligands. These predicted molecular conformations can then be clustered based on their structures to identify those closest to their crystal structure.

## 7.6 Comparison Between the kDE and BioDE Approaches

The main algorithmic difference between the BioDE and kDE approaches is that the BioDE algorithm utilizes the g.eBGF technique presented in Chapter 6, as a surrogate approximation model to speed convergence and to reject any unfeasible generated solution. This is possible through a *penalty* function that is assigned to those individuals (population members or else conformations) that attain overlapping atoms within their generated topology. Therefore, the g.eBGF algorithm is used by the BioDE model as a primary filter of molecules' feasibility. If a candidate molecular conformation passes this first filtering step (no overlapping atoms: *penalty* = 0), then the *fitness function* (*ff*) measures its VDW energy to define the individual's feasibility level. Different to this algorithmic scheme, the kDE model is a much simpler methodology that calculates the VDW energy for all candidate molecular conformations to determine their fitness level.

As demonstrated in Section 7.4.4 and Section 7.5.5, both kDE and BioDE methods are effectively pushing the molecular conformational search towards the global minimum region occupied by a large number of alternative stable conformations. Both methods succeeded in identifying molecules' stability for any type of molecular structure tested while attaining a very good convergence performance. However, given the algorithmic difference of the two approaches, the main question lies in which from the proposed direct search algorithms perform better.

Table 7.7: Comparison between kDE and BioDE approaches.

| Proteins | Number Atoms | DOF | BioDE_Conv.Gener. | kDE_Conv.Gener. | T_BioDE (s) | T_kDE (s) |
|----------|--------------|-----|-------------------|-----------------|-------------|-----------|
| 1STP     | 903          | 7   | 187/500           | 118/500         | 0.34        | 0.35      |
| 1DO3     | 2466         | 9   | 180/500           | 189/500         | 2.49        | 2.55      |
|          |              | 22  | 188/500           | 191/500         | 2.49        | 2.62      |
|          |              | 36  | 175/500           | 211/500         | 2.46        | 2.58      |
| 1NS1     | 2342         | 42  | 150/600           | 170/600         | 2.28        | 2.3       |
|          |              | 58  | 127/600           | 172/600         | 2.2         | 2.27      |
|          |              | 98  | 150/600           | 138/600         | 2.21        | 2.25      |

To evaluate and validate the kDE and BioDE models, we compared the obtained molecular structures (kDE and BioDE outputs) against their corresponding crystal structures published in PDB [Berman 2000]. Two different performance assessments were performed: an energy-oriented (lowest obtained VDW energy values) and a structural-based (RMSD) performed. To compare the BioDE algorithm against the kDE method, we have tested both methods using the same molecular structures and workstations.

Computer implementation and results demonstrate that for ligand molecules both methods perform approximately the same. For protein molecules, there is no significant computational time improvement of using the BioDE approach for identifying the molecular feasibility as shown in Table 7.7. However, the BioDE provides a convergence enhancement over the kDE method for proteins. As shown in Table 7.7, the BioDE algorithm converged about 25% faster on over 70% of the experiments performed.

Therefore, the BioDE algorithm provides convergence enhancement while identifying alternative low-energy molecular conformations.

In regards to the identified molecular structure, both the kDE and BioDE methods succeeded to converge in conformations close to the crystal structures for any tested flexible protein and for most of the examined flexible ligands. As shown in Tables 7.3 and 7.6, the RMSD values obtained by the BioDE approach are much smaller compared with those obtained by the kDE model for all the tested proteins but 1DO3 protein with 36 dof. Regarding the predicted ligand structures, it appears that both models had the same performance for all the tested ligands but CYC ligand where the kDE model calculated a smaller RMSD value.



## Chapter 8

### Conclusions, Discussion and Future Work

The scope of this chapter is to provide a summary of the research methodologies presented to study the molecular flexibility and stability mechanism. The general conclusions, including encountered challenges and limitations, are also discussed here, followed by a description of future research work.

#### 8.1 Research Summary

This research work presented three different molecular models: the g.eBGF, kDE and BioDE algorithms. Two computational geometric models (BGF and eBGF) were also implemented to assist in the development of the g.eBGF approach. The g.eBGF algorithm is responsible for rapidly and accurately identifying the molecular feasibility whereas the kDE and BioDE algorithms direct the conformational search towards stable molecular conformations. All proposed algorithms rely upon the basic algorithmic concepts for kinematically representing the molecular structure. They also integrate concepts from robotics, evolutionary-oriented optimization, computational geometry and computational biology.

The core algorithmic architecture of the BGF, eBGF and g.eBGF methods is a two layer hierarchical data structure that kinematically represents the molecular flexibility using a bounding volume hierarchy to assist in the collision detection. The BGF or BioGeoFilter approach effectively identifies the molecular feasibility for ligands (drug-like) molecules and performs really well in identifying the molecular feasibility rapidly and accurately. In addition, the BGF algorithm satisfies the haptic-rate requirement, enabling real-time ligand design.

The eBGF or enhanced BioGeoFilter algorithm presented in Chapter 5 is a significant enhancement of the BGF approach as it can model macromolecules such as proteins. The proposed eBGF method effectively studies the flexibility mechanism of proteins while addressing current limitations in protein modeling. Therefore, the eBGF algorithm is presented as a rapid and accurate filtering tool of proteins' feasibility, significantly facilitating protein modeling and design.

The generic eBGF or g.eBGF approach discussed in Chapter 6 is a generic molecular modeling tool able to represent the flexibility mechanism of any molecule independently of type, size, shape and topology. The proposed g.eBGF model is the generic enhancement of the eBGF algorithm. The g.eBGF model considers some chemically-based constraints to provide more realistic and chemically-feasible molecular conformations compared with those of the eBGF. This is a significant improvement in computational-aided molecular design.

The kDE and BioDE models presented in Chapter 7 direct the molecular conformational search towards low-energy (stable) solutions. To achieve this, both models employ our previously developed DE algorithm. The main algorithmic difference is that the BioDE algorithm utilizes the g.eBGF method as a surrogate approximation model to speed convergence. Both approaches effectively identify stable molecular conformations for any molecular structure independently of type, size, shape and topology. Both models also succeed in providing the global minimum region for any tested molecule while attaining a very good convergence performance. However, the BioDE algorithm slightly speeds the computational time for identifying stable protein solutions while significantly speeding the algorithm's convergence rate in protein conformational search.

To evaluate and validate our proposed research work, we have tested the BGF, eBGF and g.eBGF algorithms against the traditional energy calculation approach. All methods succeeded in significantly decreasing the computational time for identifying feasible molecular conformations without sacrificing accuracy.

To evaluate and validate the kDE and BioDE models, we compared the obtained molecular structures (kDE and BioDE outputs) against the corresponding crystal

structures published in [Berman 2000]. Two different performance assessments were performed: an energy-oriented and a structural-based. Both methods succeeded to converge in a smaller VDW energy value compared with the VDW energy for the corresponding crystal structure, thus identifying the molecules' stability state. The structures of the obtained molecular conformations were compared to the corresponding crystal structure using the Root Mean Square Deviation (RMSD). Both methods managed to output molecular conformations close to the crystal structure for all the tested proteins and for most of the tested ligands while attaining a very good convergence performance.

## 8.2 Future Research Work

Studying the atomic-scale processes is an open research problem that requires many disciplines to collaborate for providing reliable results and enabling bionanotechnology applications. Our proposed research work facilitates the modeling of flexible molecules and the identification of stable or low-energy conformations. This work can be used in molecular docking, nanoscale assembly problems and towards the development of an indispensable computer-aided design tool for bionanotechnology. To build a fully functional molecular system, many challenges need to be addressed and many different research pathways can be pursued.

One of the fundamental principles of Industrial Systems Engineering is that the first step in a product/system development is the idea itself, followed by the design and production stages. It is also well known that any candidate product/system modifications are better performed during the design stage for the product/system to be cost-effective. Under these assumptions, future research work lies within the real-time visualization of the molecular interactions during the design stage so that fully functional bionanoscale products can be designed and evaluated prior to actual fabrication. In this research work, new methods have been investigated that provide real-time force feedback using haptic devices. These devices are currently used to manipulate virtual molecules and to feel the forces as the molecules interact with each other providing an essential design and

visualization tool. However, to achieve a realistic molecular representation, continuous visualization as well as sense of touch to the users, a rapid molecular tool is essential that satisfies the haptic-rate requirement. To achieve haptic-rate performance, the rapid update and modeling of molecular conformations are the main prerequisites.

Focusing towards this objective, our research work presented the BGF algorithm for real-time ligand modeling that satisfies the haptic-rate requirement. Although the proposed eBGF and g.eBGF are fast molecular feasibility tools, they do not satisfy the haptic constraint. Further research work is required for speeding the identification of a protein's flexibility mechanism to allow haptic interaction between macromolecules. As shown in Table 6.1, the bottleneck function of the proposed g.eBGF algorithm is the update of the bounding volume hierarchy. The GPU-oriented modeling technique seems a promising approach for speeding the BVH update and hence, to enable haptic interactions between flexible proteins or between a flexible ligand and a flexible protein. As soon as a molecular modeling system that satisfies the haptic constraint is developed, haptic devices can be utilized to study the real-time molecular docking and/or assembly problems.

In addition, the main limitation of the proposed kDE and BioDE methods is that both methods require approximately one to three days outputting a stable molecular solution. Although these results are significantly faster than current literature, they are unsuitable for real-time haptic design. To allow haptic molecular interactions in a virtual environment, further research work is required to speed the molecular conformational search. Parallel computing is a very promising approach towards this direction. In other words, instead of using the DE algorithm presented in Section 7.3, we could utilize parallel computing such as a parallel DE algorithm to direct the molecular conformational search. This is expected to enable the haptic manipulation of molecules in a virtual environment and facilitate bionanoscale design and engineering.

An off-line improvement of the current research work is to target the molecular docking/assembly problem through a molecular path planning approach. Under this perspective, the BioDE or kDE algorithm can be enhanced by using a modified chromosome structure, which represents a candidate problem solution. Currently in the

kDE and BioDE models, the genes of the chromosome measure the torsion bond angles representing a candidate molecular conformation. The chromosome for the molecular path planning operation will depict both the torsion bond angles and the way-points along the “optimum” trajectory”. This trajectory is the “optimum” path of a totally flexible ligand towards the cavity site of a total flexible protein. The location of the cavity site will be assumed to be known and will define the last chromosome gene, signifying the molecular path planning target.

Alternatively, an on-line molecular path-planning improvement can be envisioned by utilizing the aforementioned concepts about GPUs and/or parallel computing as well as haptic-rendering approaches. Using haptics to control a flexible ligand around a flexible protein with unknown binding site may lead to the identification of the protein’s binding site. This may also provide strong insights for identifying feasible land-marks (coordinate points) along the molecules’ “optimum” trajectories. These land-marks may be used as path planning targets through the corresponding chromosome’s genes to speed the algorithm convergence.

As mentioned above, studying the molecular flexibility is only a step closer to fully understand and model the molecular behavior. Molecules are very flexible bodies in nature that usually exist in a solvent environment. Further research is required to holistically model the molecular interactions in a solvent environment. Additionally, future research work lies in studying the protein folding problem for providing structural insights for artificial macromolecular design. To conclude, bionanoscale research is still at the early stages and all the possible research ideas, concepts and pathways can be limited only by the researcher’s vision and imagination.

## References

1. Adcock S.A, McCammo JA. Molecular Dynamics: Survey of Methods for Simulating the Activity of Proteins. *Chem. Rev.* 2006; 106: 1589-1615.
2. Agarwal PK, Guibas L, Nguyen A, Russell D, Zhang L. Collision detection for deforming necklaces. *Computational Geometry: Theory and Applications* 2004; 28(2-3).
3. Angulo VR, Cortez J, Simeon T. BioCD: an efficient algorithm for self-collision and distance computation between highly articulated molecular models. *Conference on Robotics: Science and Systems*, Boston, MA, 2005.
4. Apaydin MS, Guestrin CE, Varma C, Brutlag DL, and Latombe JC. Stochastic Roadmap Simulation for the Study of Ligand-Protein Interactions. *Bioinformatics* 2002a; 18(2): S18-S26.
5. Apaydin MS, Brutlag DL Guestrin CE, Hsu D, and Latombe JC. Stochastic Conformational Roadmaps for Computing Ensemble Properties of Molecular Motion. *Proc. Workshop on the Algorithmic Foundations of Robotics (WAFR)* 2002b.
6. Apaydin MS, Guestrin CE, Hsu D, Brutlag DL, and Latombe JC. Stochastic Roadmap Simulation: An Efficient Representation and Algorithm for Analyzing Molecular Motion. *Journal of Computational Biology* 2003; 10(3-4).
7. Baxter CA, Murray CW, Clark DE, Westhead DR, Eldridge MD. Flexible docking using tabu search and an empirical estimate of binding affinity. *Proteins: Structure, Function, and Genetics* 1998; 33: 367-382.
8. Bayazit OB, Song G, and Amato NM. Ligand Binding with OBPRM and Haptic User Input: Enhancing Automatic Motion Planning with Virtual Touch. *Technical Report TR00-025, Department of Computer Science, Texas A&M University, College Station, Texas, 77843-3112, October 9, 2000.*
9. Bayazit OB. Solving Motion Planning Problems by Iterative Relaxation of Constraints. *PhD Dissertation, Department of Computer Science, Texas A&M University, May 2003.*

10. Berman HM, Westbrook J, Feng Z, Gilliland G, Bhat TN, Weissig H, et al. The Protein Data Bank. *Nucleic Acids Research* 2000; 28: 235-242.
11. Bitello R, and Lopes HS. A Differential Evolution Approach for Protein Folding. *Proceedings of the IEEE Symposium on Computational Intelligence in Bioinformatics and Computational Biology* 2006: 1-5.
12. Brintaki A and Nikolos IK. Coordinated UAV Path Planning Using Differential Evolution. *Transactions of the Operations Research International Journal* 2005c; 5(3).
13. Brintaki AN, Lai-Yuen SK. BioGeoFilter.: A Tool For Identifying Geometrically Feasible Molecular Conformations In Real-Time For Bionanomanufacturing. *Transactions of the North American Manufacturing Research Institution of SME, NAMRC 36*, Monterrey, Mexico, 2008a: 153-160.
14. Brintaki AN, Lai-Yuen SK. eBGF: An Enhanced Geometric Hierarchical Representation for Protein Modeling and Rapid Self-Collision Detection. *Transactions of the Computer-Aided Design and Applications Journal*, 2009a; 6 (6): 625-638.
15. Brintaki AN, Lai-Yuen SK. eBGF: An Enhanced Geometric Hierarchical Representation for Protein Modeling and Rapid Self-Collision Detection. *Proceedings of the International Computer-Aided Design and Applications Conference*, Orlando, FL, 2008b.
16. Brintaki AN, Lai-Yuen SK, and Nikolos IK. BioDE: A Biological Differential Evolution Approach for Molecular Design. *submitted to IEEE Transactions on Evolutionary Computation*, 2010a.
17. Brintaki AN, Lai-Yuen SK, and Nikolos IK. A Kinematics-Based Differential Evolution Method for Molecular Design. *To be presented at the IERC 2010*, Cancun Mexico, June 5-9, 2010b.
18. Brintaki AN, Lai-Yuen SK, and Nikolos IK. A Hybrid Molecular Model Towards Low-Energy Conformations. *Proceedings of the IERC09, Institute of Industrial Engineers (IIE) Annual Conference & Expo 2009*, Miami, FL, May30-June3, 2009b.
19. Brintaki AN, Lai-Yuen SK, and Nikolos IK. A Kinematics Based Heuristic Approach to Minimize Molecular Conformational search. *To be presented at the International Computer-Aided Design (CAD) Conference & Exhibition*, Dubai, United Arab Emirates, June 21- 25, 2010c.

20. Brintaki AN, Lai-Yuen SK, and Nikolos IK. A Kinematics Based Heuristic Approach to Minimize Molecular Conformational search. *Submitted at Computer-Aided Design and Applications Journal*, 2010d.
21. Brunner RK, Phillips JC, Laxmikant VK. Scalable Molecular Dynamics for Large Biomolecular Systems. Conference of High Performance Networking and Computing. *Proceedings of the ACM/ IEEE on Supercomputing 2000*; (45), ISBN: 0-7803-9802-5.
22. Chiang TH, Apaydin MS, Brutlag DL, and Latombe JC. Predicting Experimental Quantities in Protein Folding Kinetics Using Stochastic roadmap Simulation. *International Conference on Research in Computational Molecular Biology (RECOMB) 2006*.
23. Cortes J, Simeon T, and Laumond J P. A Random Loop Generator for Planning the Motions of Closed Kinematic Chains Using PRM Methods. *Proceedings of the IEEE International Conference on Robotics and Automation*, Washington, DC, May 2002.
24. Cortes J. Motion Planning Algorithms for General Closed-Chain Mechanisms. *PhD Thesis; Institute National Polytechnique de Toulouse 2003*.
25. Cortes J, Simeon T, Angulo VR, Guieysse D, Simeon MR, and Tran V. A Path Planning Approach for Computing Large-Amplitude Motions of Flexible Molecules. *Bioinformatics 2005*; 21(1): i116-i125.
26. Cortes J, Jaillet L, and Simeon T. Molecular Disassembly With Rrt-Like Algorithms. *IEEE International Conference on Robotics and Automation*, Roma, Italy, 10-14 April 2007.
27. CGAL. <http://www.cgal.org>. *Computational Geometry Algorithms Library*.
28. Chong SY, and Tremayne M. Combined Optimization Using Cultural and Differential Evolution: Application to Crystal Structure Solution From Powder Diffraction Data. *Chemistry Communication, Royal Society of Chemistry Journal 2006*; 4078-4080.
29. Damsbo M, Kinnear BS, Hartings MR, Ruhoff PT, Jarrold MF, and Ratner MA. Application of Evolutionary Algorithm Methods to Polypeptide Folding: Comparison with Experimental Results for Unsolvated Ac-(Ala-Gly-Gly)<sub>5</sub>-LysH<sup>+</sup>. *PNAS 2004*; 101(19): 7215-7222.



30. Dendzik Z, Kosmnder M, Dawid A, and Gbarski Z. Interaction Induced Depolarized Light Scattering From Ultrathin Ne Film Covering Single-Walled Carbon Nanotubes of Different Chiralities. *Molecular Structure Journal* 2005; 744-747 (3): 577-580.
31. Fischer K, and Gartner B. The Smallest Enclosing Ball of Balls: Combinatorial Structure and Algorithms. *SoCG'03*, San Diego, California, June 8-10, 2003.
32. Giannakoglou KC. Design of Optimal Aerodynamic Shapes Using Stochastic Optimization Methods and Computational Intelligence. *Progress in Aerospace Sciences* 2002; 38: 43-76.
33. Goldberg DE. Genetic Algorithms in Search, Optimization and Machine Learning. Addison-Wesley 1989.
34. Gottschalk S, Lin MC, and Manocha D. OBBTree: A hierarchical structure for rapid interference detection. *Comp. Graphics 30 (Annual Conf. Series)* 1996: 171-180.
35. Grayson P, Tajkhorshid E, Schulten K. Mechanisms of selectivity in channels and enzymes studied with interactive molecular dynamics. *Biophysical Journal* 2003; 85: 36-48.
36. Hartenburg RS, and Denavit J. A kinematic notation for lower pair mechanisms based on matrices. *Applied Mechanics Journal* 1955; 77: 215-221.
37. Holland JH. Adaptation in Natural and Artificial Systems. *The MIT Press* 1992.
38. Humphrey W, Dalke A, Schulten K. VMD-Visual Molecular Dynamics, *Molecular Graphics Journal* 1999; 14: 33-38.
39. Jones G, Willett P, Glen RC, Leach AR, and Taylor R. Development and Validation of a Genetic Algorithm for Flexible Docking. *Molecular Biology Journal* 1997; 267: 727-748.
40. Kima H, Choib J, Kimc HW, Jung S. Monte Carlo Docking Simulations of Cyclomaltoheptaose and Dimethyl Cyclomaltoheptaose with Paclitaxel. *Carbohydrate Research*, 15 March 2002; 337(6): 549-555.
41. Lai-Yuen, SK, Lee Y-S. Interactive Computer-Aided Design for Molecular Docking and Assembly. *Computer-Aided Design and Applications Journal* 2006a; 3(1-4).
42. Lai-Yuen SK, Lee YS. Energy-Field Optimization and Haptic-Based Molecular Docking and Assembly Search System for Computer-Aided Molecular Design (CAMD). *Proceedings of the 14th Symposium Haptic Interfaces for Virtual Environment and Teleoperator Systems, IEEE Virtual Reality Conference*, Alexandria, VA, 2006b: 25-29.

43. La Valle SM, and Kuffnerr JJ. Rapidly-Exploring Random Trees: Progress and Prospects. *Algorithmic and Computational Robotics, New Directions, WAFR 2000a*.
44. La Valle SM, Finn PW, Kavraki LE, and Latombe JC. A Randomized Kinematics-Based Approach to Pharmacophore-Constrained Conformational Search and Database Screening. *Computational Chemistry Journal* 2000; 21(9): 731-747, 2000b.
45. La Valle SM, Finn PW, Kavraki LE, and Latombe JC. Efficient Database Screening for Rational Drug Design Using Pharmacophore-Constrained Conformational Search. *Proceeding of the 3<sup>rd</sup> International Conference on Computational Biology, Lyon, France, 1999*.
46. Lee Y-G, Lyons KW. Smoothing Haptic Interaction using Molecular Force Calculations. *Computer-Aided Design Journal* 2004; 36 (1): 75-90.
47. Leech J, Prins J.E, Hermans J. SMD: Visual Steering of Molecular Dynamics for Protein Design. *IEEE Computational Science & Engineering* 1996.
48. Lotan I, Schwarzer F, Halperin D, Latombe JC. Efficient Maintenance and Self-Collision Testing for Kinematic Chains. *SoCG, Barcelona, Spain, 2002*.
49. Lin MC. Collision Detection Between Geometric Models: A Survey. *Proceedings of IMA Conference on Mathematics of Surfaces* 1998.
50. Liu M, Wang S. MCDOCK: A Monte Carlo Simulation Approach to the Molecular Docking Problem. *Computer Aided Molecular Design Journal*, 13 Sep 1999, 5: 435-451.
51. Michalewicz Z. Genetic Algorithms + Data Structures = Evolution Programs. *Springer Publications* 1999.
52. Morin S, Redon S. A Force-Feedback Algorithm for Adaptive Articulated-Body Dynamics Simulation. *IEEE International Conference on Robotics and Automation, Rome, Italy, 2007*.
53. Morris GM, Goodshell DS, Halliday RS, Huey R, Hart WE, Bellew RK, and Olson AJ. Automated Docking Using a Lamarckian Genetic Algorithm and an Empirical Binding Free Energy Function. *Computational Chemistry Journal* 1998; 19 (14):1639-1662.
54. Nagata H, Mizushima H, Tanaka H. Concept and Prototype of Protein-Ligand Docking Simulator with Force Feedback Technology. *Bioinformatics* 2002; 18 (1): 140-146.

55. Nikolos IK and Brintaki A., Coordinated UAV Path Planning Using Differential Evolution. *Proceedings of the 13th Mediterranean Conference on Control and Automation, IEEE*, Cyprus 2005a: 549-556.
56. Nikolos IK, Brintaki A, Zografos ES. Coordinated UAV Path Planning Using an ANN Assisted Differential Evolution Algorithm. *Proceedings of the EUROGEN 2005 Conference (Sixth Conference on Evolutionary and Deterministic Methods for Design, Optimization and Control with Applications to Industrial and Societal Problems)*, Munich, Sep. 12-14; 2005b.
57. Nikolos IK, Zografos ES, Brintaki A. UAV Path Planning Using Evolutionary Algorithms. *Springer Publications, Studies in Computational Intelligence Book Series, Innovations in Intelligent Machines Book-1* 2007; 70:77-111.
58. NIST. Nano@NIST : Maximizing the Benefits and Minimizing the Risks of Nanotechnology. [http://www.nist.gov/public\\_affairs/nanotech.htm](http://www.nist.gov/public_affairs/nanotech.htm).
59. Phillips JC, Braun R, Wang W, Gumbart J, Tajkhorshid E, Villa E, et al. Scalable Molecular Dynamics with NAMD, *Published online in Wiley InterScience*, 26 May 2005 ([www.interscience.wiley.com](http://www.interscience.wiley.com)).
60. Price KV, Storn RM, and Lampinen JA. *Differential Evolution, a Practical Approach to Global Optimization*. Springer-Verlag, Berlin Heidelberg 2005.
61. Redon S, Galoppo N, Lin MC. Adaptive Dynamics of Articulated Bodies. *ACM Transactions on Graphics* 2005; 24(3).
62. Renambot L, and Bal HE. CAVEStudy: An Infrastructure for Computational Steering and Measuring in Virtual Reality Environments. *Kluwer Academic Publishers, Cluster Computing 4* 2001:79–87.
63. Sherrill CD. Introduction to Molecular Mechanics. School of Chemistry and Biochemistry. Georgia Institute of Technology. <http://130.207.37.140/courses/chem8840/pdf/molmech-lecture.pdf>. *Web Book*.
64. Storn R, and Price K. DE - a Simple and Efficient Adaptive Scheme for Global Optimization over Continuous Space. *ICSI, Technical Report TR-95-012* 1995.
65. Taufer M, Crowley M, Price D, Chien AA, and Brooks III CL. Study of a Highly Accurate and Fast Protein-Ligand Docking Algorithm Based on Molecular Dynamics. *Proceedings of the 18th International Parallel and Distributed Processing Symposium 2004 (IPDPS'04)*.

66. Teschner M, Kimmerle S, Heidelberger B, Zachmann G, Raghupathi L, Fuhrmann A, et al. Collision Detection for Deformable Objects. *Computer Graphics Forum* 2005; 24(1): 61-81.
67. Thomsen Rene. Flexible Ligand Docking Using Differential Evolution. *Proceedings of the 2003 Congress on Evolutionary Computation*, IEEE 2003; 4: 2354-2361.
68. Thomsen R, and Christensen MH. MolDock: A New Technique for High-Accuracy Molecular Docking. *American Chemical Society, Med. Chem. Journal* 2006; 49: 3315-3321.
69. Torczon V, Trosset MW. Using Approximations to Accelerate Engineering Design Optimization. NASA/CR-1998-208460, *ICASE Report* 1998; 98-33.
70. Wang H, and Ersoy OK. A Novel Evolutionary Global Optimization Algorithm and its Application in Bioinformatics. *Electrical and Computer Engineering ECE Technical Reports, Purdue Libraries* 2005.
71. Wawer A, Seredynski F, and Bouvry P. Application of Evolutionary Computing to Conformational Analysis. In Mieczyslaw A. Klopotek, Slawomir T. Wierzchon, and Krzysztof Trojanowski, editors, *Intelligent Information Processing and Web Mining*, Springer 2004. *Proceedings of the International IIS: IIPWM'04 Conference, Advances in Soft Computing*, Akopane, Poland, May 2004: 161-168.
72. Wehrens r. Small-Molecule Geometry Optimization and Conformational Search. *Evolutionary Algorithms in Molecular Design* 2000.
73. Westhead DR, Clark DE, and Murray CW. A Comparison of Heuristic Search Algorithms for Molecular Docking. *Computer-Aided Molecular Design Journal* 1997; 11(3): 209-228(20).
74. Yang JM, Horng JT, and Kao CY. Integrating Adaptive Mutations and Family Competition with Differential Evolution for Flexible Ligand Docking. *IEEE* 2001.
75. Hui-Yuan F, Lampinen J, Dulikravich GS. Improvements to Mutation Donor Formulation of Differential Evolution. *Proceedings of EUROGEN 2003 Conference on Evolutionary Methods for Design, Optimization and Control, Applications to Industrial and Societal Problems, CIMNE*, Barcelona 2003.
76. Zhang M, and Kavvaki LE. A new method for fast and accurate derivation of molecular conformations. *Chemical Information and Computing Sciences Journal* 2004; 42: 64-70.

77. Zhang M, White RA, Wang L, Goldman R, Kavraki L, and Hassett B. Improving Conformational Searches By Geometric Screening. *Bioinformatics* 2005; 21(5): 624-630.

### About the Author

Athina N. Brintaki was born on April 26, 1978, in Athens, Greece. She received her B.S. and M.S. degrees from the Department of Production Engineering & Management at Technical University of Crete, Greece, in 2004 and 2006, respectively. In 2005, she received a graduate fellowship from the University of South Florida (USF) to continue her graduate studies and completed her Ph.D. in Industrial Engineering in 2010. From 2005-2010, she worked as a research assistant at USF, where she received the 2008 College of Engineering Research Poster Award and the 2010 Graduate and Professional Student Council Award from USF. She published 3 journal and 6 conference papers and currently has 2 journal papers submitted, 1 journal paper to be submitted, 3 working papers in different stages of completion and a number of conference and poster presentations. She continues conducting research to understand the bionanoscale processes.